Service Altimetrie & Localisation Precise

CLS COLLECTE LOCALISATION SATELLITES

cnes CENTRE NATIONAL D'ÉTUDES SPATIALES

CalVal Envisat

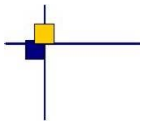

Envisat RA2/MWR ocean data validation and cross-calibration activities. Yearly report 2013.

Contract No 104685. Lot 1.2A

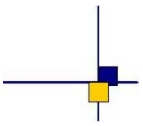

Reference : CLS-NT-13-290

Nomenclature : SALP-RP-MA-EA-22293-CLS

Issue : 1rev 1

Date : 2014,February

CLS - 8-10 Rue Hermes - Parc Technologique du Canal - 31520 Ramonville St-Agne - FRANCE
Telephone 33 5 61 39 47 00 / Telecopie 33 5 61 75 10 14

Chronology Issues :		
Issue :	Date :	Reason for change :
1.0	15/10/2013	Created
1.1	20/04/2014	N. Picot reviews taken into account

	AUTHORS	COMPANY	DATE	INITIALS
WRITTEN BY	A. Ollivier M. Guibbaud	CLS CLS		
CHECKED BY	S. Dalessio	CLS		
APPROVED BY	JP. Dumont Y. Faugere	CLS CLS		
APPLICATION AUTHORISED BY				

Index sheet :	
Context	
Keywords	Envisat, Jason-1, Jason-2, Calval, , MSL, orbits, reprocessing
hyperlink	

.

Distribution :		
Company	Means of distribution	Names
CLS/DOS	electronic copy	G. Dibarboure V. Rosmorduc
CNES	electronic copy	thierry.guinle@cnes.fr nicolas.picot@cnes.fr aqgp_rs@cnes.fr dominique.chermain@cnes.fr delphine.vergnoux@cnes.fr

List of tables and figures :

List of Tables

List of Figures

List of items to be defined or to be confirmed :

Applicable documents / reference documents :

.

Contents

LIST OF ACRONYMS

ECMWF	European Center for Medium range Weather Forecasts
GDR-A	Geophysical Data Record version A (before cycle 41 for Envisat mission)
GDR-B	Geophysical Data Record version B (after cycle 41 for Envisat mission)
GIM	Global Ionosphere Maps
IRI	Internationl Reference Ionosphere
MSL	Mean Sea Level
MWR	MicroWave Radiometer
POE	Precise Orbit Estimation
SLA	Sea Level Anomalies
SSB	Sea State Bias
USO	Ultra Stable Oscillator
PTR	Point Target Response

1. Introduction

This report is an overview of Envisat performance assessment and cross calibration studies carried out at CLS during year 2013. It is basically concerned with long-term monitoring of the Envisat altimeter system over ocean.

Before the satellite loss, Envisat GDR data was routinely ingested in the Calval 1-Hz altimeter database maintained by the CLS Spatial Oceanography Division in the frame of the CNES Altimetry Ground Segment (SALP) and funded by ESA through F-PAC activities (SALP contract N° 104685 - lot1.2.A).
In spite of the loss of the satellite on the 8th of April 2012, CLS experts teams continue to improve the mean sea level computation, taking into account analysis of new standards carried out in 2013. The continuation of this work allows to guarantee an optimal data quality level and to prepare the next reprocessing of the whole Envisat dataset.
This annual report concerns the reprocessed data from GDR cycles 6 through 92 and routine 93 to 113 spanning the 10 years (from 14-05-2002 to 08-04-2012) of Envisat life. The cycle 113 is uncomplete because of the loss of Envisat. All relevant altimeter parameters deduced from Ocean 1 retracking, radiometer parameters and geophysical corrections are evaluated and tested.
For further information about the original GDR data before reprocessing, please refer to [13].
A document concerning the impact of reprocessing on the data is also available in the frame of the reprocessing activities (see [84]).

In the mind of the next reprocessing, the performance of those updates in term of SSH and mesoscale error is presented in part 6.3.2.. The impact on Mean Sea Level trend is analysed in part 8.2.3..
Furthermore, methods of comparison to in situ dataset are also used to provide an external reference, complementary to the usual satellite cross comparisons.

Some of the results described here were presented at the OSTST meeting (Boulder, October 2013) and at the Quality Working Group (QWG) meeting (Toulouse, May 2013).
The work performed in terms of data quality assessment also includes cross-calibration with Jason-1, Jason-2 and Cryosat-2 CNES CPP data set. This kind of comparisons between coincident altimeter missions provides a large number of estimations and consequently efficient long-term monitoring of instrument measurements. This enables the detection of instrument drifts and inter-mission biases essential to obtain a consistent multi-satellite data set.

After a preliminary section describing the data used, the report is split into 6 main sections: first, **data coverage** and measurement validity issues are presented. Second, a **monitoring of the main altimeter and radiometer parameters** is performed, describing the major impact in terms of data accuracy. Then, **performances of GDR** are assessed and discussed with respect to the major sources of errors. The aim is to present the impact of the anticipated updates notably developped in 2013. Then, Envisat **Sea Surface height** is compared to other missions in terms or (SSH) differences at cross-overs and the SLA computed with **MSL** standards is monitored.

Finally, an additional part presents the **particular investigations** that have been performed during this year. These investigations are separated in two parts: one concerning the anticipated updates for the next reprocessing, the other concerns additional analysis performed in 2013.
A final part is dedicated to the Envisat error budget synthesis written in 2013 and estimated over

the whole mission. This estimation is made by comparing altimeter data to other sources (models, in situ data).

.

2. Quality overview

All the information concerning the historical data is available in 2012 ([16]) Yearly Report.
This year report concerns anticipated updates analysed after reprocessing. These updates are analysed in the mind of the next reprocessing.

Ra-2 instrumental status:
Due to the permanent RA2 S-band power drop which occurred on January 17th 2008, 23:23:40 (Cycle 65 pass 289) all the S-band parameters, including the dual ionospheric correction and rain flag remain irrelevant and MUST NOT be used from this time.
Instead, users are advised to use the ionospheric correction from GIM model, which is available in GDR data products.

Since the loss of the S-Band at the beginning of year 2008, the solar activity was in a low period, therefore the use of the JPL-GIM model correction instead of the dual-frequency correction in the SSH equation was efficient and data were weakly impacted in terms of variance. In 2011 the solar activity started to increase again and the degradation due to this correction is getting significant.
In October 2011 (cyclic report 107), a warning was sent to the community to warn about the increase of the high solar activity which degrades the data.
This year an analysis of a new combination of GIM model correction was performed, described in Part 8.2.2..
Since V2.1 data standard the USO correction is included in the range and so it does not need to be taken into account anymore.

Drifting phase:
During the drifting phase, the 35 days cycle was reduced to a 30 day pseudo cycle with a small drift estimated to +/-1.7 km per cycle maximum (at respectively 50 deg Latitude N/S) whereas it does not drift at 38 deg N and S.
The impact on the data was already described in last year yearly report. With the whole dataset in drifting phase, the analysis of the impact is now more relevant. Only a weak impact is noticed in the data quality (the visible impact concerns the SLA standard deviation) and the new Mean Sea Surface was shown to erase almost all this impact.
Note that the drift was observed to be higher than the one theoretically expected (+/-600m per cycle maximum was expected) see figure 1.

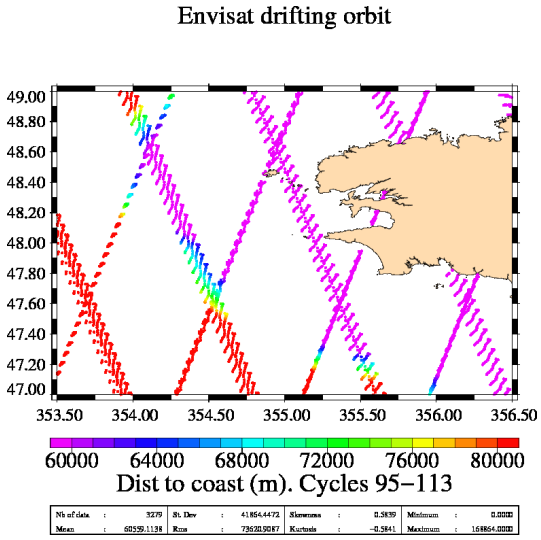

Figure 1: *Effect of the drifting phase near French coast. Cycles 95 to 113.*

Missing measurements:
The unavailability of data over ocean for the whole Envisat dataset is very low, about 3% in average.
The MWR unavailability is also rather stable and low, in average around 2% on the whole dataset.

Long term monitoring of RA-2 and MWR parameters:
The ocean-1 altimeter and radiometer parameters are consistent with expected values. They have a very good stability and high performances, comparable to Jason-1 and Jason-2. A very good availability on every surface and very low editing ratios over ocean are observed since the beginning of the mission. The high frequency content of Ku-band Ra-2 parameters is very stable.

Concerning the radiometer wet tropospheric correction, a degradation was noticed using the MWR after reprocessing in SLA computation. This degradation was systematic for all cycles. Investigations have been processed this year and a new MWR correction has been computed by CLS experts team to correct this degradation and to recover the quality obtained before reprocessing.
This new correction named V2.1b is described in Part 8.1.1..

Mean Sea Level:
Comparisons between Jason-1 and Envisat Mean Sea Level trend estimated at CLS were carried on.
These studies are possible thanks to:
- The availability of a comparison to a long Jason-1 reprocessed time series.
- The availability of a comparison to in situ datasets (Argo TS profile and Tide gauges) ingested to provide an external source of calibration. These activities are developed in [21] and [22].

With V2.1+ updates (see detailled content in 6.2), Envisat reprocessed data enables to provide a Mean Sea Level very close to Jason-1 time series.
The first year of the mission (before 2004) still presents a strange behavior, visible on some alimetric parameters. On the rest of the period, differences between both missions can be analyzed

more and more precisely. For instance, wet tropospheric correction still remains a source of error in the trend computation for all missions. Using the ECMWF operational model for the whole mission is not totally satisfactory due to the frequent jumps induced by the model upgrades, which are removed in the case of cross comparisons.
The impact of the new version of MWR wet tropospheric correction developped this year will be focused on in this report in Part 8.2.3.. Another invstigation concerns the GIM model used in MSL computation after the loss of the S-band, it is described in Part 8.2.2.

3. Data used and processing

3.1. Data used

Envisat Geophysical Data Records (GDRs) from cycle 6 to cycle 113 have been used to derive the results presented in this report, for the routine part.
All cycles from 6 to 92 were reprocessed into a standard homogeneous (so called V2.1 version) to the current production since cycle 92 (September 2010). Furthermore, cycles 6 to 9 were processed for the first time, though giving access to 3 additional month of data in 2002. This corresponds to ten years spanning from May 14th 2002 to April 8th 2012.

The Envisat GDR data are generated using two softwares: the IPF, from Level0 to Level1B, and the CMA, from Level1B to Level2.
Conversely to the previous yearly reports, the standard of the whole data is the same: the so-called V2.1 version, resulting from :
- IPF 6.04.L2 Version
- and CMA 9.3 Version

For any information concerning the historical data, please refer to the previous yearly report ([15]).

For cycles 47-48, the altimeter instrument was switched to B-side during 37 days, from the 15/05/2006 14:21:50 to the 21/06/2006 11:37:32 (cycle 47 pass 794 to cycle 48 pass 847), as indicated by a dedicated flag in the input data.

3.2. Processing

3.2.1. GDR products and quality assessment method

To perform this quality assessment work, conventional validation tools are used including editing procedures, crossover analysis, collinear differences, and a large number of statistical monitoring and visualization tools. All these tools are integrated and maintained as part of the CNES SALP altimetry ground segment and F-PAC (French Processing and Archiving Center) tools operated at CLS premises. Each cycle is carefully analyzed before data release to end users. The main data quality features are reported in a cyclic quality assessment report available on http://www.aviso.altimetry.fr/en/data/calval/systematic-calval/validation-reports.html. The purpose of this document is to report the major features of the data quality from the Envisat mission.

As for all other existing altimeters, the Envisat GDR data are ingested in the Calval 1-Hz altimeter database maintained by the CLS Spatial Oceanography Division. This allows us to cross-calibrate and cross-compare Envisat data to other missions. In this study data from Jason-1 (GDRs cycles 1 to 374) and Jason-2 (GDRs cycles 1 to 138) are used. Jason-1 is the most suitable for Envisat cross calibration as it is available throughout the Envisat mission and has been extensively calibrated to T/P (Dorandeu et al., 2004b [35]). Since January 2010 a reprocessing of Jason-1 products in GDR C is available. Therefore, since January 2011 a new homogeneous Envisat/Jason-1 data set is available.

Comparisons between Jason-1 and Envisat altimeter and radiometer parameters have been carried out using 10-day dual crossovers for SSH comparison and 3-hour dual crossovers for altimeter and radiometer comparisons. The geographical distribution of the dual crossovers with short time lags strongly changes from one Envisat cycle to another. Indeed, contrary to Envisat which is sun-synchronous, Jason-1 observes the same place at the same local time every 12 cycles (around 120-day). Following the method detailled in Stum et al. (1998) [102], estimates of the differences are computed using a 120 day running window to keep a constant geographical coverage.

3.2.2. Particular updates added to the GDR products

In addition to the new homogeneous dataset provided by the V2.1 reprocessing only few updates were performed for the validation process. The corrections are directly read from GDR products except for 3 terms:

- **GOT 4.7 ocean tide** is used because its quality was already shown to be better than the FES 2004 or GOTOO available in the products (Yearly report 2009 [13]). Note that for the next reprocessing, the GOT 4.8 version may be used. Performance of this version is analysed in Part 8.1.3..

- **Sea ice flag**: An additionnal flag to the one available in the products was developped to detect data corrupted by sea ice (see 4.3.1.). This flag is more severe than the one available in the product and enables to get rid of an optimized number of spurious data for validation purposes.

- **Filtered dual-frequency ionosphere correction**: A 300-km low pass filter is applied along track on the dual frequency ionosphere correction to reduce the noise of the correction. This correction is applied up to the cycle 64 before the S-Band Power drop (17th January 2008) then the GIM ionospheric correction is used. The new method of filtering developped in 2012 and described in [16], based on an iterative filtering process, will be used for the next reprocessing. Relative SSH performance are summarized in 8.1.2..

The few updates still necessary to complete the analysis are listed in the product disclaimer document available at http://earth.esa.int/dataproducts/availability/ [87]. Note that:

- **No S-Band anomaly is present in the data anymore**: Users are yet advised that the S Band anomaly flag available in the GDR must not be accounted for.

- **No more auxiliary files needed: the USO drift is now directly/properly corrected in the range.**
  The whole data serie, including the reprocessed data have to be used without any USO auxiliary file.
  Yet, during the reprocessing, some erroneous jumps in the USO computation of some products were identified.
  To avoid those erroneous jumps, users are advised to consider an appropriated editing of the data (see part 4.3.2.).
  The number of tracks impacted are synthetized in the "Anomaly report" table in Appendix of Yearly Report 2011 (see [15]).

3.2.3. Anticipated updates

This report concerns the dataset after reprocessing accounting for a list of updates developped and analysed for the next reprocessing. The performance of some evolutions has already been analysed in [16] and concerns:
- the F-PAC PTR correction;
- the GDR-D orbit standards;
- An updated wet tropospheric correction, used after reprocessing but degrading the mesoscale error;

This year the list of anticipated updates grows up and new standards have been analysed. The use of these alternative corrections for the next reprocessing is not yet ensured:

- A new **radiometer wet tropospheric correction** which corrects the degradation observed after reprocessing (V2.1) and improves the performance of SSH at crossovers to reach the one obtained before reprocessing.This new correction is here named V2.1b and is described in Part 8.1.1..

- The ionosperic correction used for the next reprocessing will be **the filtered correction obtained by iterative filtering** and analysed in 2012 (see 8.1.2.).

- The **GOT 4.8 ocean tide** may be used for the next reprocessing. Performance are better than the 4.7 version, as explained in Part 8.1.3..

- The MSS used for the Mean Sea Level trend estimation is currently the **CNES 2011 Mean Sea Surface**, but alternative corrections could be considered.

Finally, particular investigations have been performed this year to analyse several aspects of SSH computation:

- Impact of Envisat altitude consideration in GIM model computation (see 8.2.2.)

- Significant Wave Height analysis: evolution towards a climate dedicated multimission product (see 8.2.4.);

- Impact of orbits based on the latest gravity field: GFZ-GRGS EIGEN6S2 (see 8.2.1.);

4. Missing and edited measurements

This section mainly intends to analyze the hability of the Envisat altimeter system to correctly sample ocean surfaces. This obviously includes the tracking capabilities, but also the frequency of unavailable data and the ratio of valid measurements likely to be used by applications after the editing process.

4.1. Missing measurements

From a theoretical ground track, a dedicated collocation tool allows determination of missing measurements relative to what is nominally expected. The cycle by cycle percentage of missing measurements over ocean has been plotted in Figure 2. The measurement unavailability over the whole mission is about 7% in average. Twelve cycles have more than 10% of unavailability. Passes 1 to 452 of cycle 15 have not been delivered because of a wrong setting of RA-2. Several long RA-2 events occurred during cycles 6, 7, 13, 14, 16, 22, 34, 48, 51, 53, 56 which resulted in a significant number of missing passes.
Since May 2008, following an improvement of the data dissemination the average ratio of missing RA2 measurements over ocean is much smaller than the previous years.
On the plot 2, the major impact on the data availability noticed is the signature of the maneuvers to change the orbit on cycles 94-95 (see the cyclic report).
More anecdotally, a collision avoidance and a priority conflict with ATV were also noticed for cycle 101, with a weak impact on data.
Note that the last cycle of Envisat life (113) lasted 19 days and the percentage of missing data is also significant.

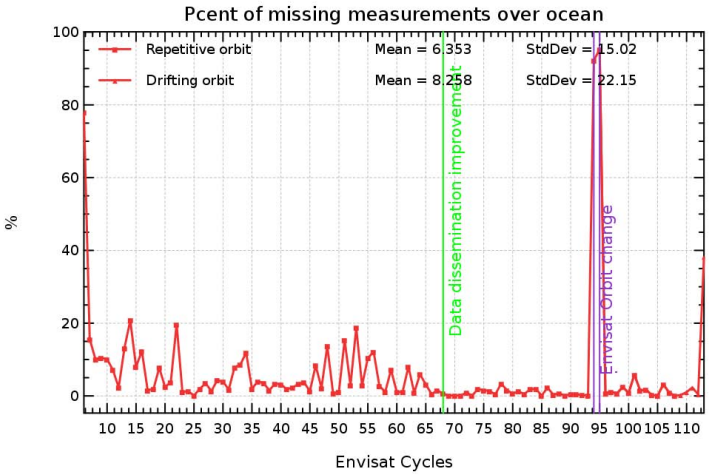

Figure 2: *Monitoring of the percentage of missing measurements relative to what is theoretically expected over ocean*

Figure 3 shows an example of missing measurements for the last complete cycle 112 . The measurements which are missing over the Himalaya are due to the IF Calibration Mode occurring on ascending passes only. This procedure was not always the same: for cycles prior to 55, it was performed over the Himalaya on both ascending and descending passes and for cycles 56 to 66 it was performed on ascending passes only but on the Rocky Mountains as well as on the Himalaya. Afterward, it is performed on ascending passes above the Himalaya only.

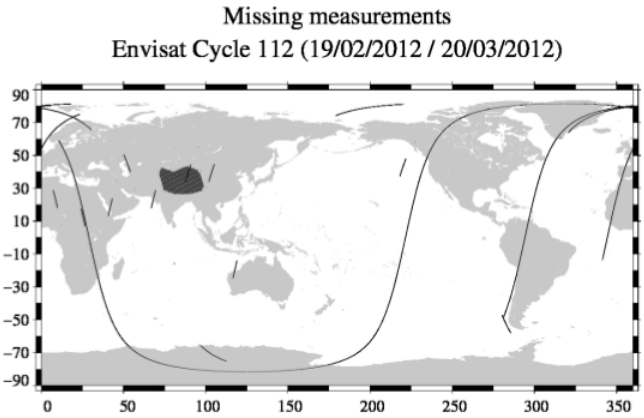

Figure 3: *Envisat missing measurements for the last entire cycle (112)*

It has been noticed that some pass segments were regularly missing. Figure 4 shows the pass segments missing more than 5 times over the 11 last cycles of the reprocessing period (cycles 82-92). Some of them are explained (PLO permanent acquisition sites (ESA/Rome, GAVDOS/ Creta), others are not. Apart from that, the data retention rate is very good on every surface observed. This might be due to the tracker used by Envisat Ra-2, the Model Free Tracker (MFT).

Note that for the drifting phase cycles, this plot cannot be updated due to the method of projection on the theoretical track.

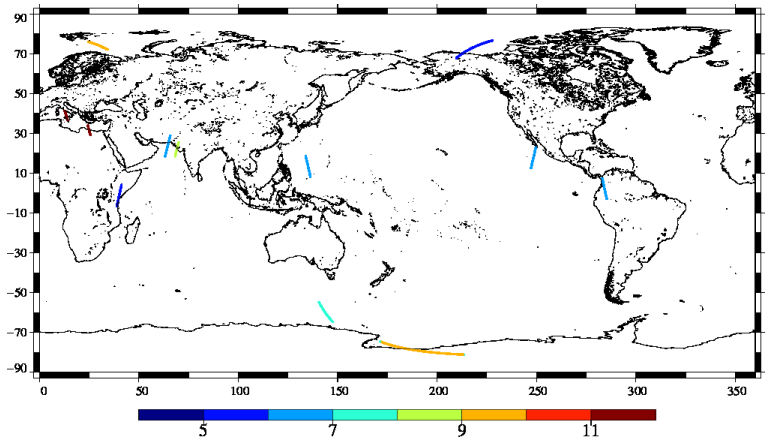

Figure 4: *Pass segments unavailable more than 5 times between cycles 82 and cycle 92. The color indicates the occurrence of unavailability*

Finally, the list of instrument and platform events is available in part 11. Apart from instrumental and platform events, up to 3% of measurements can be missing because of data generation problems at ground segment level: LRAC or PDHS level1 data generation problems or ingestion problems on F-PAC side.

4.2. Missing MWR data

The Envisat MWR exhibits nearly 100% (Dedieu et al., 2005) of availability since the beginning of the mission. However, MWR corrections can be missing in the GDRs due to data generation problems at ground segment level. When the Land/sea radiometer flag is set to land over ocean, it means that the radiometer data is missing. The percentage of missing MWR corrections over ocean has been plotted in Figure 5.
Some cycles are impacted by long period of radiometer missing, such as cycle 33, 58, 101-102 and 110 for the most impacted. Note that the beginning of the period (before cycle 15) is more concerned by lack of MWR data.

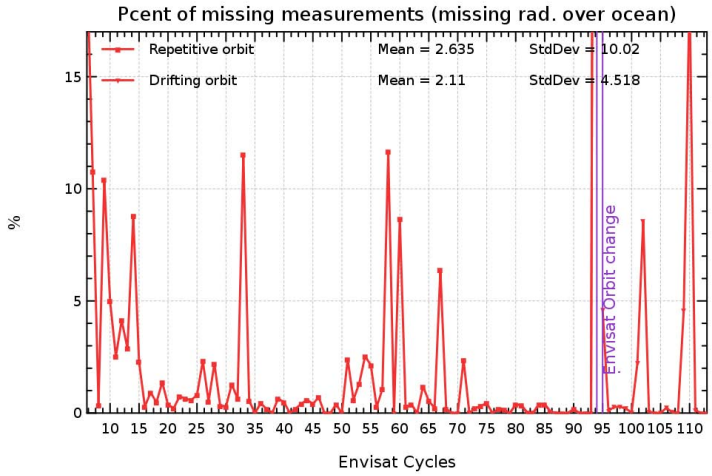

Figure 5: *Cycle per cycle percentages of missing MWR measurements*

4.3. Edited measurements

Data editing is necessary to remove altimeter measurements having lower accuracy. It consists in:
- First: removing data corrupted by sea ice.
- Then, removing measurements out of thresholds tuned for several parameters.
- The third step uses cubic splines adjustments to the ENVISAT Sea Surface Height (SSH) to detect remaining spurious measurements.
- The last step consists in removing entire pass where SSH-MSS mean and standard deviation have unexpected values.

4.3.1. Measurements impacted by Sea Ice

Since Envisat operates between 82N and 82S of latitude, sea ice detection is an important issue for oceanic applications. In the GDR, an ice flag is available but for CalVal purpose, a more severe method of flag was developped to get rid of any spurious data during validation phase. A study performed during the validation phase showed that the combination of altimetric and radiometric criteria was particularly efficient to flag most of the data over ice. The method is described in detail in (Faugere et al, 2003 [44]). We employ the peakiness parameter (Lillibridge et al, 2005 [69]) in conjunction with the MWR- ECMWF wet troposphere difference which appears to be a good means to complement the peakiness parameter in all ice conditions.

The ratio of flagged measurements over ocean is plotted on Figure 6.

In September 2007 (cycles 61-62) and 2011 (cycles 106-107) occured lower values of flagged data for the Northern Hemisphere zone (see blue curve Figure 6), due low ice extend records.
This was observed by different Envisat instruments including its RA2 altimeter. For the first time, an altimeter satellite could observe open ocean surfaces up to 82°N above North East Siberia during September-October 2007. Inaccurate Mean Sea Surface or tide models in this area might explain low SLA performances. See further details on http://www.aviso.altimetry.fr/en/

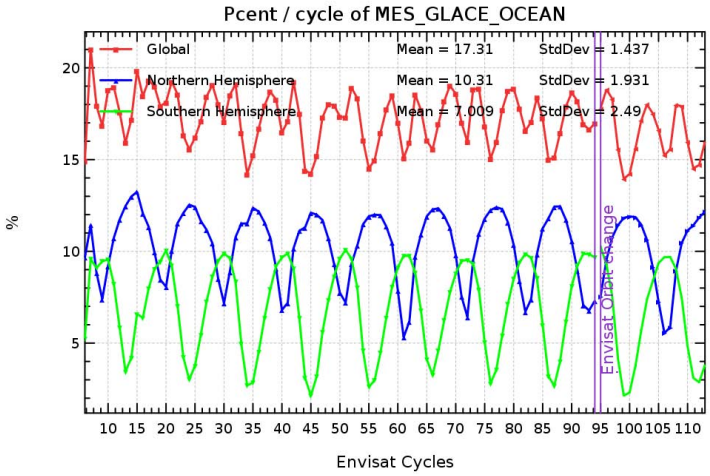

Figure 6: *% of edited points by sea ice flag over ocean*

applications/ice-and-cryosphere/sea-ice/arctic-sea-ice-extent-as-observed-by-envisat-altimeter.html.

A record-breaking maximum of flagged data also occurred for the Southern Hemisphere zone around cycles 95-96 (end of 2010), see green curve Figure 6.

4.3.2. Editing by thresholds

The second step of the editing procedure consists in using thresholds on several parameters. The minimum and maximum thresholds used in the routine quality assessment are given in table 1.

Parameter	Min thresholds	Max thresholds
Sea surface height (m)	−130	100
Variability relative to MSS (m)	−2	2
Number of 18Hz valid points	10	–
Std deviation of 18Hz range (m)	0	0.25
Off nadir angle from waveform (deg2)	−0.200	0.160
Dry troposphere correction (m)	−2.500	−1.900
Inverted barometer correction (m)	−2.000	2.000
MWR wet troposphere correction (m)	−0.500	0.001
Dual Ionosphere correction (m)	−0.200	−0.001
Significant waveheight (m)	0.0	11.0
Sea State Bias (m)	−0.5	0
Backscatter coefficient (dB)	7	30
Ocean tide height (m)	−5	5
Long period tide height (m)	−0.500	0.500
Earth tide (m)	−1.000	1.000
Pole tide (m)	−5.000	5.000
RA2 wind speed (m/s)	0.000	30.000

Table 1: *E*diting criteria

The thresholds are maintained constant throughout the ENVISAT mission, so that monitoring the number of edited measurements allows a survey of data quality. The percentage of edited measurements over ocean for the main altimeter and radiometer parameters has been plotted in Figure 7.
For almost all the plots, Cycle 6 presents high values of edited percentage. This is probably due to the instrument tests (shift of band emission, see cyclic report...) and to the small amount of available data (only 242 passes produced over 1002). Similarly, cycles 95 and 96 have few data

(orbit change maneuvers). This metric is not fully relevant for these cycles.
The RMS of elementary measurements has the strongest ratio among the altimeter parameters, more than 1% in average with a slight annual oscillation probably due to sea state seasonal variations.
The number of elementary measurements has a surprisingly low ratio compared to other missions except for cycles 14 and 20 when wrong configuration files were uploaded on-board after a RA-2 event.
The square of the off-nadir angle derived from waveforms leads to very stable editing ratio. Variations of this parameter can reveal actual platform mispointing, if any, but can also reveal waveform contamination by rain or by sea-ice. It is indeed computed from the slope of the waveform trailing edge. No seasonal signal is visible which may prove that the sea-ice detection method is efficient. Note also a small decrease of the value after the orbit shift, as already reported in the commissionning phase and stressed at ESA QWG Meetings 16 and 17.
The dual frequency ratio shows a very slight increasing trend from cycles 15 to 65 until the S-Band drop (on A-Side cycle 65 and during cycle 47-48 on B-Side configuration).
The editing on Ku-band SWH and sigma0 threshold are stable, though slightly higher than for historical data processing because the null SWH class now includes more data.
Concerning MWR ratios, it presents a significant annual signal. This signal was investigated and shown to be due to a residual annual signal in the ice coverage of Artic shelf.

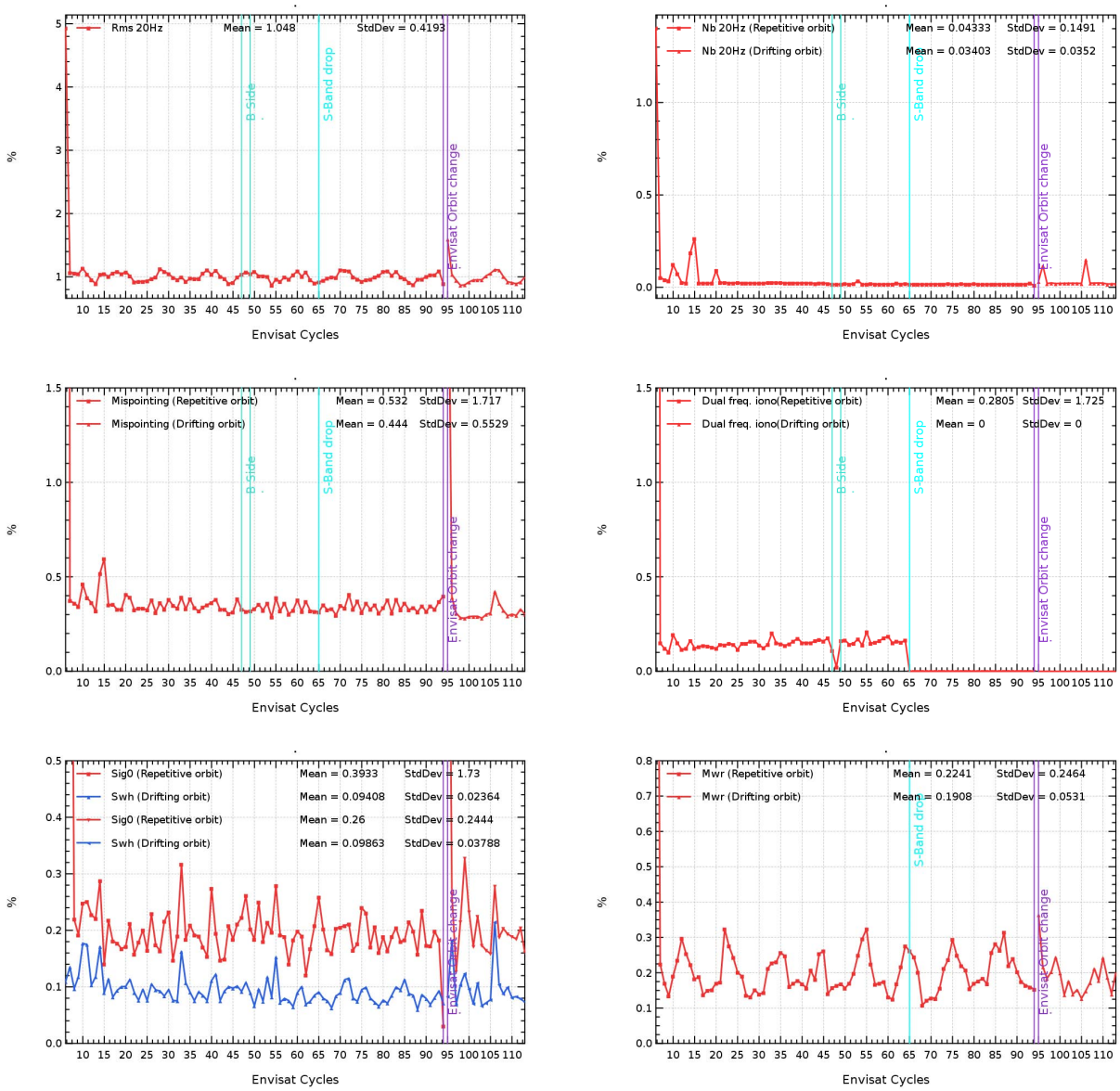

Figure 7: *Cycle per cycle percentages of edited measurements by the main Envisat altimeter and radiometer parameters:* ***Top-Left****) Rms of 20 Hz range measurements > 25 cm,* ***Top-Right****) Number of 20-Hz range measurements < 10,* ***Middle-Left****) Square of off-nadir angle (from waveforms) out of the [-0.2 deg2, 0.16 deg2] range,* ***Middle-Right****) Dual frequency ionosphere correction out of [-40 , 4 cm],* ***Bot-Left****)Ku-band Significant wave height greater than 11 m, Ku band backscatter coefficient out of the [7 dB, 30 dB] range,* ***Bot-Right****) MWR wet troposphere correction out of the [-50 cm, -0.1 cm] range.*

4.3.3. Editing on SLA

It is necessary to apply additional editing criteria on SSH-MSS differences in order to remove remaining spurious data. The first criterion consists in removing measurements with SSH-MSS greater than 2m. The second criterion was necessary to detect measurements impacted by

maneuvers. Maneuvers are necessary to compensate the effect of gravitational forces but can have a strong impact on the orbit quality. Two types of maneuvers are operated to maintain the satellite ground track within the +/-1km deadband (and +/-200m after cycle 54, see 8) around the reference ground track: in-plane maneuvers, every 30-50 days, which only impact the altitude of the satellite and out-of-plane maneuvers, three times a year, to control the inclination of the satellite (Rudolph et al., 2005). The out-of-plane maneuvers are the most problematic for the orbit computation. The second criterion consists in testing the mean and standard deviation of the SSH-MSS over each entire pass. If one of the two values, computed on a selected dataset, is abnormally high, then the entire pass is edited.
Note that the cross-track deadband can't be computed on drifting phase because of the lack of theoretical track (see 8).

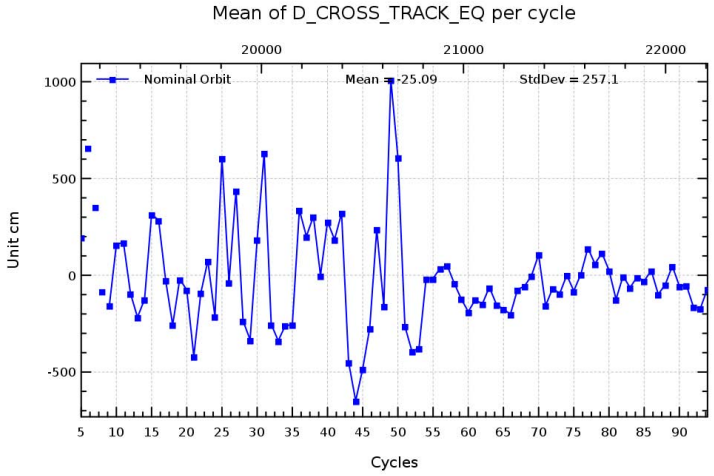

Figure 8: *Cross track deadband measured at equator by comparison to a theoretical track before the drifting phase.*

A specific study has been performed to determine how to compute the statistics, and what threshold should be applied. The statistics have to be computed on very stable area. The criteria for selecting the area and the thresholds are:

- The latitude: the range value can be degraded near the ice, despite the use of the ice flag. Moreover, the MSS is less accurate over 66 $^\circ$, as it has been computed without Topex, Jason-1 and Jason-2 data.
- The oceanic variability: the standard deviation of SLA can be very high because of the mesoscale variability. Areas with high oceanic variability have to be removed to detect the abnormally high standard deviation.
- The bathymetry and distance from the coast: A lot of corrections (tides for example) are less accurate in low bathymetry areas and near the coast (Japan sea).
- The sample: The statistic have to be computed on a significant number of points

All those criteria have been tested and combined as part as a specific study in a previous yearly report. The conclusion is that two criteria are needed:

1st criteria:
for small portion of pass (less than 200 points) the sample is not big enough to compute reliable statistic. The selection must not be severe: Selected areas: |latitude|<66 $^{\circ}$, variability<30cm, bathymetry>1000m, distance to coast>100km Threshold: 30 cm on mean and standard deviation
2nd criteria:
for other passes Selected areas: |latitude|<66 $^{\circ}$, variability<10cm, bathymetry>1000m, distance to coast>100km Threshold: 15 cm on mean and standard deviation

The percentage of edited measurements over ocean on these criteria has been plotted in Figure 9. On cycles 11, 12, 21 and 26, several full passes have been edited because of bad orbit quality related to out-of-plane maneuver or lack of Doris data (cycle 11).The special operation on RA-2 Chirp Bandwidth impacted the SSH editing ratio on cycle 47. Most of the data edited on this criteria are due to the jumps noticed on reprocessed USO correction (several hundreds of meters) and identified under the anomaly report number [IDEAS-PR-11-05520].
On cycle 56 an USO anomaly recovery, occurred at the beginning of cycle and impacted the SSH statistic editing per pass. The behavior of the Ultra Stable Oscillator (USO) clock frequency on this cycle is chaotic. The transitions between anomaly and normal mode has been very straight and the USO correction does not allow us to well correct some passes.

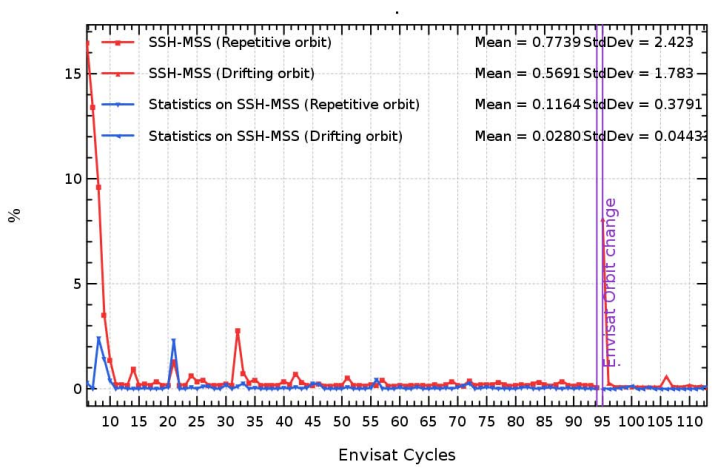

Figure 9: *SSH-MSS out of the [-2, 2m] and edited using thresholds on the mean and standard deviation of SSH-MSS on each pass*

As plotted above, some cycles are particularly impacted by a substantial editing on the two criterion previously defined.

For cycle 6 to 9, different adjustments performed during this calibration phase have impacted the homogeneity of processing.
During **cycle 6**, 26 tracks are edited on the SLA criterion, on only 242 workable passes (760 tracks missing). Data was impacted by a DORIS event, orbit was extrapolated for this period with degraded performances. The **cycle 7** was impacted by some RA2 bandwidth tests, on 2002/06/18 and between 2002/06/26 and 2002/06/29 (20MHz for these two periods, 22 tracks rejected). For this cycle 95 tracks are impacted by wrong USO correction values too.

For **cycles 8 and 9**, respectively 90 and 33 tracks are rejected on this two SLA criterion, because of wrong USO correction.
For **cycle 14**, 6 passes (from 20/03/2003 11:07:17 to 20/03/2003 16:08:08) are entirely edited on SLA threshold. For these passes, USO correction was found to reach abnormal values (more than 150m) directly impacting the SLA.
Cycle 21 is impacted by a combination of events; 10 passes between 2003/10/27 and 2003/10/30 are impacted by short period of wrong USO correction applied to the range. During this cycle, high values of SLA were also observed consecutively to two altimeter restarts (pass 242 to 247, and pass 366 to 389). The SLA during instrument heating seemed to be badly corrected by the IPF USO correction, whereas the F-PAC USO expertise correction looked correct for these high values. Finally, this cycle is impacted by an exceptionally high solar activity (two strong magnetic storms on 2003/10/30 and 2003/11/21), degrading the orbit quality and then the SLA, which is rejected for 16 tracks. For cycle 21, the data rejected on SLA criterion approximates 3.5%.
During **cycle 32**, 25 tracks are entirely rejected by SLA values. These passes are impacted by jumps of several meters visible on the SLA, caused by wrong USO correction periods. This cycle is the most impacted by SLA values out of thresholds on the whole reprocessing period caused by wrong USO correction, except cycles 6 to 9.
On cycle 106, a mishandling of the USO counter clock impacts 4 tracks.
For the last cycles of the Envisat time serie (108 to 113), no particular editing has been noticed.

Note that the correction developed for expertise in F-PAC is not affected by these jumps. Yet the impact is rather weak: on the whole mission, around 300 tracks, were impacted by this anomaly (including around 200 before cycle 10).

5. Long term monitoring of altimeter and radiometer parameters

All GDR fields are systematically checked and carefully monitored as part of the Envisat routine calibration and validation tasks. However, Ku-band parameters are mainly presented here, as they are the most significant in terms of data quality and instrumental stability. Furthermore, all statistics are computed on valid ocean datasets after the editing procedure.

5.1. Number and standard deviation of 20Hz elementary Ku-Band data

As part of the ground segment processing, a regression is performed to derive the 1 Hz range from 20 Hz data. Through an iterative regression process, elementary ranges too far from the regression line are discarded until convergence is reached. The mean number and RMS of Ku 20Hz elementary data used to compute the 1Hz average are plotted in figure 10. These two parameters are nearly constant, which provides an indication of the RA-2 altimeter stability. The mean number of Ku 20Hz values over one cycle is about 19.97. This value is very high compared to other altimeters. It is almost not disturbed in wet areas or near the coast. The two drops on the Ku-band on cycles 14, 15 and 20 are due to wrong setting of the RA-2 just after recovery. Higher values correspond to higher waves occurring during the austral winter. The mean value is about 9.0 cm. This value represents a rough estimation of the 20 Hz altimeter noise (Zanifé et al. 2003 [117], Vincent et al. 2003a [115]). Assuming that the 20Hz measurements have uncorrelated noise, it corresponds to a noise of about 2 cm at 1Hz. It is consistent with the expected noise values.

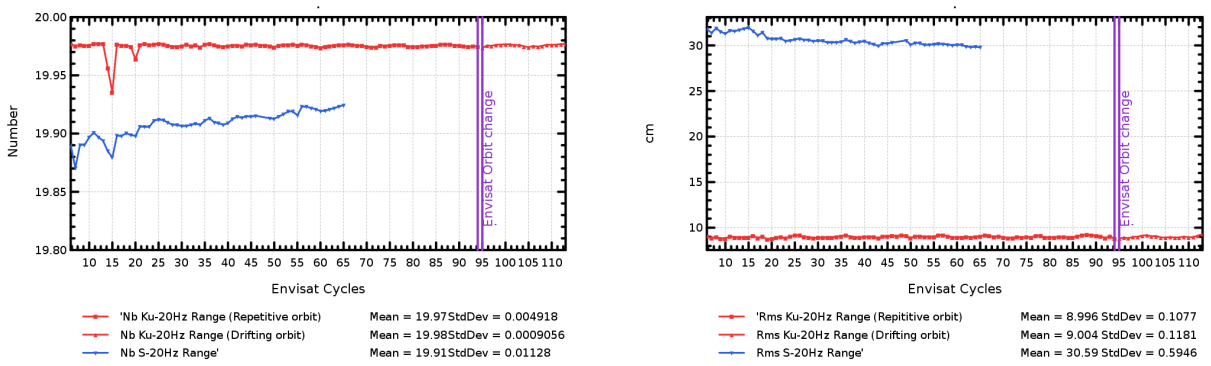

Figure 10: ***left)*** *Mean per cycle of the number of 20 Hz elementary range measurements used to compute 1 Hz range.* ***right)*** *Mean per cycle of the standard deviation of 20 Hz measurements.*

The corresponding S-Band parameters have a less stable behaviour. The S-Band mean number and RMS of 20Hz measurements have respectively an increasing and decreasing trend. This drift, as well as the jump noticed around cycle 18 appearing on reprocessed data is not understood yet but should be investigated further (impact on the MSL drift at the beginning of the period?).

The histogram of RMS of Ku Range on cycle 112 is plotted in figure 11.

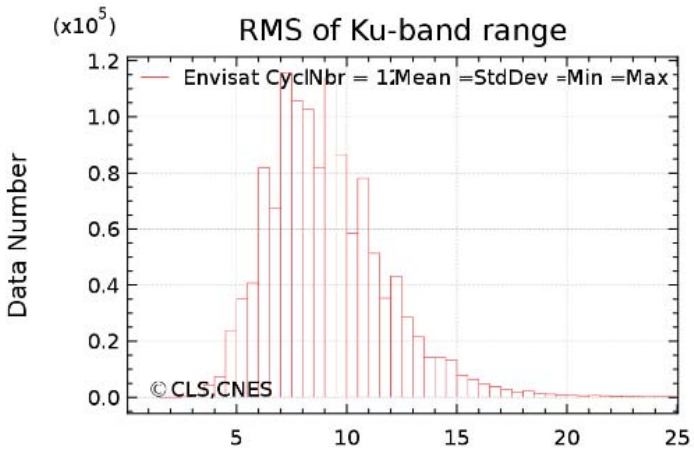

Figure 11: *Histogram of RMS of Ku range (cm). Cycle 112 .*

5.2. Off-nadir angle from waveforms

The off-nadir angle is estimated from the waveform shape during the altimeter processing. The square of the off-nadir angle is plotted in Figure 12. The mean value presents a slight decreasing trend up to cycle 65 around a value of 0.005 deg2.
Note as well that a smaller value is noticed for the cycle 48, for which altimeter was turned to its B-Side for a short period (cf. details in part 3.1).
At the end of the period, as noticed during the mini commissionning phase and QWG 17 the mispointing stabilises at a slight lower value than before the orbit change. No reason has been found to explain this behaviour. However the value is so low that it has no impact in terms of data quality.

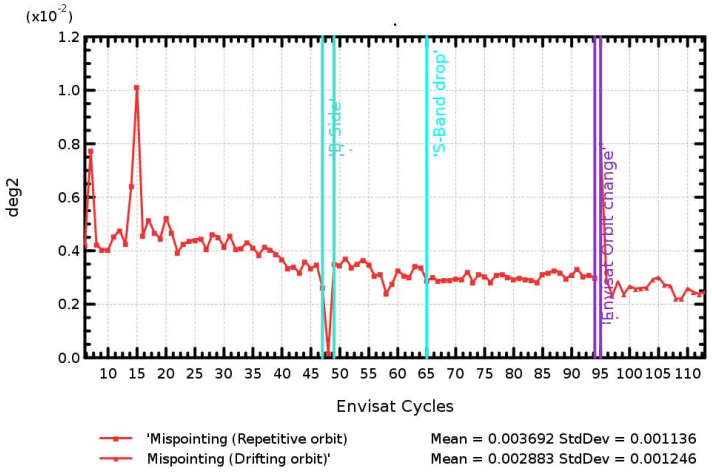

Figure 12: *Mean per cycle of the square of the off-nadir angle deduced from waveforms (deg^2).*

The histogram of the squared mispointing is plotted in figure 13.

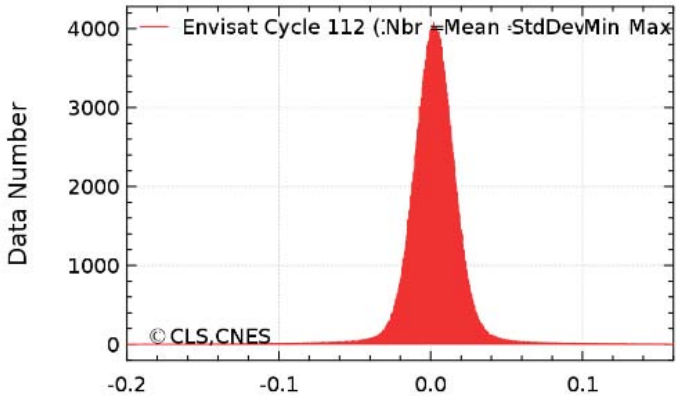

Figure 13: *Histogram of off-nadir angle from waveforms (deg²). Cycle 112 .*

5.3. Significant Wave Height

The cycle by cycle mean and standard deviation of Ku and S-Band SWH are also plotted in figure 14. Its monitoring reflects sea state variations (with a clear annual signal). The mean value of Ku SWH is 2.5 m. The S-Band mean SWH is drifting and rather lower (around 2m). The cycle by cycle mean of Envisat-Jason-1 differences is plotted in Figure 14.
These differences are quite stable (or slightly drifting before cycle 65) and centered around 0 since the V2.1 evolution on Envisat side (processing parameter modification (SigmaP)). Note that a study was performed on the SWH to understand the behavior of small waves, considered, by some users as degraded (see [15]).
As for range parameters, some strange behaviours on S-Band SWH are also noticed (see Figure 14): drifts on the standard deviation notably and odd behaviour before 2004 (cycle 22) on the mean.

The histogram of Ku SWH for the last complete cycle is plotted in figure 15.

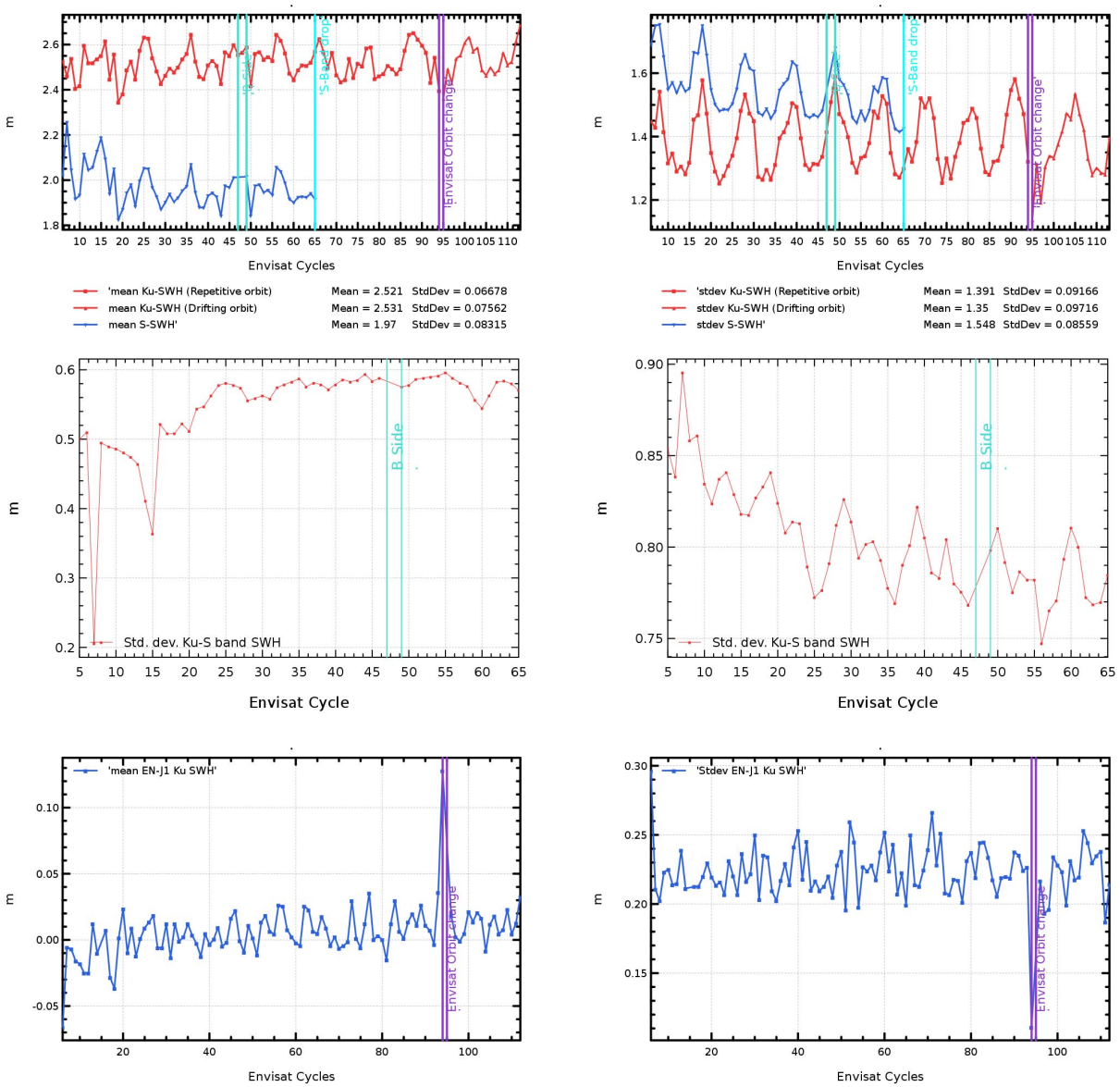

Figure 14: *Global statistics (m) of Envisat Ku and S SWH* ***top****) Mean and Standard deviation.* ***Middle:*** *Mean and standard deviation of Ku-S band SWH* ***bottom****) Mean Envisat-Jason-1 Ku SWH differences at 3h EN/J1 crossovers.*

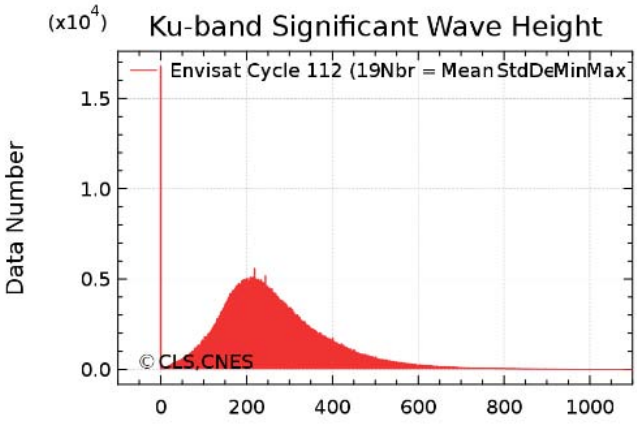

Figure 15: *Histogram of Ku SWH (m) Cycle 112 .*

5.4. Backscatter coefficient

The cycle by cycle mean and standard deviation Ku and S-Band Sigma0 are plotted in Figure 17, until 2011. Note that a -3.5 dB bias has been applied (Roca et al., 2003 [91]) on the Ku-band Sigma0 in order to be compliant with the wind speed model (Witter and Chelton, 1991 [116]). The mean values in Ku band are stable, around 11 dB. The mean difference between Envisat and Jason-1 Ku-band Sigma0 is -3 dB. This high value is explained by the fact that, Envisat Sigma0 value has been biased and not Jason-1. This mean difference has increased by 4.10-2dB/year between cycles 38 and 140 Jason-1 (corresponding to cycle 13 to 41 of Envisat) and remains constant afterwards. This drift was checked to be unchanged after correcting it from the atmospheric attenuation computed with an homogeneous reprocessed set of brightness temperature. These sigma0 differences obviously impact the wind consistency between the two satellites. Note that the wind from the ECMWF model, which does not assimilate Jason-1 data, shows a very good agreement with the Jason-1 wind with a slope close to 6 cm/s/yr whereas Envisat wind trend is much lower, 1.3cm/s/year (see [4]). This trend difference could mean that the Envisat wind slightly drifts. Yet caution must be brought to this as Envisat is rather homogeneous to ERA-Interim reprocessed data, ECMWF solution free of most jumps and discontinuities seen in the operational model (see 16)... The global stability of this parameter was extensively studied in Ablain et al. 2012 submitted in Marine Geodesy (see [10]) and summurized in 2011 Jason-1 yearly report ([6], available on Aviso web site).
A slight decrease of Ku Sigma0 standard deviation for Envisat/Jason-1 difference is observed after orbit change.

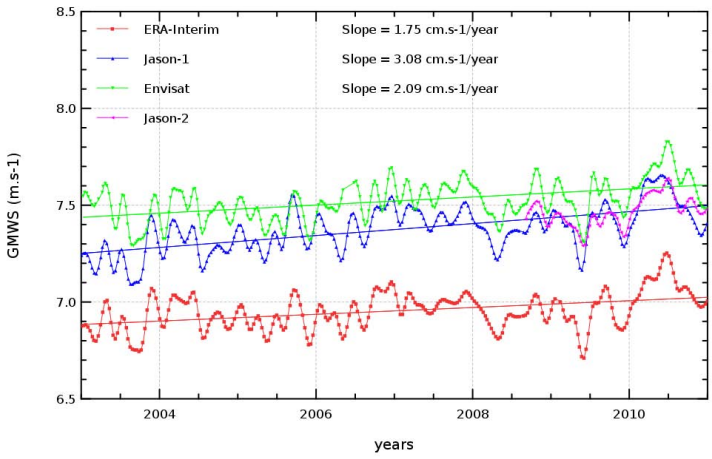

Figure 16: *Wind speed from different sources (EN, J1, J2 and ERA-Interim model).*

Histograms of Ku Sigma0 for the last complete cycle is plotted in figure 18. The Ku Sigma0 histogram has a good shape.

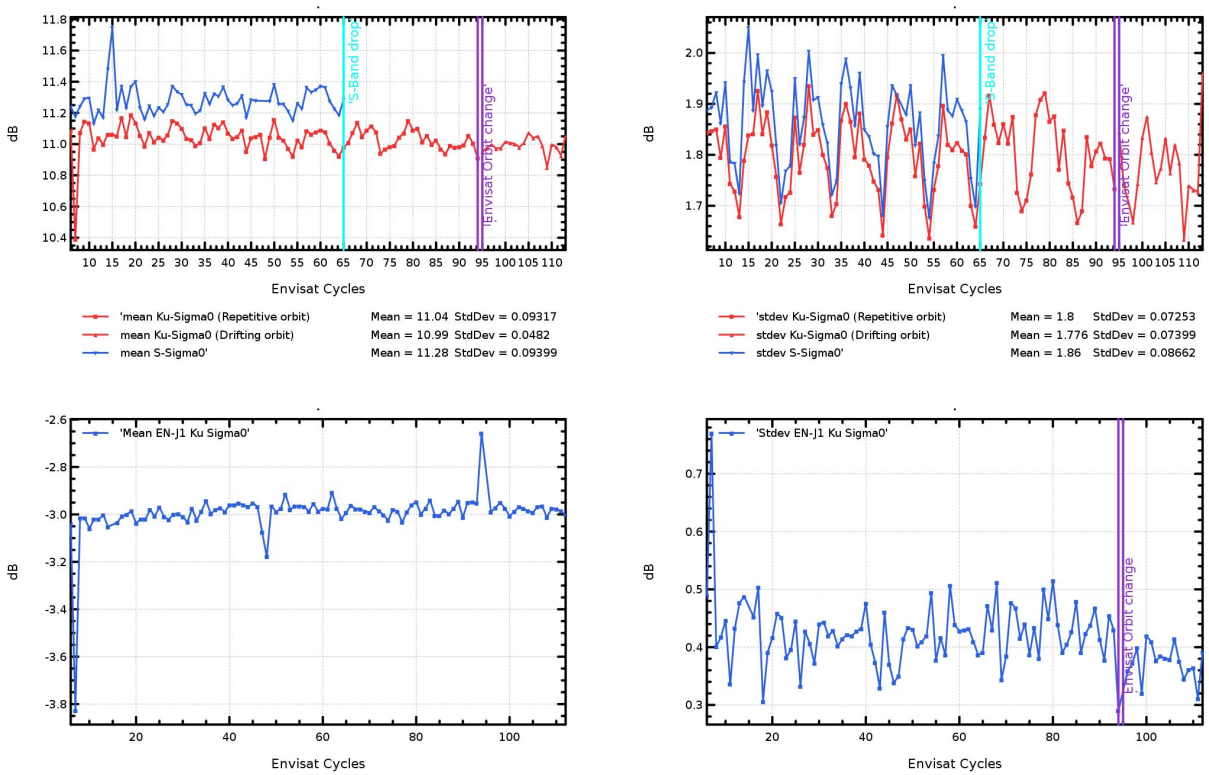

Figure 17: *Global statistics (dB) of* ***Top****) Envisat Ku and S Sigma0 Mean and Standard deviation.* ***Bottom****) Mean Envisat-Jason-1 Ku Sigma0 differences at 3h EN/J1 crossovers.*

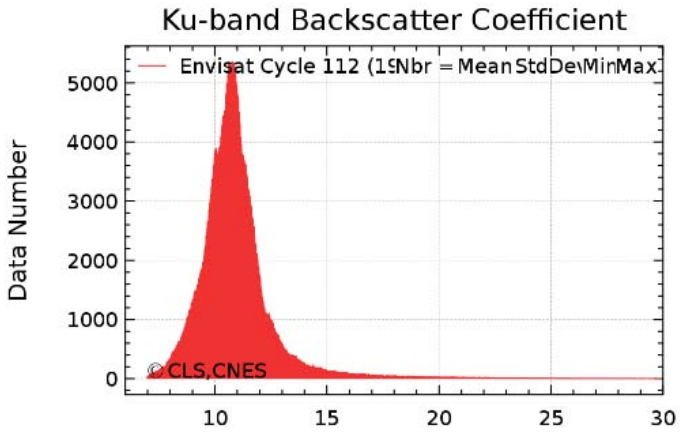

Figure 18: *Histogram of Ku Sigma0 (dB). Cycle 112 .*

5.5. Dual frequency ionosphere correction

As performed on TOPEX (Le Traon et al. 1994 [65]) and Jason-1 (Chambers et al. 2002 [32]) it is recommended to filter dual frequency ionosphere correction on each altimeter dataset to reduce noise. A 300-km low pass filter is thus applied along track on the dual frequency ionosphere correction. Note that in 2012, a new filtering method was developped in order to improve the current filtering process. This is developped in [16] and could enable to add this filtered field directly in the GDR, which is not feasible with the current method.
As previously mentioned, the JPL GIM ionosphere corrections are computed to assess the dual frequency altimeter based ionosphere correction. After the S-Band loss of Envisat (January 17th 2008), it was prefered to the DORIS correction also available in the products to replace the bifrequency correction for its better performences. The same GIM model is used to compute the GIM corrections on Envisat and Jason-1. The quality of Envisat's ionosphere correction can thus be assessed by monitoring the dual-frequency -GIM based ionosphere correction on Jason-1. The cycle by cycle mean of dual frequency and JPL GIM ionosphere correction are also plotted in figure 19. Different trends are observed on the two curves.

The cycle by cycle mean of dual frequency and JPL GIM ionosphere correction are plotted in figure 19. The mean value of the two corrections clearly follows the solar activity periods (11 year solar cycle): decreasing from the beginning of Envisat mission to 2008 and increases again since late 2009, after a short stable period. The mean differences is surprisingly stable around -0.8 cm whereas Jason-1 GIM-Dual presents a bigger bias for higher solar activities. This bias increasing for high values of ionospheric correction is also noticed, on Envisat, when comparing ascending (night time) and descending passes (in the daytime). This would suggest that the beginning of the mission is affected by an error which should be further investigated.
The standard deviation of the difference is plotted in figure 19. Here as well, the first year seems to have a chaotic behavior compared to Jason-1. Notice that, in this reprocessed series, a homogeneous sea state bias (SSB) has been used to correct the Ku and S-Band Ranges (Labroue 2004 [59]).

Concerning the discrepancies between both missions, note that, in terms of noise, the higher noise for Jason-1 is due to an higher noise in the C band (used for Jason-1 bifrequency ionosphere) than in S-Band (used for Envisat one). The filtering step applied on both ionospheres from the products enable to have comparable noise level for both missions. In terms of bias, differences are likely due to the difference of altitude for both missions, but the stability of Envisat ionosphere difference (Bifrequency-GIM) can also be seen as an anomaly at the beginning of Envisat mission (before cycle 22), reducing the dependency between the absolute value and the bias on this correction (observed on Jason-1). This would deserve more investigations.

In 2012, the solar activity continued to increase which has an impact on the data quality. The mean difference of SSH at cross-over is polluted by the signature of the ionospheric signal with a mid-scale impact.

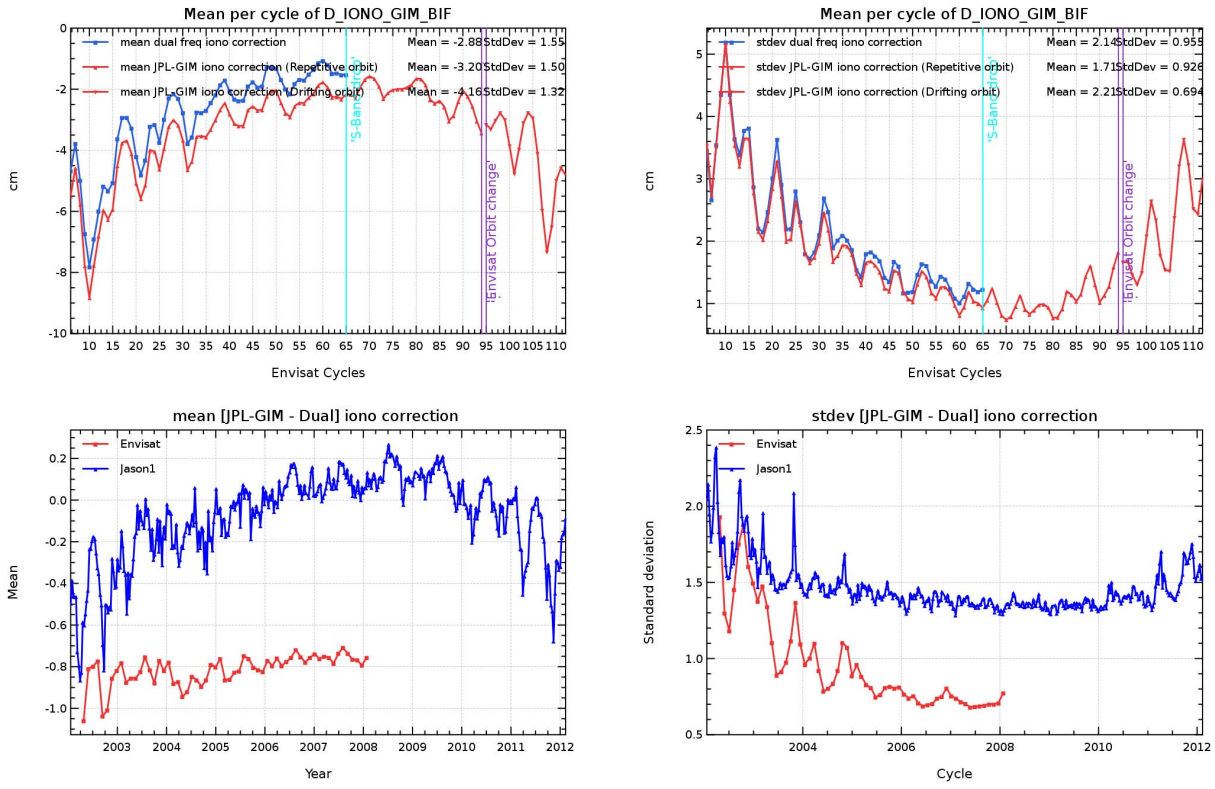

Figure 19: *Comparison of global statistics of Envisat dual-frequency and JPL-GIM ionosphere corrections (cm).* ***Top****) Mean and standard deviation per cycle of Dual Frequency and GIM correction.* ***Bottom****) Mean and standard deviation of the differences for Envisat and Jason-1*

5.6. MWR wet troposphere correction

A neural network formulation is used in the inversion algorithm retrieving the wet troposphere correction from the measured brightness temperatures (Obligis et al., 2005 [79]). As an example, the scatter plot of MWR correction according to ECMWF model for cycle 112 (last complete cycle) and 113 is given in figure 20.

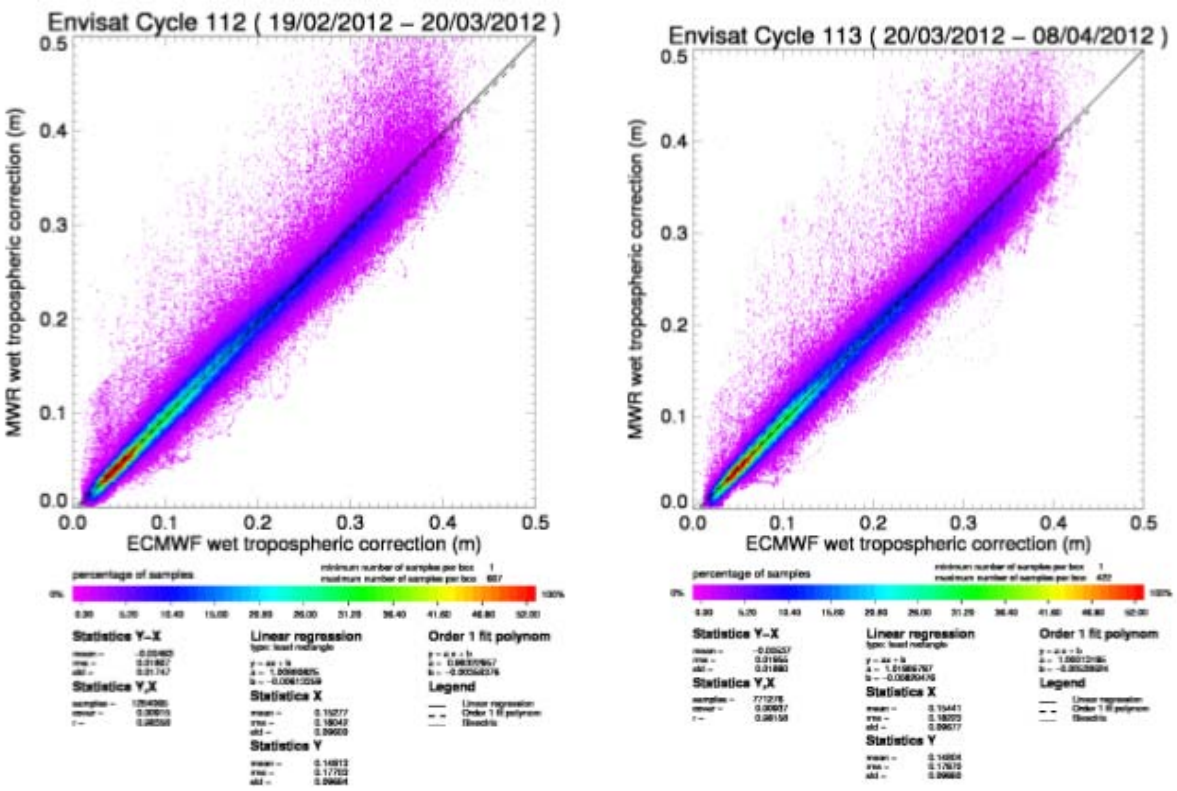

Figure 20: *Scatter plot of MWR correction according to ECMWF model (m) (cycle 112 & 113)*

Since the beginning of the mission, the stability of the instrumental parameters has been closely looked at. In particular, different behavior is observed depending on the brightness temperature values. A complete monitoring of all the radiometer parameters is available in the cyclic Envisat Microwave Radiometer Assessment available at http://earth.esa.int/pcs/envisat/mwr/reports/ ([86]). Mean and standard deviation of Radiometric correction for Jason1, Jason2 and Envisat is plotted in figure 21 (top). It is also completed by (MWR-ECMWF model) monitoring, enlighting finer jumps and discrepancies in figure 21 (bottom). This difference is not really stable, though the global mean remains small. An annual signal of about 1.5mm of amplitude can be seen. Successive jumps on the ECMWF side (marked out by vertical lines on the plots (see ECMWF web site [37])) also have an impact on the stability of the difference [radiometer wet tropospheric correction-ECMWF model]. To minimize the unhomogeneities on model side, ERA Interim is taken as a reference on figure 22. The standard deviation is very much stabilized but the annual signal on the mean remains.

Note that the 1.8cm of standard deviation is greater than the value obtained before the repro-

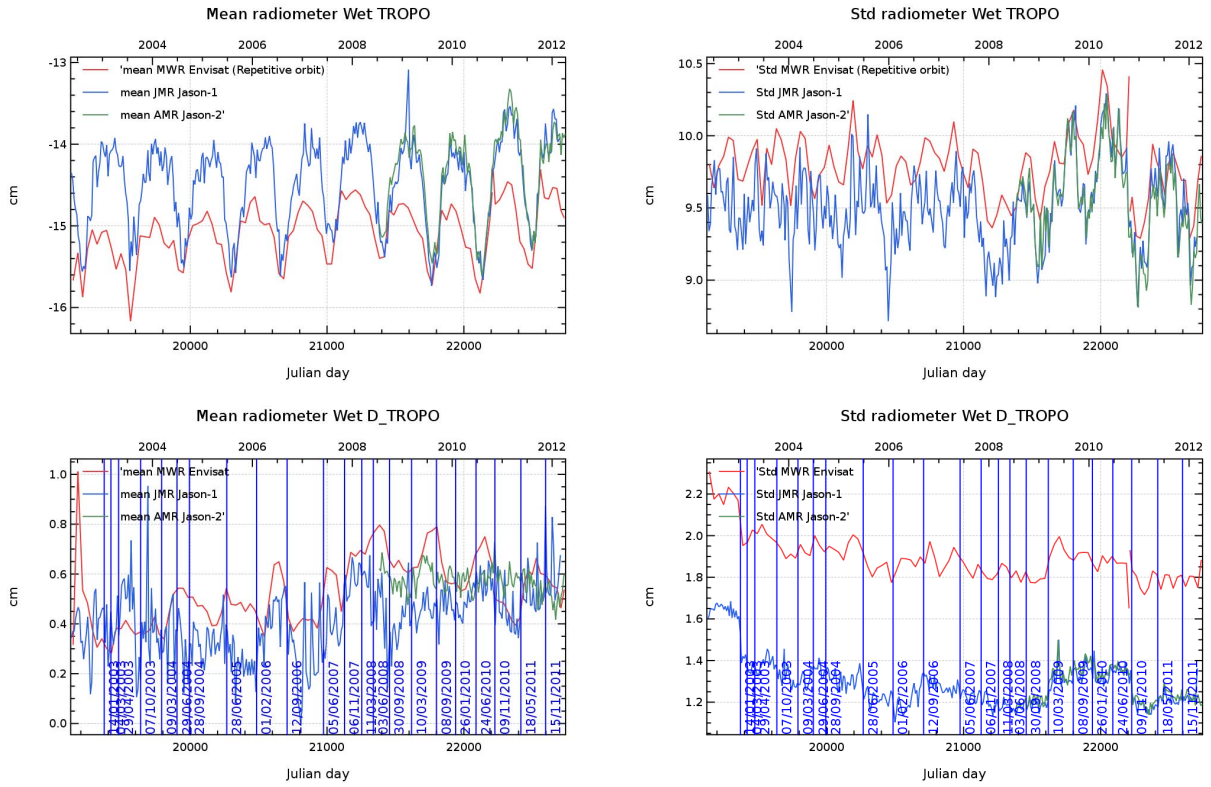

Figure 21: *Comparison of global statistics of Envisat MWR and ECMWF wet troposphere corrections (cm).* ***top****) Mean and standard deviation per cycle of MWR, JMR and AMR corrections* ***Bottom****) Mean and standard deviation per cycle of the differences versus ECMWF model. Vertical lines represent the major events.*

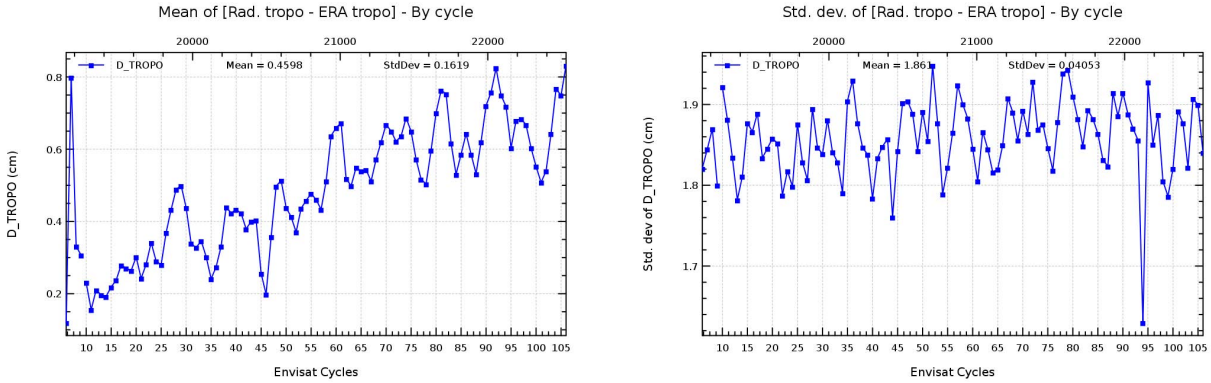

Figure 22: *Mean and standard deviation per cycle of the differences of MWR correction versus ERA-Interim*

cessing (1.6cm). In fact, the analysis made after reprocessing enabled to evidence a degradation of this correction visible on SSH performance at crossovers (see [16]). A new wet tropospheric correction has been developped in 2013 and does not present anymore this degradation (see 8.1.1.). Particularly the comparison with the wet tropospheric models is described in 8.1.1.4.).

6. Sea Surface Height performance assessment

One of the main objectives of the Calibration and Validation activities is to assess the performance of the whole altimeter system. This means that the quality of each parameter of the product is evaluated, in particular if it is likely to be used in the Sea Surface Height (SSH) computations. Conventional tools like crossover differences and repeat-track analyses are systematically used in order to monitor the quality of the system.

6.1. SSH definition

The standard SSH calculation for Envisat is defined below.

$$SSH = Orbit - Altimeter\ Range - \sum_{i=1}^{n} Correction_i$$

$$\begin{aligned}
\sum_{i=1}^{n} Correction_i \;=\; & Dry\ troposphere\ correction : new\ S1\ and\ S2\ atmospheric\ tides\ applied \\
+\; & Combined\ atmospheric\ correction :\ Dynamic\ atmospheric\ correction \\
+\; & and\ inverse\ barometer \\
+\; & Radiometer\ wet\ troposphere\ correction \\
+\; & ionospheric\ correction\ /GIM\ model\ after\ cycle\ 64 \\
+\; & Non\ parametric\ sea\ state\ bias\ correction \\
+\; & Geocentric\ ocean\ tide\ height \\
+\; & Solid\ earth\ tide\ height \\
+\; & Geocentric\ pole\ tide\ height
\end{aligned}$$

As said in 3.2.1., the plots presented here concern the whole Envisat serie, on a basis of the V2.1 standard, improved for some terms, as explained further.

The following table 2 presents the updates computed after reprocessing to improve the SSH performance. Some of these updates have ever been analysed in previous yearly report and a part of them were studied this year, presented in this report.

Altimetric correction	V2.1 product	Alternative correction	Analysed updates
Orbit standard	GDR-C	GDR-E	Impact of the new 10-days gravity field (see 8.2.1.)
Range	/	PTR	/
			.../...

Altimetric correction	V2.1 product	Alternative correction	Analysed updates
MWR Wet tropo.	After reprocessing degraded version	V2.1b (see 8.1.1.)	/
Ionospheric corr.	Dual frequency filtered iono.	Iteratively filtered iono. (see 8.1.2.)	Impact of Envisat Altitude in GIM model computation (see 8.2.2.)
Sea state bias			
Ocean tide	GOT 4V7	GOT 4V8 / GOT 4V10	Performance assessment of GOT 4V8 tide model (see 8.1.3.)

Table 2: *A*ltimetric correction updates

6.2. Improved performances of GDR: anticipating the next reprocessing

SSH crossover differences are computed on a one-cycle basis, with a maximum time lag of 10 days, in order to reduce the impact of ocean variability which is a source of error in the performance estimation. The mean of crossover differences represents the average of SSH differences between ascending and descending passes. This difference can reflect orbit errors or errors in geophysical corrections but also includes geophysical variability. The fact that Envisat is Sun-synchronous can play a role since the ascending passes and descending passes respectively cross the equator at 10pm local time and 10am local time. Thus all the parameters with a daily cycle can induce errors resulting in ascending/descending differences. The error observed at crossovers can be split into two types: the time invariant errors and the time varying errors.

In 2012 and 2013 V2.1 reprocessed dataset was enhanced on several aspects. The V2.1+ dataset is an anticipation of future reprocessing in an expertise database maintained at CLS and for DUACS purpose. This dataset brings together the following altimetric corrections updates:
- PTR with an impact on Global Mean Sea Level (see [15] and Ollivier 2012 et al.);
- POE standard with an impact on Regional Mean Sea Level (see [15] and Ollivier 2012 et al.);
- Sea Surface Bias with an impact on performances at crossovers and on mean of SLA (see [16], particular investigation on SSB).
- The GOT 4V8 Ocean Tide Height is now the new correction used in SSH computation (see 8.1.3.)
- The iterative filtered ionospheric correction is now used in SSH computation (see 8.1.2.);
- Finally, a new radiometer wet tropospheric correction has been developped by CLS experts team to correct the degradation of mesoscale error observed after reprocessing.This new correction is named V2.1b and is detailled in 8.1.1..

This last update is the one which has the greater impact on SSH quality at crossovers. The global impact of all these updates is analysed in the following part.

6.3. Global improvements of SSH quality

6.3.1. Estimation of performance: reduction of the mesoscale error

To estimate the performance of a new standard, the analyse is made on SSH behaviour using this updated correction compared to a reference correction. If we consider the SSH computation at monomission crossovers, we evaluate the relevance of altimetric data on crossed tracks, so at the same localisation in two different moments. If the crossover time selection is limited to 10 days and with some relevant selections (bathymetry, oceanic variability,...), we can consider that the satellite could see the "same" ocean surface in the "same" conditions, omitting the high or low frequency content and the related impacts on SSH data. With this method, we also estimate the quality of signal in terms of **mesoscale error**. The standard deviations of SSH at crossovers using a study or a reference standard are compared and gives us a good estimation of the mesoscale error potentially made.
In terms of presented results, the quality of SSH is said as "better" if the standard deviation of SSH at 10-days crossovers considering the new standard is reduced from the one computed with the reference standard (negative difference represented in green on the plots).

6.3.2. Envisat SSH quality: monomission analysis

6.3.2.1. Effect of Envisat Orbit change

The effect of the drifting orbit on Envisat is very weak and can hardly be evidenced on previous plots. It can however be evidenced when filtering some wavelength only as shown on zoom over 14 months on figure 23.

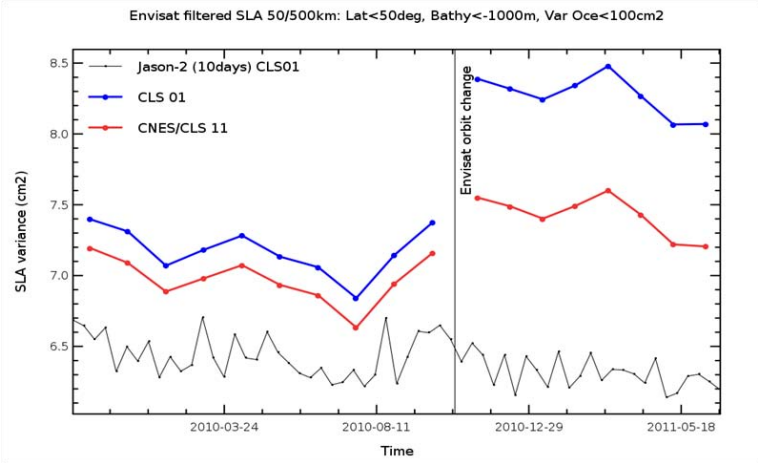

Figure 23: *Impact of the SLA reference out of the repeat track on the wavelength between 50km and 500km.*

6.3.2.2. Time varying SSH differences at crossovers

The variance of crossover differences conventionally gives an estimate of the overall altimeter system performance. Indeed, it gathers error sources coming from orbit, geophysical corrections, instrumental noise, and part of the ocean variability. The standard deviation of the Envisat SSH crossover differences has been plotted in Figure 24. Without any selection, a seasonal signal is observed because variations in sea ice coverage induce changes in ocean sampling by altimeter measurements. When only retaining deep ocean areas, excluding high latitudes (higher than 50 deg.) and high ocean variability areas, the standard deviation then gives reliable estimate of the altimeter system performances. In that case most of the cycles have a standard deviation between 5 and 6cm. But there are some exceptions that can be explained. Cycle 11 has a relative high value because of missing Doris data. Cycles 15 or before cycle 10 are higher because of the low number of crossover points. There are less than 10000 crossovers whereas other cycles lead to more than 20000. Cycle 21 has a strong value (6.8 cm) because of the combined effect of 2 maneuvers, intense solar activity between these 2 maneuvers, and lack of laser measurements between these two maneuvers.

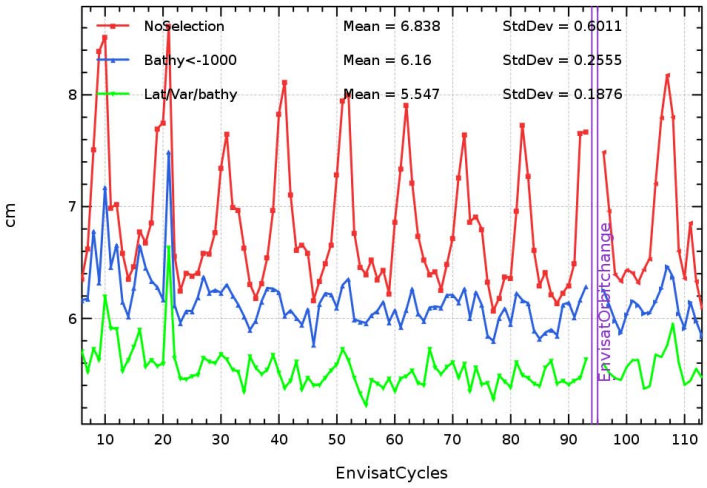

Figure 24: *Standard deviation (cm) of Envisat 10-day SSH crossover differences depending on data selection (with a maximum time lag of 10 days). Red: without any selection. Blue: shallow waters (1000 m) are excluded. Green: shallow waters excluded, latitude within [-50S, +50N], high ocean variability areas excluded.*

6.3.2.3. Regional analysis of mesoscale error

The mesoscale error estimation improvement is shown on figures 25 and 26 with reference to V2.1 and V1 respectivelly.

The variance of SSH at crossovers is globally descreased on the dataset with all the developped updates; the gain reaches 1.8cm^2 compared to the V2.1 dataset after reprocessing (for a selection far form coasts, latitudes$<$ 50 deg and low oceanic variability).

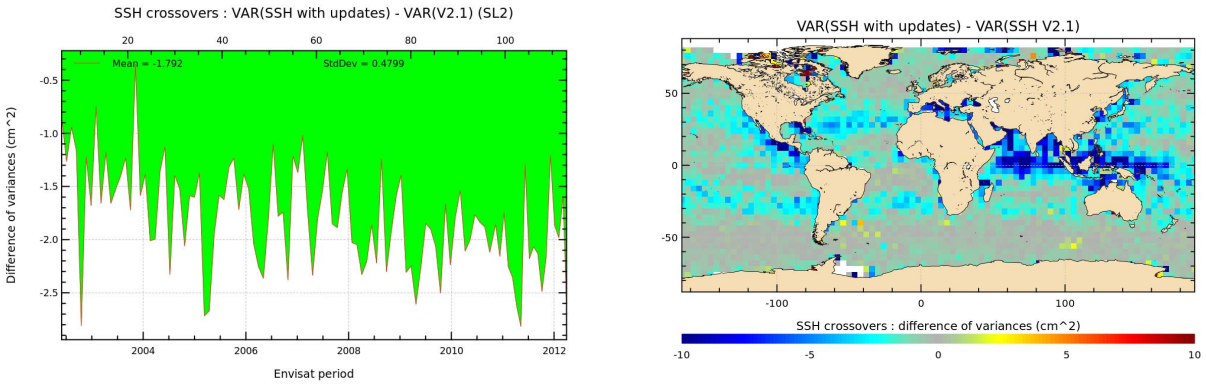

Figure 25: *Improvement of mesoscale precision, comparing V2.1+ updates to V2.1*

The comparison to GDR before reprocessing (V1) is showed on Figure 26. In this case, the gain reaches 3.2cm^2 for the same selection, and globaly distributed. This global gain is important and results from all the improvements developped for the reprocessing in 2011 and after, notably the last updates which will be taken into account in the next reprocessing.

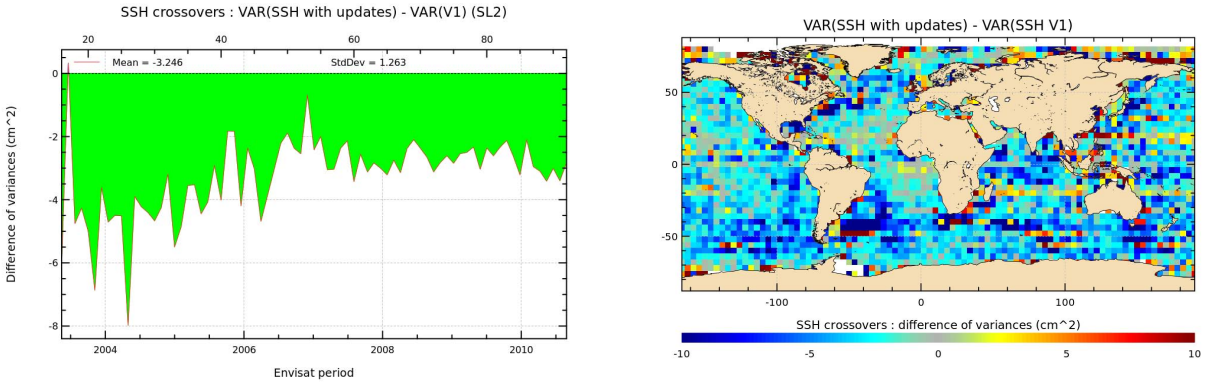

Figure 26: *Improvement of mesoscale precision, comparing V2.1 with updates (GDR-D orbits, F-PAC PTR, V2.1b wet tropospheric correction, iterative filtered iono, GOT 4V8 tide model) to V1 version (before reprocessing)*

6.3.3. Multimission performance analysis

6.3.3.1. Cross comparisons with Jason-1 and Jason-2

Intercalibration are made between Envisat and the Jason's missions to compare performance at crossovers. SSH for each mission is computed on the same area excluding latitudes higher than 50deg, shallow waters and using exactly the same interpolation scheme to compute SSH values at crossover locations. A step of average per box is also performed.

For the comparison with Jason-1 and Jason-2, the crossovers are taken into account in a limit of 10 days to avoid the effect of low frequency phenomenon. For Envisat/Jason-1 cross comparison, Envisat is considered as a primary mission which implies that the mean of SSH at crossovers is computed over the Envisat cycle duration (35/30 days). for Jason-2/Envisat, considering that Jason-2 is the primary mission, this mean is computed over 10 days. This difference of computation may have influence on the mean of standard deviation by cycle.
Figure 27 presents the maps of X-SSH mean per box for one Envisat cycle, computed on 35 days (cross comparison with Jason-1) or 10 days (cross comparison with Jason-2). We note that this mean per box can really differ from one box to the other, this phenomenon is notably visible on the mean computed over 10 days (27, right). With a mean over 35 days, long wave length effects are more visible and the standard deviation of X-SSH mean per box is lower than the one computed over 10 days, as you will see on figure 30.

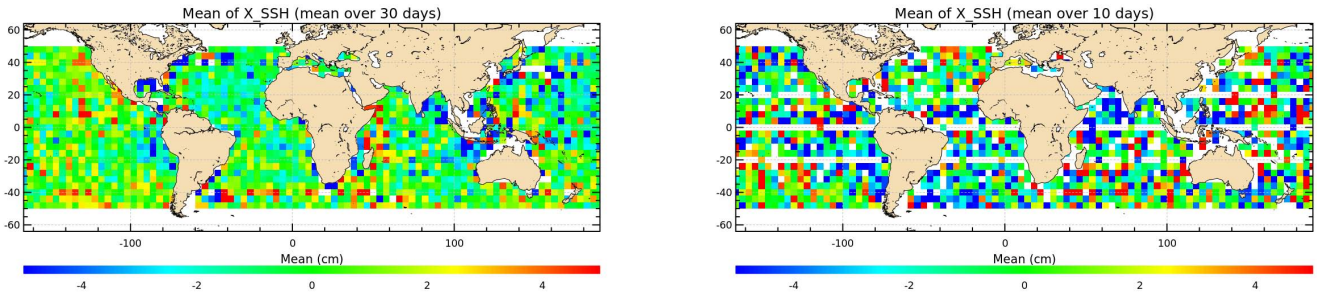

Figure 27: *Mean (cm) of X-SSH at Envisat monomission crossovers* ***Left****: from Envisat/Jason-1 cross-comparison (mean on 35 days)* ***Right:*** *from Jason-2/Envisat cross-comparison (mean on 10 days) , with 4 by 4 average per box and shallow waters excluded, latitude within [-50S, +50N], high ocean variability areas excluded.*

Figure 29 presents the mean of SSH difference at dual-crossovers using the ECMWF wet tropospheric model. A global bias of 37*cm* is observed between Envisat and Jason-1 (29, left). This bias is in agreement with the absolute calibration studies (see for instance Bonnefond et al. OSTST).
The Envisat/Jason-1 mean difference has a particular signature which could indicates that this difference includes ionospheric correction difference. Some other corrections are different, such as sea state bias.
On Envisat/Jason-1 differences, an interannual long wave signal is visible, notably before 2004 where a strong drift is observed (before cycle 25). A similar observation can be made at the end of the serie with a different drift observed after cycle 75. These particular points are not fully understood at the moment.
In terms of mean, the difference observed between Envisat and Jason-2 was 28cm (47.4cm for Envisat, 18.5cm for Jason-2);
After Jason-2 reprocessing, this 18.5cm bias is explained and so removed on Jason-2 side to have a mean difference of 47.4cm now.
On Jason-2/Envisat difference, the impact of Jason-2 reprocessing and PTR correction are visible.

On Envisat/Jason-1 difference (figure 29, left), a strange behaviour is observed on Envisat cycle 79/80 (May/June 2009). This behaviour is not explained yet, but seems to appear on Envisat/Jason-2 difference too (figure 29, right), on Jason-2 cycles 30 to 40. The difference between Jason-2 and Envisat during this period is reduced under 47cm.
This strange behaviour is not visible on Jason-2/Jason-1 difference, as presented on figure 28 extract from the Jason-2 reprocessing report ([93]).
Some other discrepancies are visible for Jason-2 cycles 96, 112 and 113, with no founded reason at the moment. Correlation with strange behaviors on Envisat side at the end of dataset, could be highlighted.

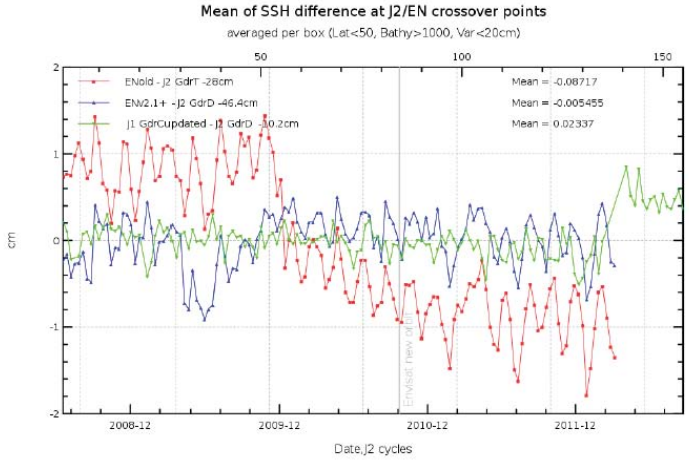

Figure 28: *Mean of J1-J2 SSH differences at dual crossovers (cm) on global ocean with selection*

These results suggest that some problems could be present on Envisat side. These suspicious results should be analysed to better understand the behaviour of Envisat SSH at multi-missions crossovers.

Performances at crossovers are compared on figure 30, in terms of standard deviation at dual crossovers. The standard deviation of Envisat/Envisat and Jason-1/Jason-1 SSH crossover

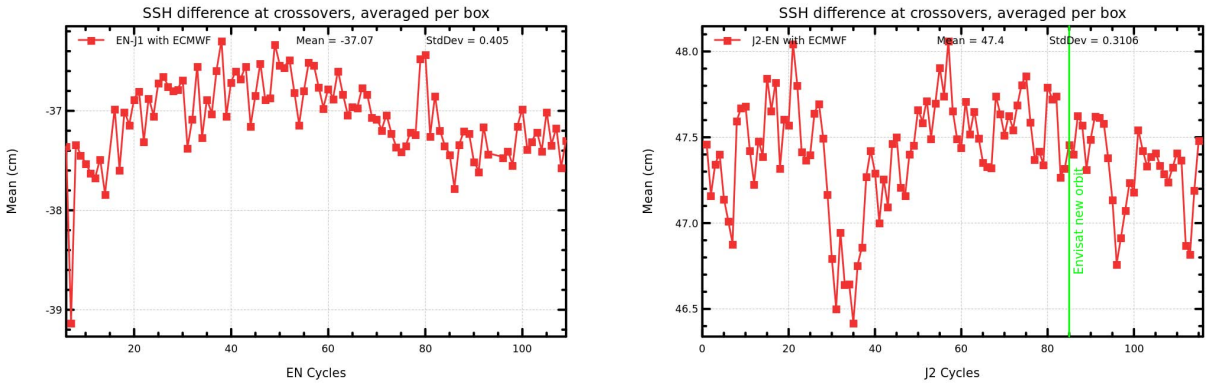

Figure 29: *Mean of* ***Left:)*** *EN-J1* ***Right:)*** *J2-EN SSH differences at dual crossovers (cm) on global ocean - Envisat dataset with updates*

differences are respectively $3cm$ and $2.5cm$ after an average per box.
The standard deviation of SSH is greater for Envisat, compared to Jason-1 but it decreases along the period to reach a similar value as Jason-1 at the end of the Envisat period.
The same comparison is made for Envisat and Jason-2 after reprocessing, on the right figure of 30.
The performances of the three missions are very good and close to each others.

Investigation on these particular behaviors on SSH difference would be interesting to refine our knowledge of SSH for each mission and to detect eventual problems on one or the other mission.

Note that the results are different for Envisat in the two configuration. This result from the computation of the mean and standard deviation over the whole series, as explained previously (see figure 27).

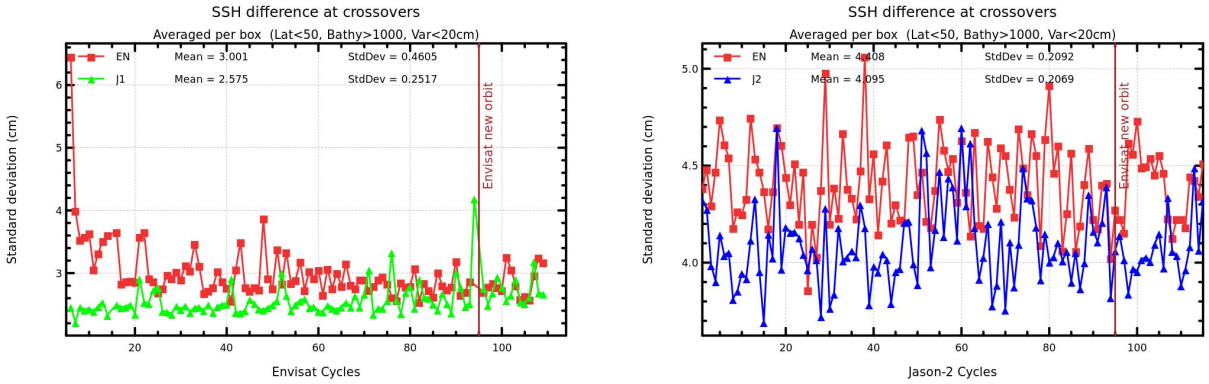

Figure 30: *Standard deviation (cm) of 10-day SSH crossover differences* ***Left****: from Envisat with all updates/Jason-1 cross-comparison (mean on 35 days)* ***Right:*** *from Jason-2/Envisat with all updates cross-comparison (mean on 10 days), with 4 by 4 average per box and shallow waters excluded, latitude within [-50S, +50N], high ocean variability areas excluded.*

The cross comparison between altimetric missions allows to estimate the intrinsic consistency of mission's data for mesoscale. Evaluating difference of SSH at dual-crossovers allows to compare the

two missions in terms of errors. If the differences are low (gray on the following maps figure 31), the consistency between the two missions is revealed for mesoscale consideration. This consistency can be in errors determination too: the considered SSH can be prone of the same error for the two missions. In this case, these diagnosis allows to confirm error detection and to limit the future analysis domain.
Figure 31 presents the intrinsic consistency of Envisat data for mesoscale consideration, with updated dataset by year since 2003.
We observe some remaining desagreements notably concerning ionospheric correction signature growing up at then end of the serie, when the solar activity gets higher. A great difference of SSH is also observed in South Pacific (blue patch on the maps), which seems to grow up since 2003 to 2011. For the moment this phenomenon is still not fully understood.

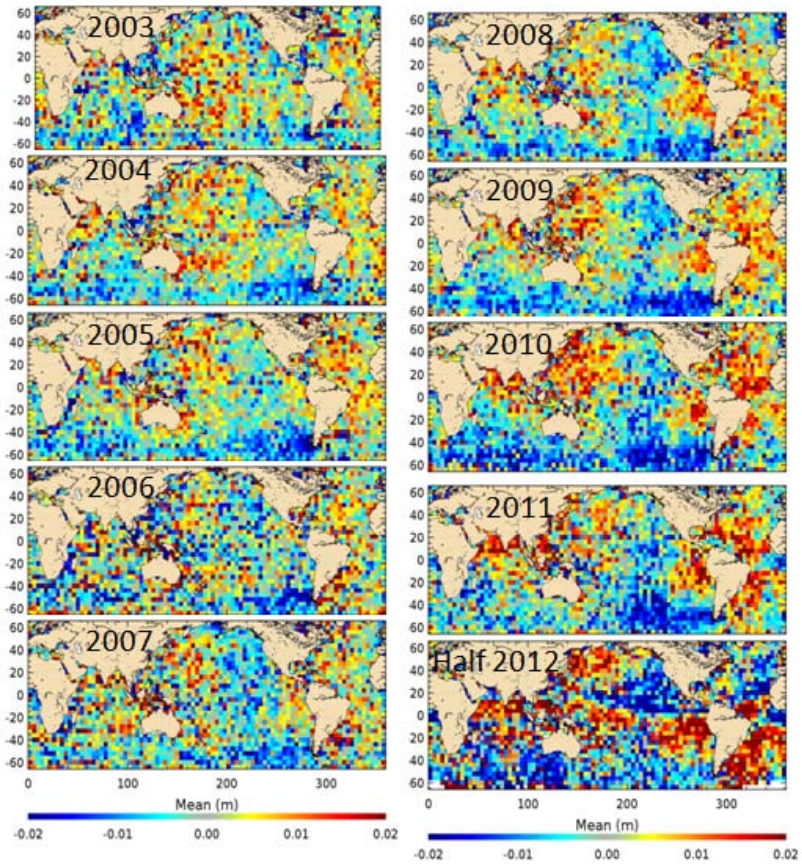

Figure 31: *Envisat difference of SSH at monomission crossovers by year since 2003 using updated dataset*

The next figure 32 represents mesoscale error between Envisat and Jason-1, with updated dataset for Envisat and GDR-D orbit standard for Jason-1. Remaining patterns are linked to a combination of differences between the two missions: radiometer wet tropospheric correction, ionospheric correction, sea state bias computation, ... Differences can also be caused by orbit errors on the two missions. The same estimation has been made using the new 10-days gravity field for Envisat (see 8.2.1. figure 57).

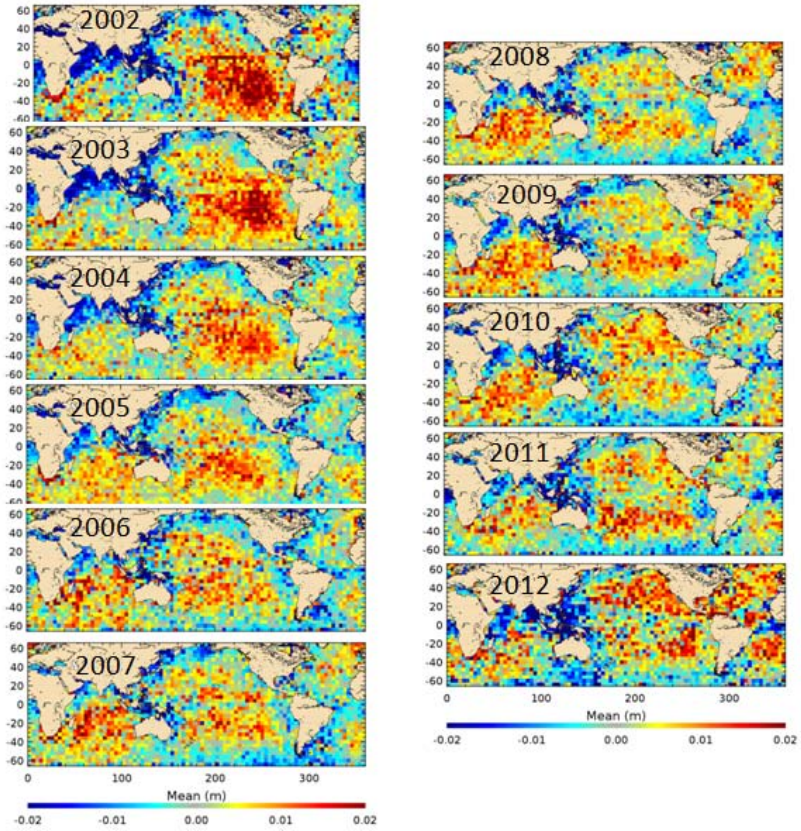

Figure 32: *Envisat/Jason-1 difference of SSH at dual-crossovers by year since 2003 using updated dataset for Envisat and GDR-D for Jason-1*

The similar comparison is made between Envisat and Jason-2 on year 2011. The results are presented in Figure 33, using model wet tropospheric correction.
The remaining North/South observed with GDR-D standards bias (Figure 33, right) comes from the different SSB model used for the two missions.

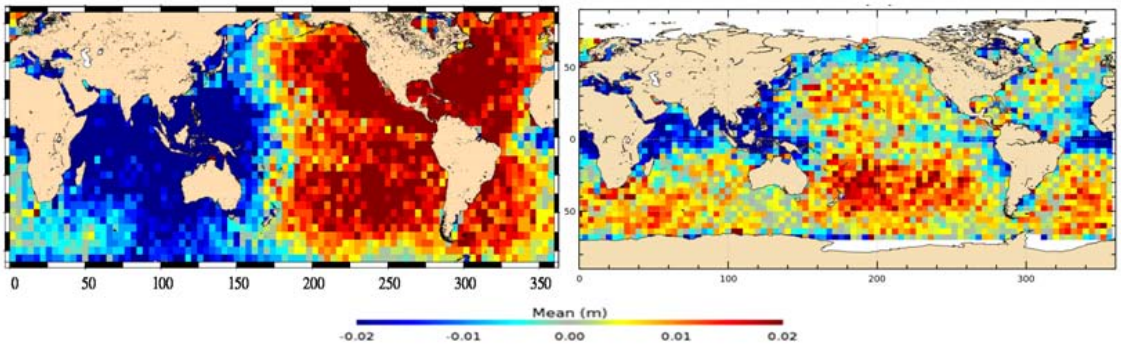

Figure 33: *Difference of variance of SSH at crossovers for 2011 using* ***Left:*** *Envisat V2.1/Jason-2 with GDR-C standard* ***Right:*** *Envisat V2.1+ with updates/reprocessed Jason-2 dataset*

6.3.3.2. Cross comparison with Cryosat-2

With the loss of Envisat in April 2012, an important part of the global altimetric network disappeared. Notably at high latitudes and between Jason-1 and Jason-2 data tracks, we focused on the potential of Cryosat-2 to constitute a new reference for multimissions studies. Available Cryosat-2 data are provided by CNES CPP delayed time reprocessing, in LRM mode. Results are promising; Figure 34 shows the SLA computed for Envisat, Jason-1, Jason-2 and Cryosat-2 for 2010/2011. The patterns are similar for all the missions, showing that Cryosat-2 could be used for studies in complement of Envisat. The Figure 35 shows as well that the difference of variance of SSH at crossovers for Jason-2/Cryosat-2 has an order of magnitude comparable or even lower than the one obtained with Envisat/Jason-1 cross-comparison.

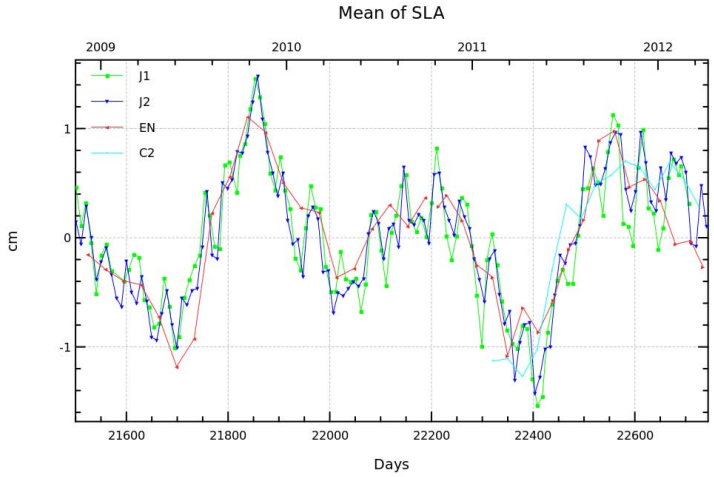

Figure 34: *Comparison of SLA for Envisat V2.1 dataset, Jason-1, Jason-2 and Cryosat-2 (selection on bathymetry, latitudes and oceanic variability)*

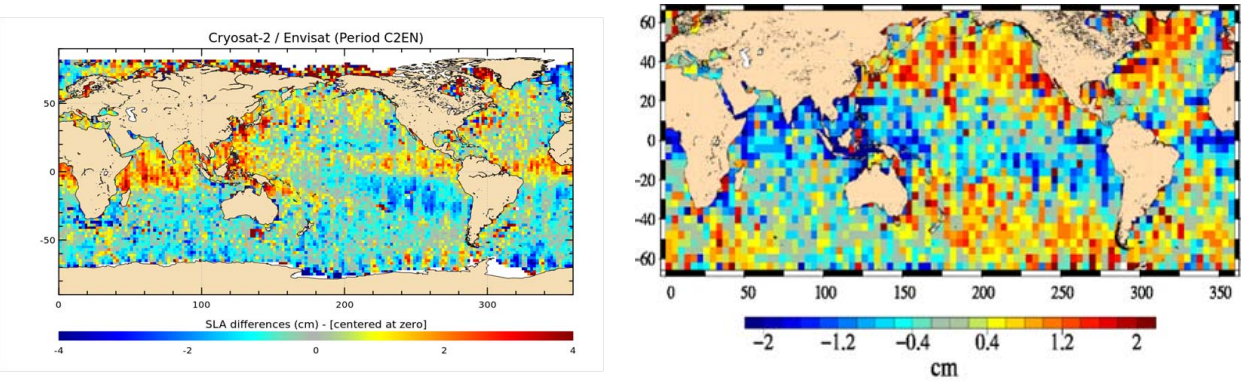

Figure 35: ***Left****: Difference of SLA along track: Cryosat-2/Envisat* ***Right:*** *Difference of SSH variance for multimission crossovers: Cryosat-2/Jason-2*

Cross comparisons with Cryosat-2 are important for inter-missions error analysis after Envisat loss. It allows to ensure the continuity of analysis and to improve our knowledge of altimetrics results and the global quality of altimetric system. Particularly the cross-comparison between Cryosat-2 and Jason-2 allows to be confident in use of Cryosat-2 as a new reference solution for multimissions studies.

7. ENVISAT Mean Sea Level Trend

Observing and understanding our climate evolution is a challenge in which altimetry can play a role through, notably, ocean topography monitoring studies. For the last two decades, satellite altimetry has provided reliable time series, highlighting a rise of around 3mm/year at global scale (Cazenave et al. 2004 (see [28], Ablain et al. 2009 (see [9])) of the Mean Sea Level (MSL).
By now, most Sea Level rise studies are based on the 3 NASA/CNES missions: TOPEX/Poseidon (1993-2005), followed by Jason-1 over (2002- onwards) and Jason-2 (from 2008 onwards). The primary role of these missions is the accurate measurement at global and regional scales for climate applications (OSTM/JASON-2 science and operation requirements, 2005). Additionally to these missions, the ESA polar orbiting satellite ERS-1 (1991 - 2000), ERS-2 (1995-2011),Envisat (onwards from 2002) and Cryosat-2 (onwards from 2010) have been successively launched, providing a precious and precise complementary data set to the NASA/CNES missions. ERS1, ERS2, Geosat-Follow-On (GFO), Envisat and SARAL/Altika enable a better restitution of the mesoscale variability at all latitudes and more especially between 66 and 82 deg where no Topex, Jason-1 and Jason-2 data are available. Their strong added values in multi-mission merged products such as SSALTO/Duacs Aviso products was already extensively shown in several publications concerning mesoscale variability studies (Pascual et al. 2006 (see [85], Le Traon et al. 2003 (see [67])).
Up to now, the quality and performances of ENVISAT mission were shown to be very good (Faugere et al 2006, see [48]) and with similar level of accuracy as Jason-1 and Jason-2's for mesoscale applications (Ollivier et al 2010, see [14]). Yet, Envisat GDR have long been suffering from an inhomogeneous time series and from major events affecting data quality which prevented users from using them directly for climate oriented studies. Dedicated updates and post processing enable to now obtain an homogeneous data set. Thanks to this homogenizing work, fine cross-calibration analysis with other missions and in situ methods are possible. They allow to highlight some remaining differences and particularities of Envisat data.

7.1. Envisat MSL becoming more relevant!

Since Envisat launch, some discrepancies between its Mean Sea Level trend and other mission's were investigated.
However after many improvements and updates over the whole time series, its similarity to Jason-1's MSL (used for climate studies) and to tide gauges after 2004 is very encouraging.
In 2012 a paper was published (Ollivier et al. 2012 [82])) to describe the data analysis process that enabled to improve considerably the pertinence of this oceanic indicator. For this, multimision and in situ comparisons analysis enable to identify errors in the datasets, to identify there origin and to solve them, thanks to fruitful exchanges with experts (Level 0 and 1 instrumental experts and orbit experts).
As already extensively developped in [15] and [16], the update of two major terms enabled to improve respectively the global and regional MSL:
- The Time Delay Calibration Factor of the Point Target Response (instrumental correction called PTR correction in this document)
- The new standard of GDR-D orbit, which better accounts for the time variable gravity field estimated from Grace data.

Since 2010, Envisat MSL is available on Aviso web page at: http://www.aviso.altimetry.fr/en/data/products/ocean-indicators-products/mean-sea-level.html. In 2012 Envisat time series was updated

with the new reprocessed dataset as well as from the PTR instrumental correction, insuring a better consistency between other missions and in situ data set.
The description of the processing and the table of corrections used are available at http://www.aviso.altimetry.fr/en/data/products/ocean-indicators-products/mean-sea-level/processing-corrections.html.

Last updates in 2013 allow to continue to analyse the fine discrepancies between Envisat and other missions mean sea level trend. The impact of new radiometer wet tropospheric correction and all other updates have been studied this year, maintaining the high quality of multimissions mean sea level trend.

7.2. MSL recipe

7.2.1. Mean Sea Level computation details

In order to have comparable time resolution between Envisat and Jason-1, each point of the MSL monitoring are computed with quarter of Envisat cycle (35/4 = 8.75 days) periodicity: the closest fraction of cycle from 10 day-Jason-1 periodicity. Envisat's time series are computed by first averaging the data in 2x2 deg boxes and then by computing a global average with a weighting depending on the latitude (between 66deg N/S) following Dorandeu and Le Traon 1999 [33]. Time series are then smoothed with a 10 points (87.5 days) sliding window. This step enables to smooth the noise and to reduce the SNR (Signal to Noise Ratio) on the slope computation. The Sea Level Anomaly (SLA) formula is given below.

$$SLA = Orbit - Altimeter\ Range - Mean\ Sea\ Surface - \sum_{i=1}^{n} Correction_i$$

with :

$$\begin{aligned} \sum_{i=1}^{n} Correction_i &= Dry\ troposphere\ correction \\ &+ Dynamic\ atmospheric\ correction \\ &+ Wet\ troposphere\ correction \\ &+ Ionospheric\ correction \\ &+ Sea\ state\ bias\ correction \\ &+ Ocean\ tide\ height \\ &+ Solid\ earth\ tide\ height \\ &+ Geocentric\ pole\ tide\ height \end{aligned}$$

Now the geophysical corrections provided in the GDR products are totally homogeneous and described in part 3.2.2..
In this part are presented analysis on Mean Sea Level trend computation, using the anticipated updates and new corrections developped in 2013. The impact of these updates on global and regional mean sea level is presented in the following parts.

.

The table 3 presents the geophysical corrections for each Envisat period used in the Mean Sea Level computation this year.

	Cycles 6-64	Cycle 65-94	Cycle 95 onwards
Orbit	GDR-D		
Range	From GDR + PTR correction (V2.1+)		
DAC	MOG2D-HR		
Iono corr	Iteratively filtered Dual-Frequency with S-Band SSB	GIM+bias	
MWR Wet tropo	Updated composite		Updated MWR
MWR Dry tropo	Gaussian grids S1-S2 atmospheric tides applied		
SSB	Homogeneous to GDR-C		
Solid Tides	From GDR		
Pole Tides	From GDR		

Table 3: *G*eophysical corrections used following the periods

This year, some analysis have been made on global and regional Mean Sea Level trend, notably based on the anticipated updates:
- The impact of the **V2.1b wet tropospheric correction**, (updated correction described in 8.1.1.), on regional and global MSL;
- The analysis of **Envisat altitude consideration in GIM (Global Ionosphere Maps) model computation** (see 8.2.2.);
- A new modelisation of **the 10-days gravity field used in orbit solution** was analysed and compared to the one used in GDR-D (see 8.2.1.).
- A new MSS is used in MSL computation, the **CNES 2011 Mean Sea Surface**.

7.2.2. Impact of GIA on altimetric and is-situ MSL comparison

The altimetric MSL presented here doesn't take into account the GIA (Glacial Isostatic Adjustment) which represents the response of the earth's enveloppes to the mass redistribution since the last glacial maximum. This phenomenon is important to compute a precise MSL and has to be included in the MSL computation for altimetric and in-situ data.
Figure 36 presents the regional correction trend associated to this effect.
For in-situ data, the correction is made with a model directly applied in MSL computation. But for altimetric MSL, an uniform correction of $-0.3mm/y$ is applied, corresponding to the mean of GIA, without considerating the regional impact of this phenomenon. Then the global mean sea level trend given by altimetry with GIA consideration is increased by $0.3mm/y$. Then the comparison between altimetry and in-situ MSL computation has to be made considering this value on altimetry side.

A more precise method is to correct altimetric MSL by a model to apply the regional impact of GIA, as it is made for in situ data. This has no significant impact on the global average trend, but the dispersion between altimetric and in-situ MSL trends would be reduced which would give relevance to the comparison between the two MSL computation methods.
As a consequence, to improve the consistency between in-situ and altimetry MSL, the regional impact of GIA has to be considered at the same way on both side.

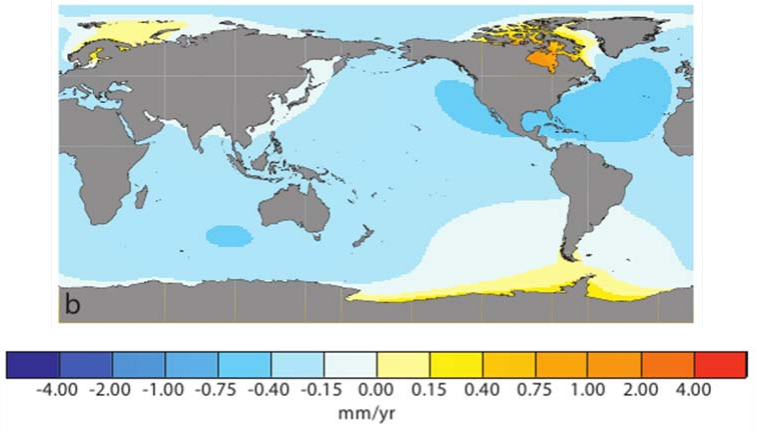

Figure 36: *Regional impact of GIA on altimetric MSL trend*

7.3. MSL global time series

The global MSL computed with the updated dataset is presented in figure 37. The effect on global MSL is largely dominated by the PTR evolution as demonstrated in [15].
The new updates have a weak effect on global MSL, the impact is limited to $0.03mm/y$ on the whole Envisat period, comparing to V2.1 dataset (see [16]).

Updated Envisat MSL exhibits a 2.4mm/yr trend (not taking into account the GIA post rebound, see 36) on the whole dataset. The difference between Envisat and Jason-1 is reduced to 0.26mm/y on the whole Envisat period, as seen on the Figure 37. The consistency with Jason-2 is also very good in terms of interannual signal (the too short period for J2 does not enable to conclude any significant absolute trend).
Yet the beginning of the period (before 2004) remains suspicious. This behaviour could be the result of a combination of suspicious effects (ionospheric correction, wet tropospheric correction, ...) but this question is not yet resolved.
If we consider the period 2004-2012, the difference between Envisat and Jason-1 reaches $1.2mm/y$. The difference of trends for Envisat with or without considering the first year reaches $0.8mm/y$, which is higher than on Jason-1 ($0.2mm/y$).

The comparison to in-situ data is presented in table 4.
The studies are also detailed in [113] to evaluate the different impacts of the standards on the comparison to Tide Gauges and TS profiles.

For comparison with in tide gauges, the correction of GIA is not applied in 4 nor on in-situ side neither on altimetry side. The detailled results of altimetry/Tide Gauges comparisons are available

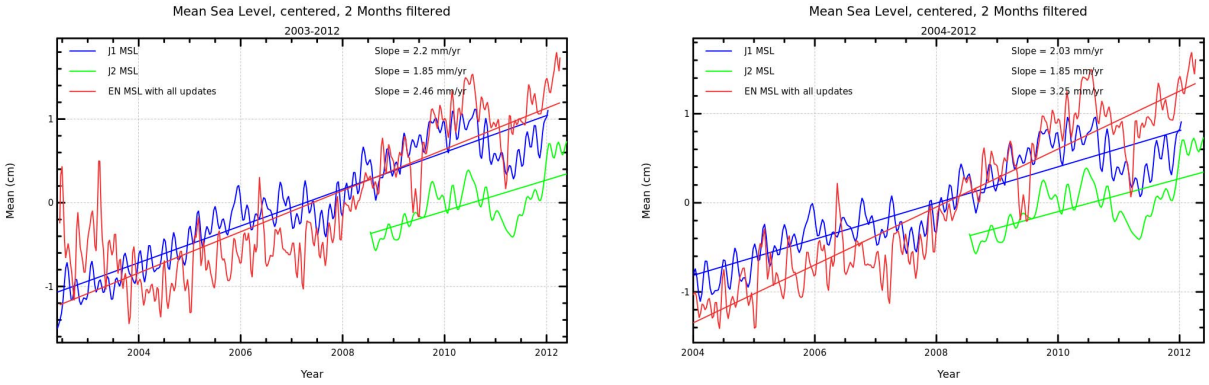

Figure 37: *MSL computed with last updates: PTR, updated tropo. correction and GDR-D orbit for the period* ***Left****: 2003-2012* ***Right****: 2004-2012*

MSL trends (mm/yr, **without correction of GIA**)	**Altimeter MSL**	**MSL drift vs Argo+GRACE**	**MSL drift vs tide gauges**
Jason-1	2	0.7	0.4
Envisat	3.2	2.3	1.1
Trend differences	1.2	1.6	0.7

Table 4: *Altimeter MSL trends of Jason-1 and Envisat and MSL drifts compared with in-situ measurements over the period 2004 / January 2012.*

in Altimetry/Tide Gauges 2013 annual report ([18]). In this cited report, correction of GIA is applied and the difference between altimetry and in-situ data reaches $0.7mm/y$ for Envisat (here $1.1mm/y$ without GIA correction, last column of 4). The observed difference contains the effect of GIA on altimetry side ($0.3mm/y$) and the use of GDR-D orbit standard. The impact of GDR-D orbit standard on altimetric Mean Sea Level trend was estimated at $+0.2mm/y$ with GDR-D.
The difference of MSL trend between Envisat and Jason-1, comparing altimetry and tide gauges data, reaches $0.7mm/y$. This value is reduced using updates, compared to after reprocessing value (see [16], $0.9mm/y$).
The associated error over this period is estimated to be ± 0.7 mm/yr, taking into account the spatial sampling restricted to coastal areas and the terrestrial crustal movements. Considering both Jason-1 and Envisat time series, the comparison with tide gauges suggests that the drift is greater for Envisat mission (1.1 vs 0.4 mm/yr).

Finally, to complete this study and make the results reliable, the altimeter MSL is then compared with Argo and GRACE data over the same period (2nd column of table 4). Note that the MSL computation method using Argo T/S profiles has changed this year which can impact the interannual differences between altimetry and in-situ data and the trend evolution too. For all the details concerning the methods and results, see Altimetry/Argo T/S profiles 2013 annual report [19]).
The difference of trends between Envisat and Jason-1, each compared to Argo profiles, reaches $1.6mm/y$ which is close to the difference given by altimetry alone. Note that the correction of

GIA is not applied in table 4, which is a difference with the results presented in [19]. Applying the correction of GIA on the both sides, the MSL difference between altimetry and Argo T/S profiles reaches $1.7mm/y$ for the periode 2004-2012.
Note that the error over this period is estimated to be around ±0.8 mm/yr, taking into account the errors associated with both types of data, their processing and the colocation process. Moreover, absolute MSL drifts referenced to Argo and GRACE data also suggest that the Envisat MSL drift is greater than the one of Jason-1 (2.3 vs 0.7 mm/yr).

Thus, the comparison with different types of in-situ data allow to confirm that the MSL drift seems to be greater for Envisat than for Jason-1 over the period 2004-2012.

7.4. MSL regional time series

The regional MSL is presented on figure 38. The V2.1+ updates allows to improve the regional MSL computed. The effect on regional MSL is largely dominated by the orbit standard evolution (see impact of Orbit alone in [15]). Geographic trends differences are now homogeneous with few geographical patches (excepts a slight difference in the Indian Ocean (blue) and along the magnetic equator (yellow)).

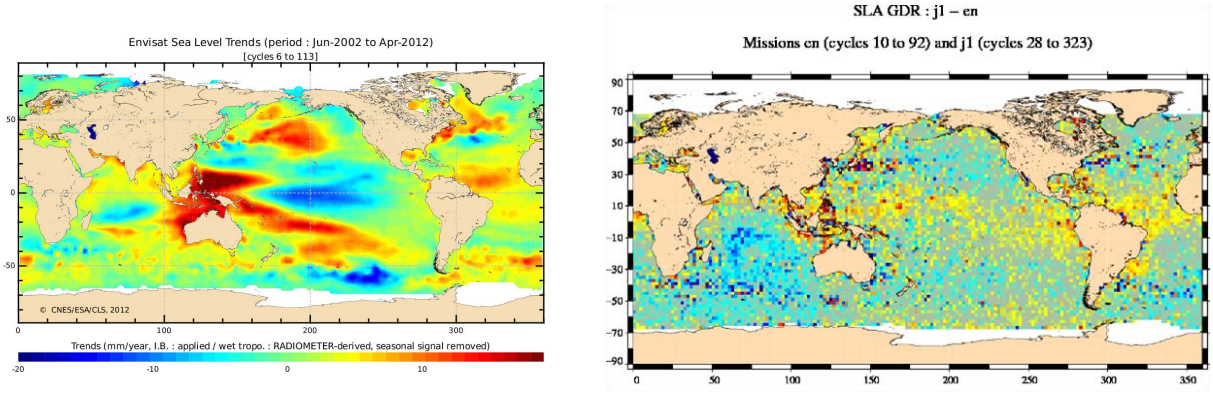

Figure 38: *Left: Regional absolute MSL for EN. Right: Difference EN/J1 after reprocessing with updates (V2.1+)*

The regional MSL difference between Envisat and Jason-1 was computed using the new 10-days gravity field modelisation (presented in 8.2.1.). The results is available on left map of figure 58.
The improvement is limited but the Envisat-Jason 1 difference is more homogeneous, notably in South Pacific area.

7.5. Impact of wet tropospheric correction models on MSL

In 2013 tests on Mean Sea Level continued to be performed, notably concerning the wet tropospheric correction models used in MSL computation. ECMWF and ERA-Interim model have been used to highlights the observed discrepencies between radiometer and model. ERA Interim model was notably tested as a reference on the long term stability.
Observed results are described in the next table (Table 5). Figure 39 shows the MSL trends for

the different configurations:

Correction used	Global MSL Trend
MWR	2.5mm/yr
ERA Interim	2.9mm/yr
Difference with models	Global MSL trend difference
MWR-ECMWF	0.25mm/yr (0.6mm/yr before rep.)
MWR-ERA Interim	0.4mm/yr

Table 5: *M*SL trends in mm/year

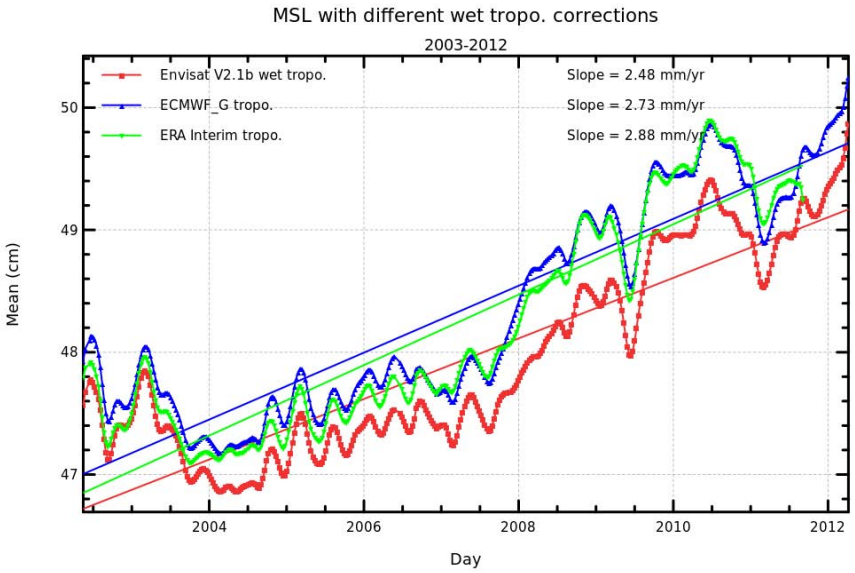

Figure 39: *MSL computed with wet tropospheric corrections (V2.1b Radiometer, ECMWF model and ERA-Interim model)*

The difference of trends between ERA-Interim and radiometer tropospheric correction is more important than the difference between the ECMWF and radiometer tropospheric correction (0.4mm/y against 0.25mm/y). But the long term stability is by construction more reliable for ERA-Interim.

8. Particular Investigations

8.1. Anticipated updates for the next reprocessing

8.1.1. V2.1b Radiometer Wet tropospheric correction

8.1.1.1. Reminder: observed degradation after reprocessing

The degradation of the V2.1 MWR wet tropospheric correction compared to the one used before reprocessing was near 1.5cm^2 when avoiding the high latitudes, low bathymetry and high oceanic activity, as seen on figure 40 left, and it could reach locally 5cm^2 in wet areas (figure 40, right).

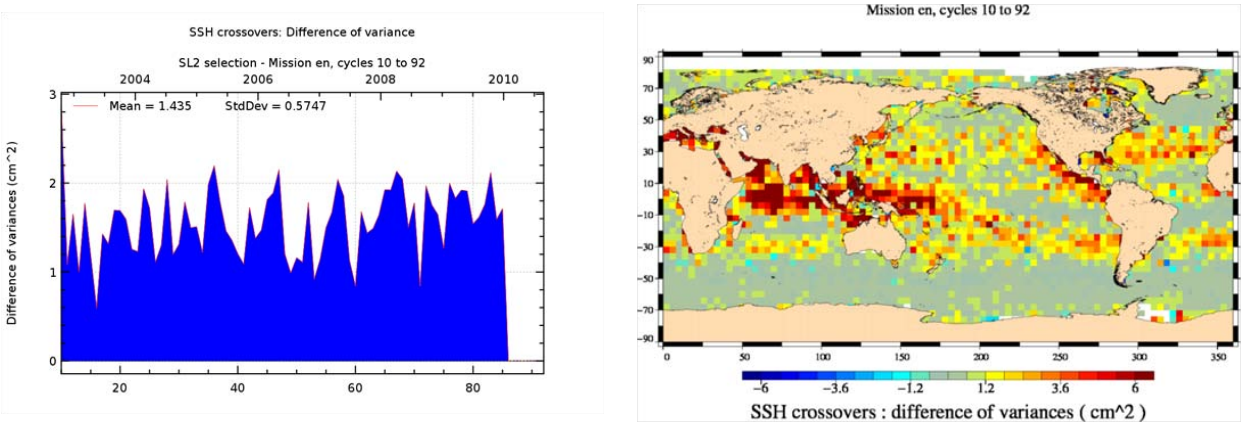

Figure 40: *Impact of the MWR correction in V2.1 against routine GDR (before rep.), over cycles 10 to 92;* ***Left:*** *Variance difference of SSH at crossovers per cycle* ***Right****: Map of this difference.*

After analysis of this degradation, a new radiometer wet tropospheric correction, named V2.1b, was computed during summer 2013 and an analysis was carried out to compare its performance with the one obtained after and before reprocessing.

8.1.1.2. Increase of the valid data number

We observe that the number of valid points increases using the new V2.1b MWR correction, mainly at high latitudes for low tropospheric content. The number of points out of threshold ($-0.5m < x < -0.001m$) is also decreased.

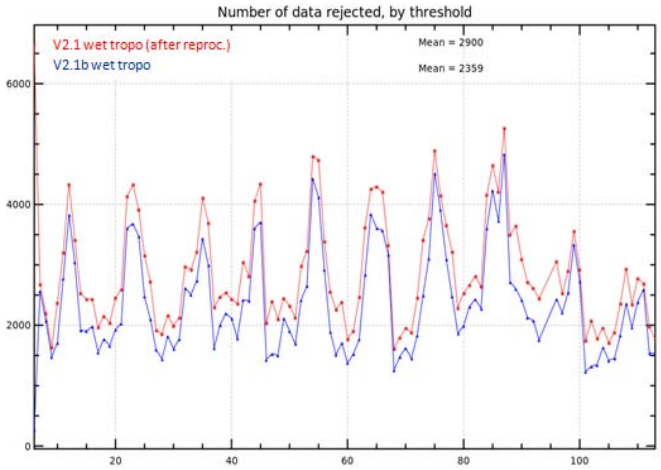

Figure 41: *Number of rejected data with **red**): MWR after reprocessing **blue**): V2.1b MWR*

8.1.1.3. Reduction of the variance of SSH at crossovers

The mesoscale error lower than 10 days is decreased comparing to the V2.1 MWR, as shown on figure 42. The error is reduced from 1.3cm^2, in the order of magnitude of the degradation observed after reprocessing. The error made on SSH at crossovers with V2.1b MWR wet tropospheric correction is similar to the one observed before reprocessing, as shown on figure 43. The variance by the radiometer wet tropospheric correction on its own is negligeable compared to before the reprocessing before cycle 85 and reach -1.5cm^2 for cycles after (after cycle 85, the routine GDR was already in V2.1 standard then the observed gain corresponds to the "V2.1b"-"V2.1" gain). The quality observed before reprocessing on this point is here recovered.

On figure 44, we can observe the 3 expected behaviors of MWR correction, comparing to before reprocessing:
- Before cycle 41, the variability is due to side lobes;
- Between cycle 41 and 85, only a milimetric bias is observed;
- After cycle 85, the observed bias is mainly due to wet areas.

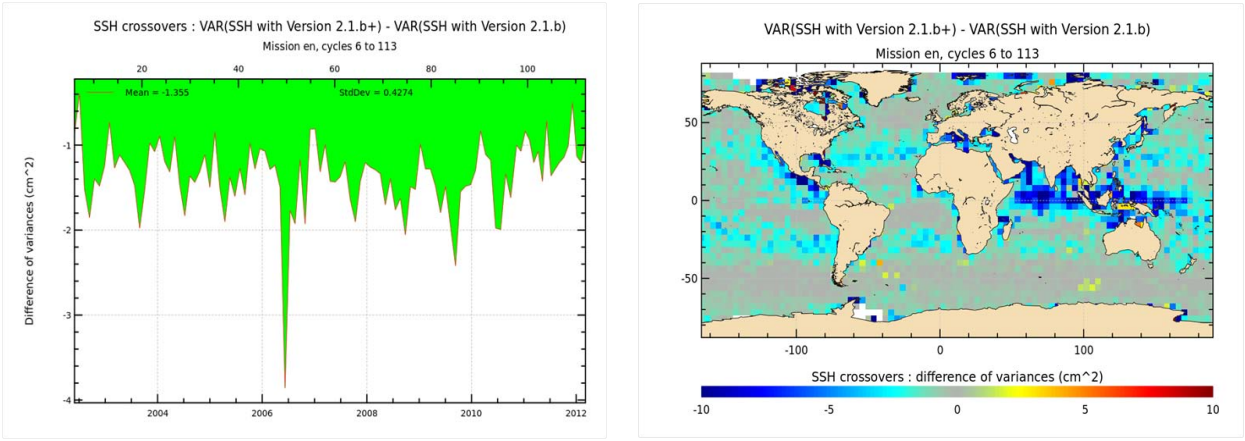

Figure 42: *Impact of the MWR correction in V2.1b against V2.1, over cycles 6 to 113;* ***Left:*** *Variance difference of SSH at crossovers per cycle* ***Right****: Map of this difference.*

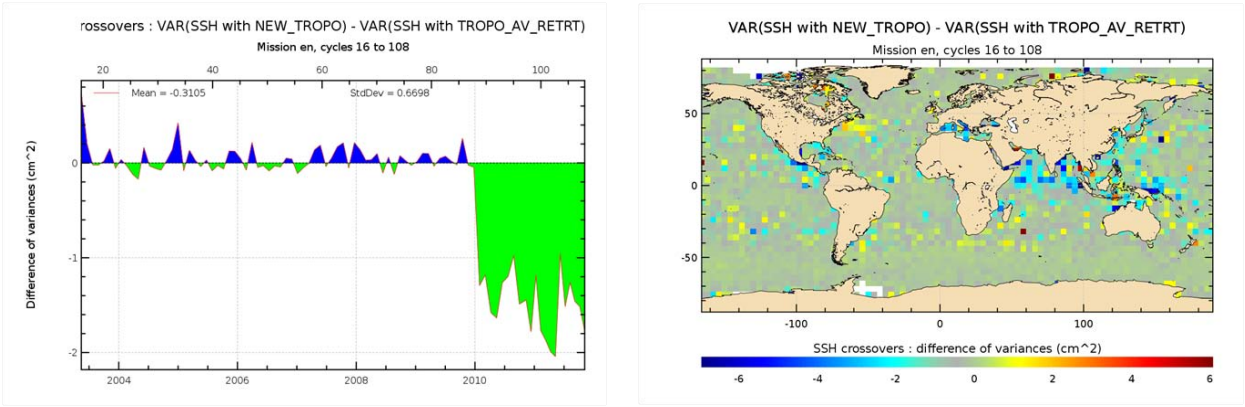

Figure 43: *Impact of the MWR correction in V2.1b against V1, over cycles 6 to 113;* ***Left:*** *Variance difference of SSH at crossovers per cycle* ***Right****: Map of this difference.*

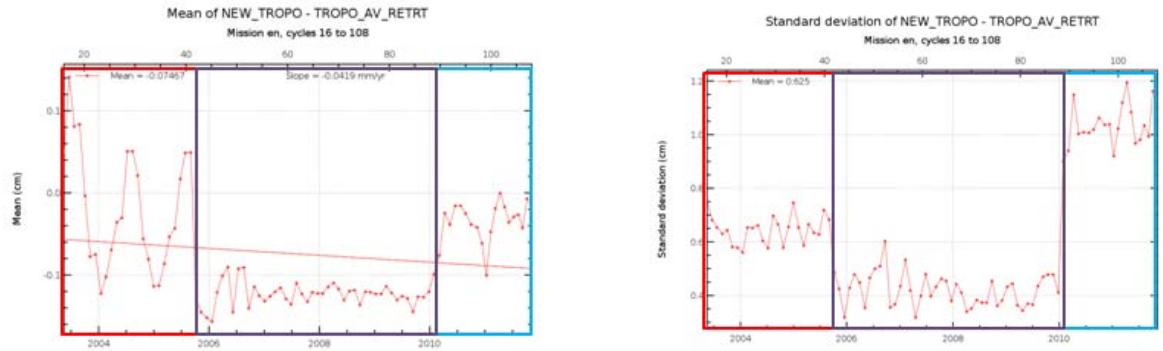

Figure 44: *Mean and standard deviation of V2.1b - V1 (before rep.) MWR on the whole Envisat dataset*

8.1.1.4. Comparisons to ERA Interim and ECMWF model

The figure 45 shows the mean and standard deviation of ERA-Radiometer wet tropospheric correction.
The standard deviation reaches $1.6cm^2$ which is the value obtained before reprocessing. After the reprocessing and with a degraded radiometer wet tropospheric correction (see [16]), this value was greater and reached 1.8cm. The V2.1b radiometer wet tropospheric correction is also comparable to the one used before reprocessing concerning the standard deviation against ERA Interim model.

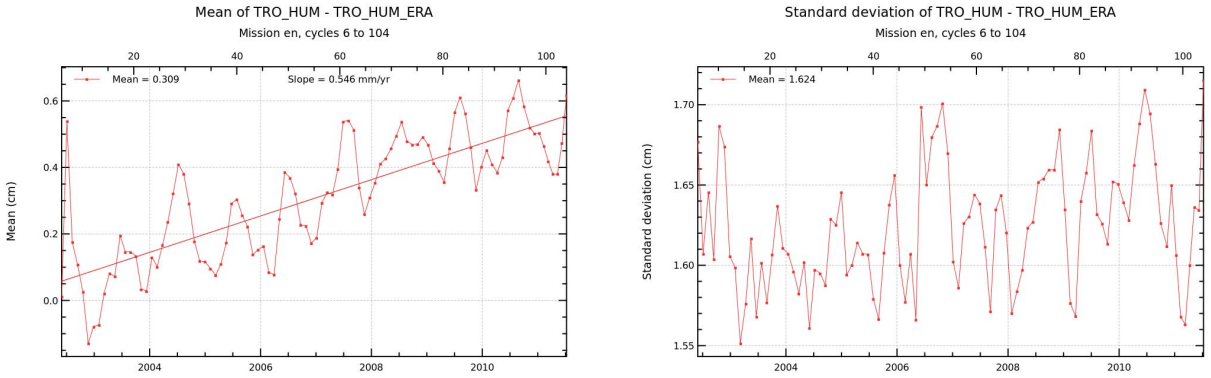

Figure 45: *Mean and standard deviation per cycle of the differences of MWR correction versus ERA-Interim*

The comparison with ERA-Interim model shows that the performance at crossovers is increased by $2.2cm^2$ using MWR radiometer against ERA, excluding high ocean variability areas, high latitudes and shallow water, as visible on figure 46. Without any selection, the reduction of mesoscale error at crossovers reaches $1.3cm^2$.
These two results are similar to the comparison with the ECMWF wet tropospheric correction model, as seen on figure 47.

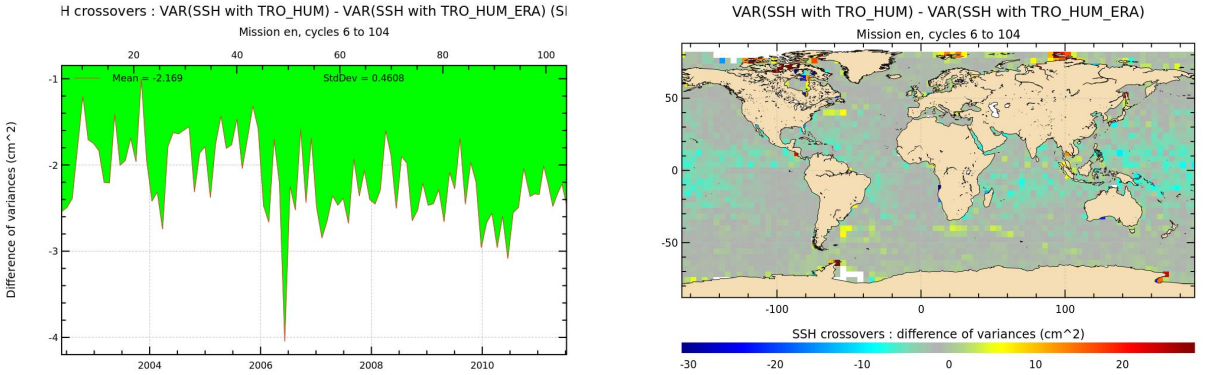

Figure 46: *Impact of the MWR correction in V2.1b against* ***ERA Interim model****, over cycles 6 to 104;* ***Left:*** *Variance difference of SSH at crossovers per cycle* ***Right****: Map of this difference.*

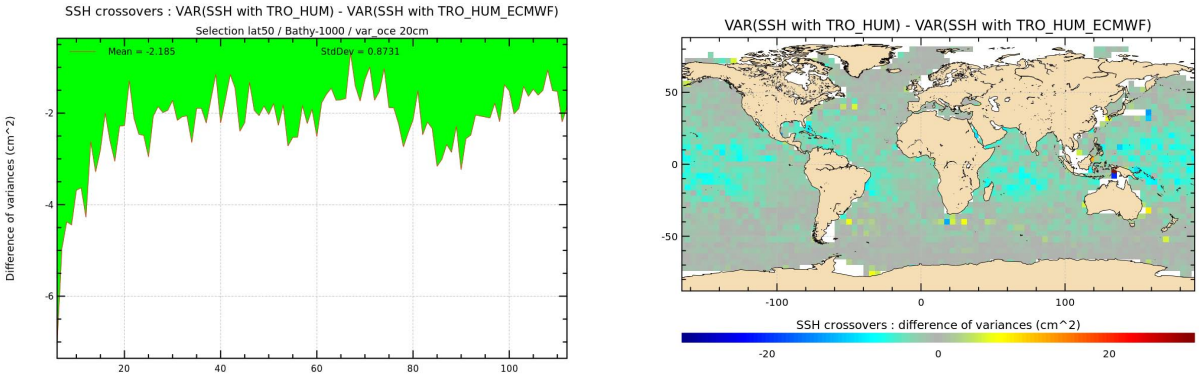

Figure 47: *Impact of the MWR correction in V2.1b against* ***ECMWF model****, over cycles 6 to 113;* ***Left:*** *Variance difference of SSH at crossovers per cycle* ***Right****: Map of this difference.*

In comparison with other missions, Envisat improves the model in the same order of magnitude ($2.2cm^2$) than Jason-1 ($2.6cm^2$) or Jason-2 ($3cm^2$), which is visible on figure 48. Note that this difference with V2.1 MWR version was $1cm^2$.

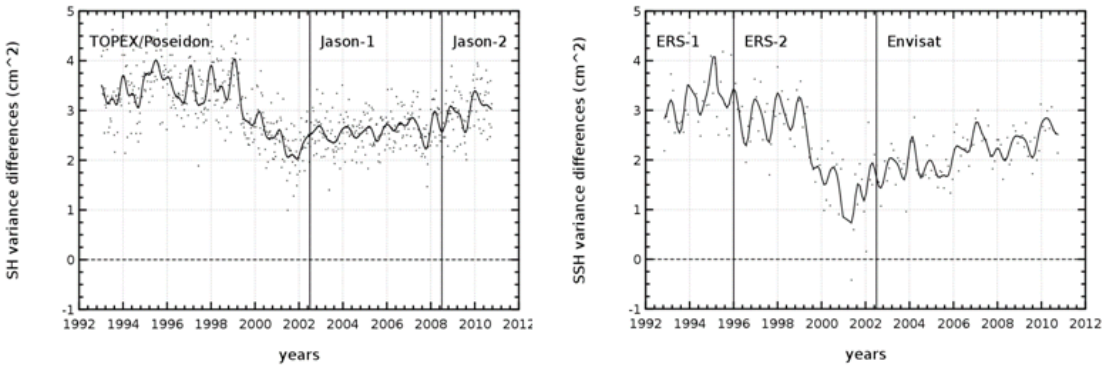

Figure 48: *Difference of variance of SSH at crossovers using ERA-Interim model/Radiometer wet tropo correction for* ***Left:)*** *3 channels radiometers* ***Right:)*** *2 channels radiometers*

We observe on figure 49 that V2.1b gives a better agreement with models than V2.1, notably with ERA-Interim reprocessed series which has a reduced number of inhomogeneities.

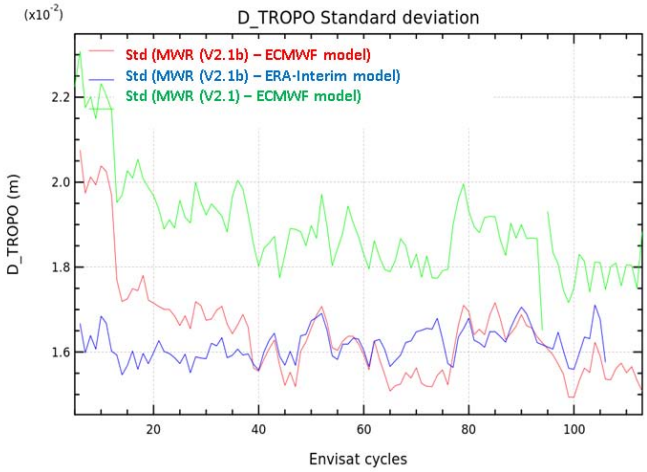

Figure 49: *Standard deviation of wet tropospheric corrections: [radiometer - models] on the whole Envisat serie*

Note that the impact of the V2.1b MWR correction on MSL is very weak; some effects are visible near coasts, ice shelves and wet areas but the global impact on trend is limited to $0.06mm/y$, as shown on figure 50.

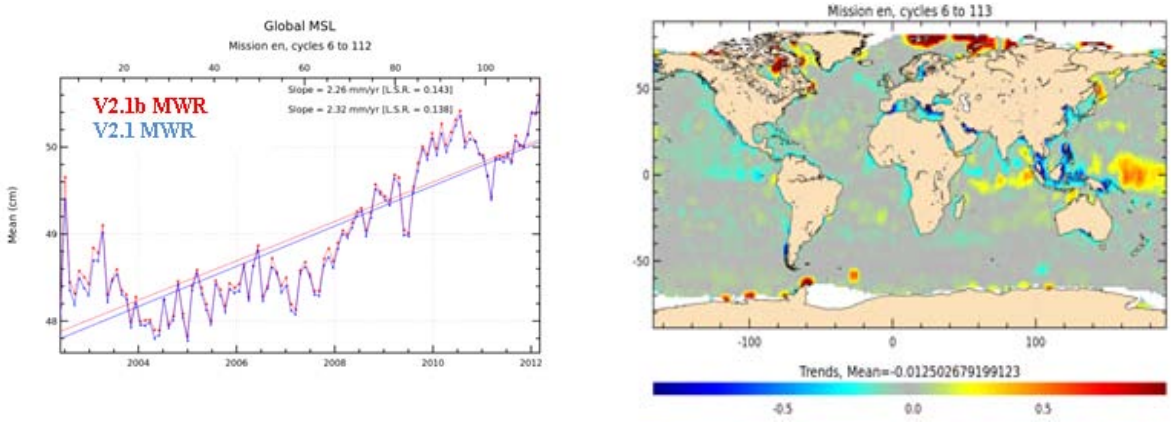

Figure 50: *Global (**Left**) and regional (**Right**) Mean Sea Level trend using V2.1b MWR version*

Note that:

- The MWR products in version V2.1b will be soon **available for users** on esa ftp site (ftp://diss-na-fp.eo.esa.int), completed by a technical note describing the Netcdf files format and synthesizing the results presented here;
- **The V21.b MWR correction will be used for the whole Envisat dataset next reprocessing.**

8.1.2. A new approach for dual-frequency ionospheric correction filtering

A study was carried out on possible improvement of the ionospheric correction filtering method. Envisat dual-frequency ionospheric correction is very noisy and needs to be filtered before being used to correct SLA. Presently, users are advised to filter frequencies lower than 300km before using it in the SLA computation. In the delivered products, the dual-frequency ionospheric correction is provided without any filter.
In the current method, dual-frequency ionospheric correction data are filtered after the CalVal editing process, which brings together a selection of data on different criterion: flag,thresholds, statistics on SLA along tracks,... After the complete validation process, dual-frequency ionospheric correction data are considered as valid if all the described criterion are respected, which create a strong dependency between ionospheric terms and other corrections or SSH which has no reason to be.
Valid values of dual-frequency ionospheric correction can be rejected because of SSH, and as a consequence, no associated filtered values can be computed.

The main advantage of the proposed new filtering method is to suppress this dependancy.
The first difference is the data selection step; in this iterative method, the selection is made only on range standard deviation and elementary data number. A selection is also made to suppress ice data. Thus this selection allows to apply the iterative filtering on a larger number of data.

The method is based on an iterative process: between each iteration, selection of valid data is based on difference between filtered data and not filtered data. Data are conserved if they respect a statistic criteria calculated from standard deviation of previous iteration filtered data. After the filtering step, an interpolation is made to fill potential gaps in filtered correction.
As well, filtered values are available wherever the dual-frequency correction is defined.

The increase of filtered ionospheric correction data number reaches more than 6% for Envisat, compared to filtered value selected after validation process.
For Jason-1 and Jason-2, this percentage is around 5%.

In terms of performance, the variance of SSH at crossovers is decreased using the iterative filtered ionospheric data compared to the dual-frequency ionospheric data for Jason-1 and Jason-2, and overall similar for Envisat. Indeed for Envisat we observe a slight degradation of this difference of variance for few cycles before 20. Geographically, this degradation is visible in high ionospheric content areas.
Tests have been performed with different widths for the Lanczos filter window (λ in the following slides, expressed in number of points). Results for Envisat are sensitive to the λ used for filtering, notably before cycle 20, where a slight degradation of quality is observed. With a λ limited to 50 points instead of 100, the observed degradation is reduced for these cycles (high solar activity period), without degrading the slight gain observed for the rest of the period.
After investigations, a different behaviour appears on even tracks and odd tracks, particularly for the beginning of the Envisat serie.
The degradation seems to be more important for odd tracks (night), probably linked to the characteristics of orbit (heliosynchroneous).

This new filtered correction is used for Duacs Delayed Time reprocessing 2013. The feasibility of

adding this correction in GDR will be assessed by ESL team.

.

A new approach for dual-frequency ionospheric correction filtering

M. Guibbaud, A. Ollivier, M. Ablain

Overview

Dual-frequency ionospheric correction is very noisy and needs to be filtered before correcting for SLA ➔ Users are advised to filter frequencies lower than 240km.

But in the products, this filter is not provided.

Current method :

Done during CalVal process AFTER editing step (= selection of data on different criteria, flag, thresholds and statistics on SLA terms, …)

- ➔ Introduce a dependancy between ionospheric correction and SSH which has no reason to be
- ➔ No filtered ionospheric correction for SLA rejected data, whatever the reason of rejection

New filtering method:

Possibly done in the product generation chains (for implementation, see ESL team)

- ➔ Reducing the dependancy between ionospheric correction an data selection based on SLA
- ➔ Keeping filtered values wherever the dual-frequency correction is defined

ENVISAT Altimetry Quality Working Group Meeting (#19)

The new filtering method

1st STEP : Very light selection : Selection only on ice, range standard deviation and data number.

2nd STEP : Iterative filtering process: between each iteration, selection of valid data is based on difference between filtered data and not filtered data.

Use of a Median filter,
then a Lanczos filter

3rd STEP : Interpolation by spline: to fill the gaps

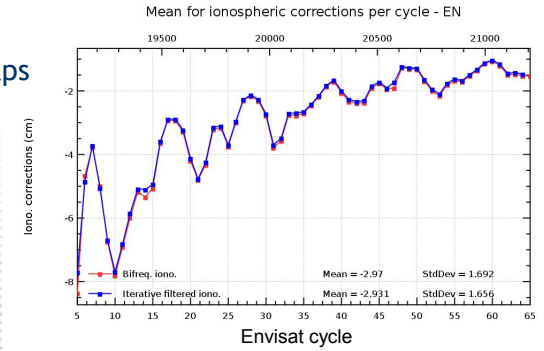

1- valid data number increase

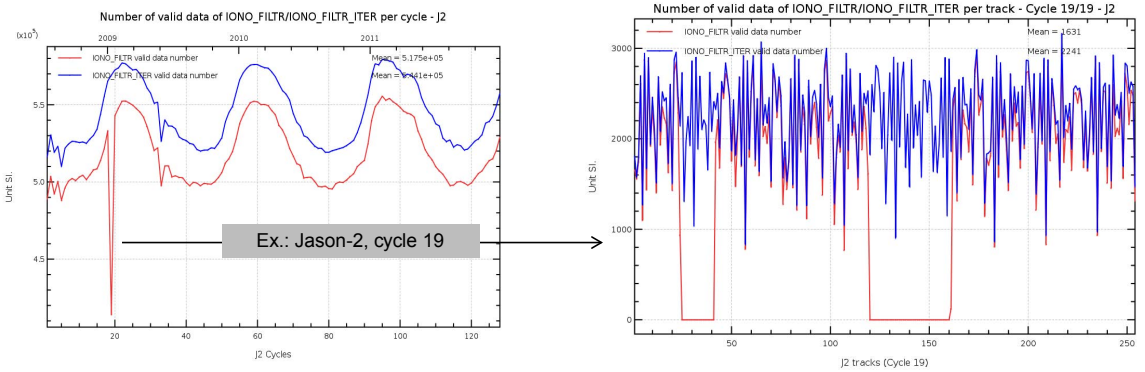

➔ Cycle 19: No MWR correction for tracks 24 to 42, and 119 to 161 => validation flag is « false » => no current ionospheric correction for this period, but existing iterative iono. correction

Recovery of iono for over edited SLA

Statistics/Mission	Jason-1 (c 1 to c368)	Jason-2 (c 1 to 128)	Envisat (c 1 to 64)
% of data gained/cycle	+ 4.7%	+5.1%	+6.2%

1- valid data number increase: geographical coverage

Jason1 – Iterative iono correction

Data gained, compared to current filtering method – c200

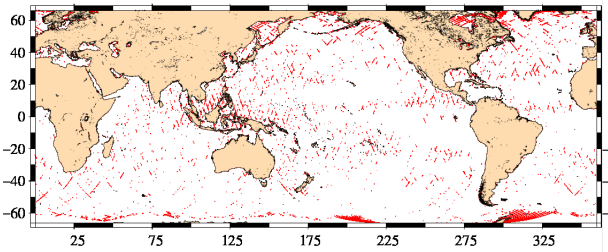

Jason2 – Iterative iono correction

Data gained, compared to current filtering method – c70

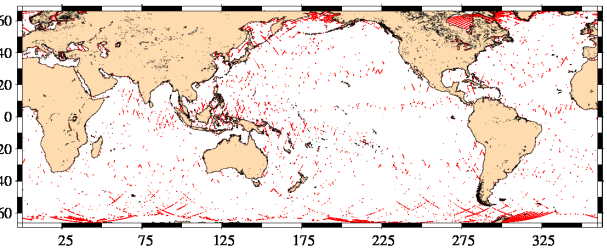

Envisat – Valid iterative iono. correction

Data gained, compared to current filtering method –c50

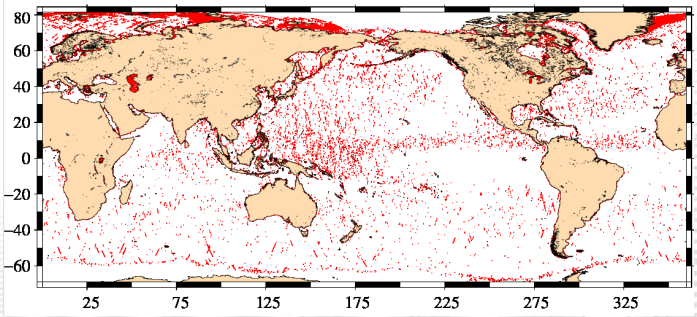

1- valid data number increase

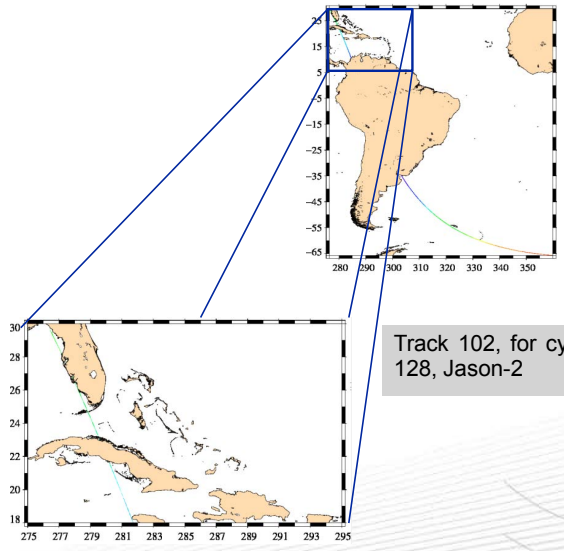

Track 102, for cycle 1 to 128, Jason-2

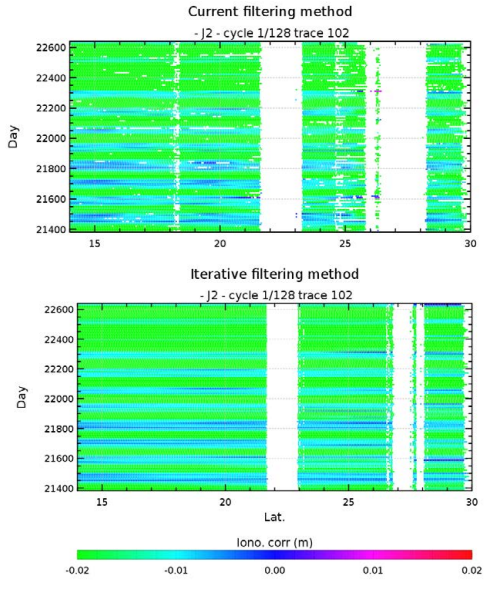

Better coverage in coastal areas

1- valid data number increase

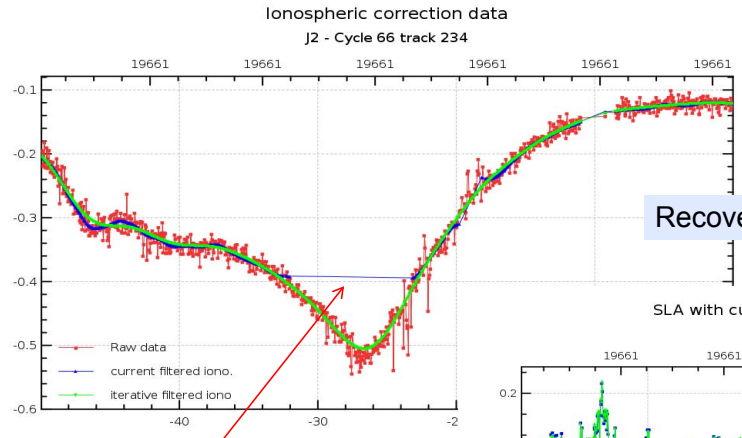

Recovery of SLA for over edited iono

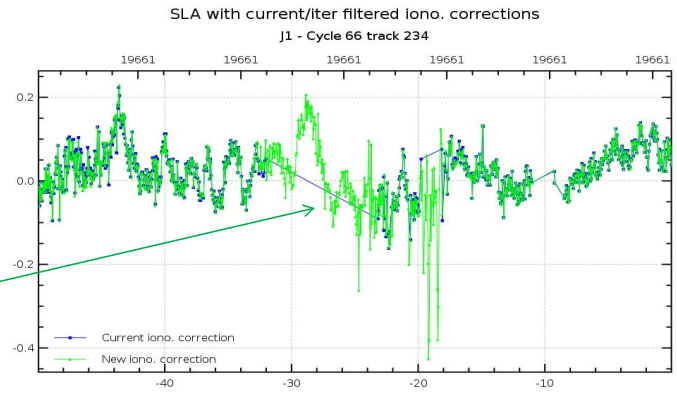

Current filtered iono. correction is not defined => *SLA is not defined*
BUT
With iter. filtering method, iono. correction is defined => SLA exists and is valid

2- Performances improvement

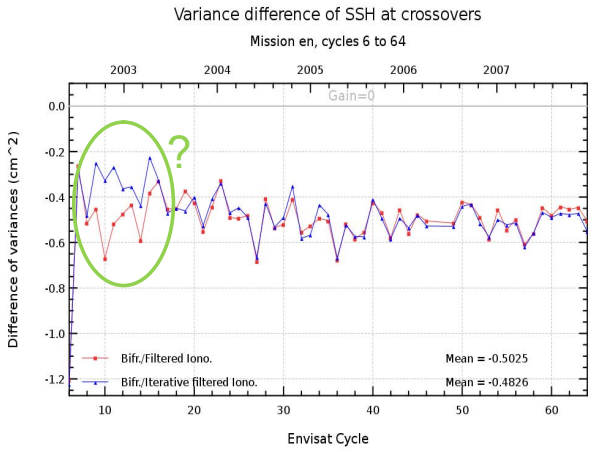

Case of Envisat

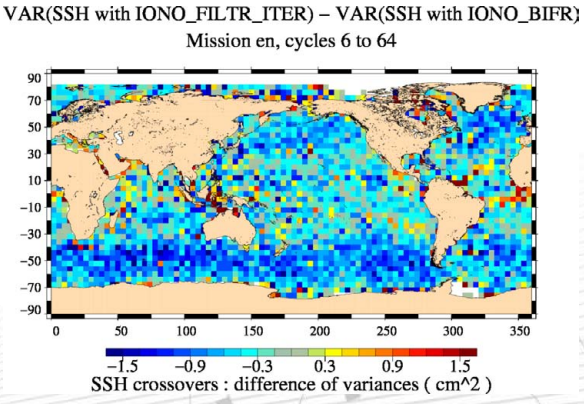

- Gain of SSH variance at crossovers for the filtered methods (0.5cm² by cycle)
- Global geographical improvement with filtered ionospheric correction.

- Why the improvement is more pronounced for current filtering method between cycle 8 & 15 (04/2003)?

2- Performances improvement

Statistics on SSH at crossovers for Jason1/Jason2/Envisat
Current filtering method Versus *Iterative Filtering method*

Statistics/Mission	Jason-1 (c 1 to c368)	Jason-2 (c 1 to 128)	Envisat (c 1 to 64)
SSH variance difference at crossovers	-0.22 cm^2	-0.23cm^2	0cm^2

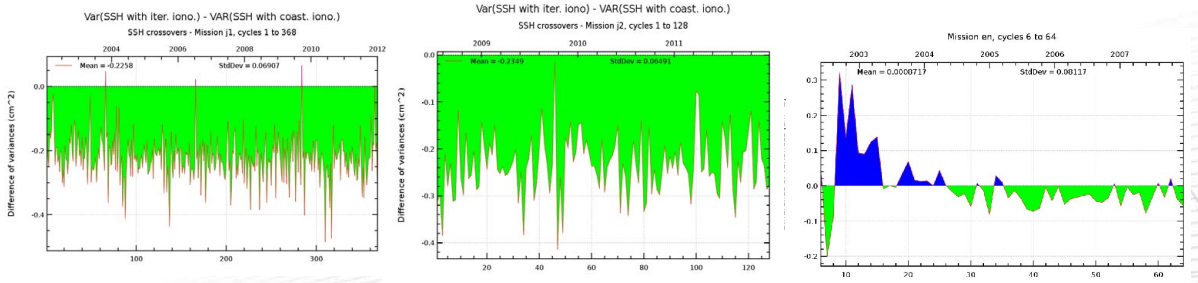

For Envisat:
- Very light degradation (0.2cm^2) for high solar activity period ➔ why?

2- Performances improvement

Geographical impact on SSH at crossovers – Jason-1/Jason-2/Envisat

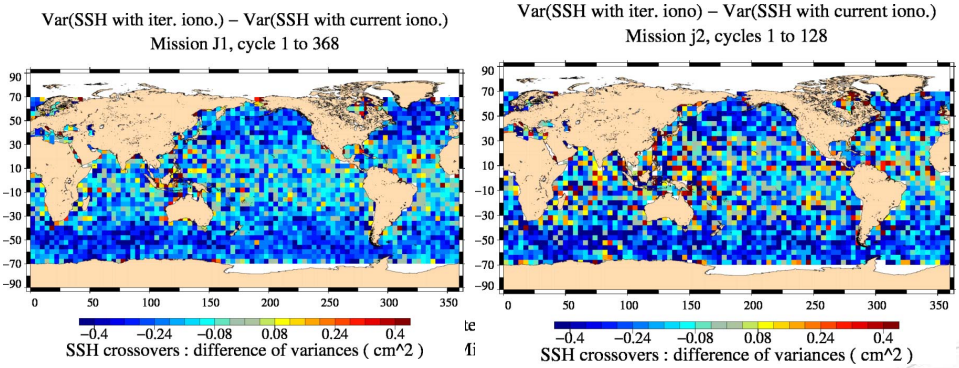

J1/J2: Decrease of variance of SSH at crossovers

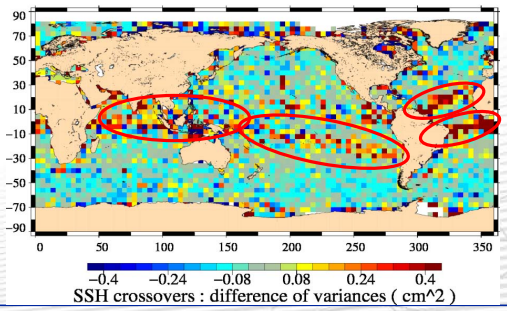

Envisat: degradation in high solar activity areas

3- Envisat: particular investigations

Envisat = heliosynchroneous mission: different behavior on even/odd tracks

Behavior different from Jason-1: specific study needed.

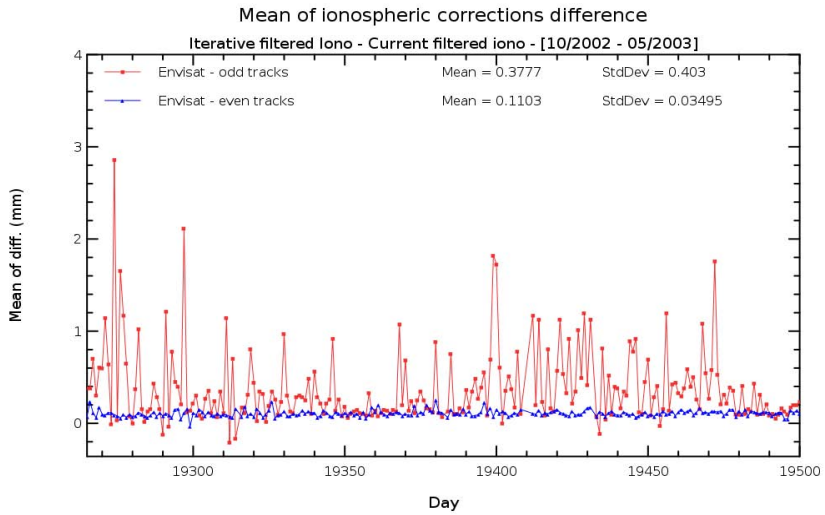

Analysis of observed degradation on variance at crossovers before cycle 25 for Envisat

Analysis of track 3 of cycle 11 (degraded variance at crossovers)

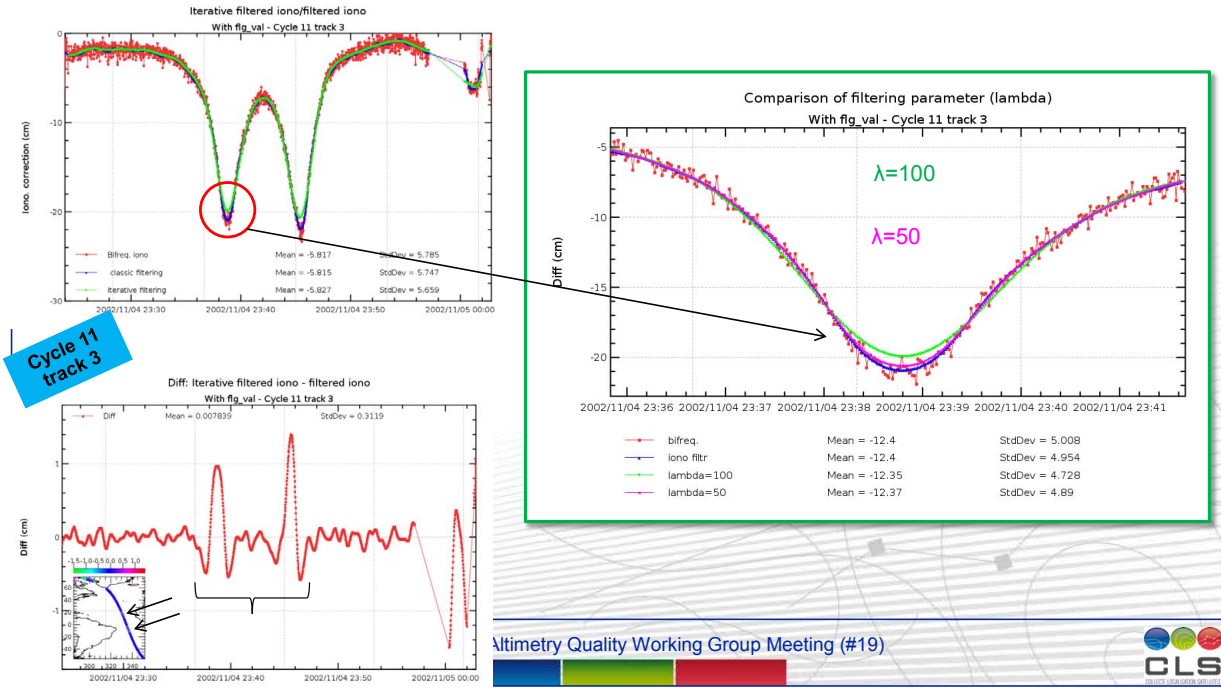

Envisat: example on cycle 11

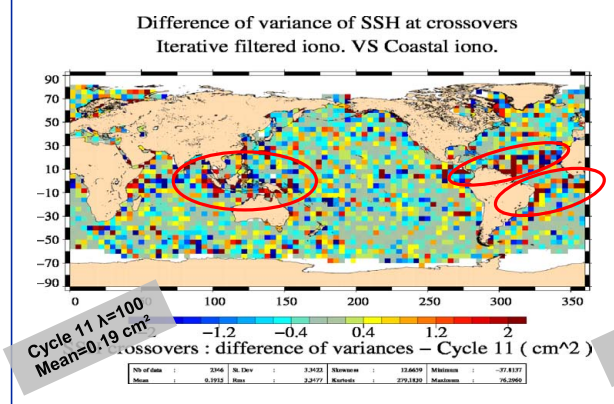

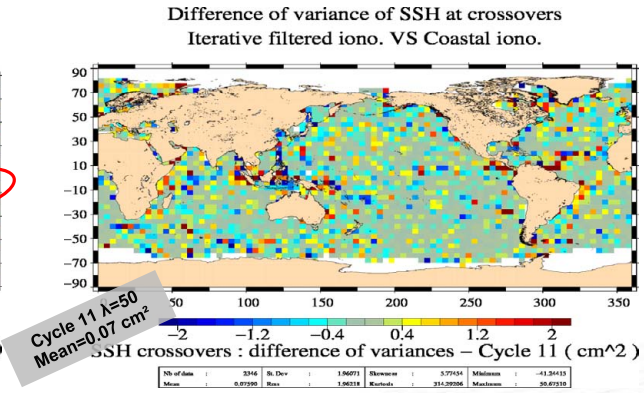

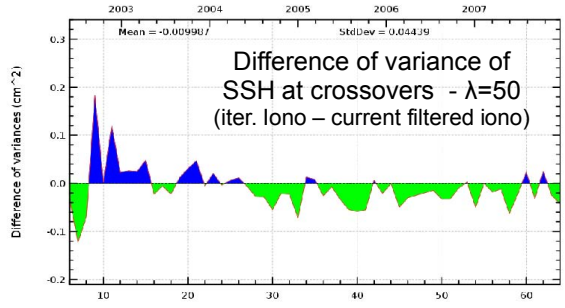

For λ=50, the global gain on the whole period is very slightly positive.

The degradation is reduced for cycles in high solar activity period without degrading the slight gain observed for the rest of the period.

Conclusion and prospects

- Gain of ionospheric correction valid data:

➔ Increase of valid data number for filtered ionospheric correction with the iterative method (wherever the dual-frequency ionospheric correction is defined, typically if MWR is missing)
➔ Increase of SLA potentially valid data number

- Performances of the system increased:

➔ Significant gain in SSH consistency at crossovers compared to :
  - bifrequency ionospheric correction: improved for the 3 missions
  - current filtered ionospheric correction: improved for Jason-1 and 2, similar for Envisat (heliosynchroneous and lower altitude).

Will be used for Duacs Delayed Time reprocessing 2013.
Feasibility of introduction in GDR to assess by ESL team.

8.1.3. GOT 4V8 ocean tide model performance assessment

The tide model GOT 4.8 is the version of the GOT model produced by R. Ray in 2011. The difference with GOT4.7 is due to a better processing of the dry tropospheric correction for altimeter data (correcting for S1 and S2 effects). The model GOT is described in [89].
GOT4.8 and GOT4.7 models have been compared in term of reduction of the altimeter residual variance and MSL signals ; 7.5 years of along-track residuals and crossovers data of ENVISAT missions have been used for the comparisons. The impact of the new model is very weak when using ENVISAT data due to its sun-synchronous characteristic. However, thanks to more appropriated crossovers DT in some areas, we notice a raise of the variance when using GOT4.8 model in the Hudson bay and in the Norvegian and the Barents seas. The global impact on SSH at crossovers is limited to $0.05cm^2$ with an amplitude of annual signal reaching $0.5cm^2$, as shown on figure 51.

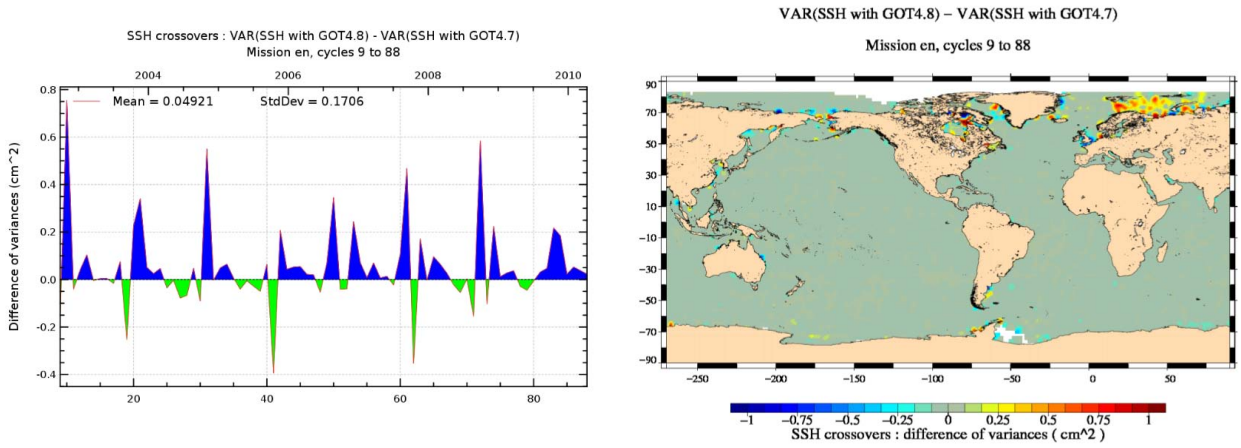

Figure 51: *Difference of variance of SSH at crossovers, comparing GOT 4V8 and GOT 4V7 Tide models*

The impact on global Mean Sea Level trend is negligeable, as presented in figure 52. Regionally the impact is limited to areas cited above. A very weak decrease of trend is visible notably in Pacific ocean and is limited to $0.025mm/y$.

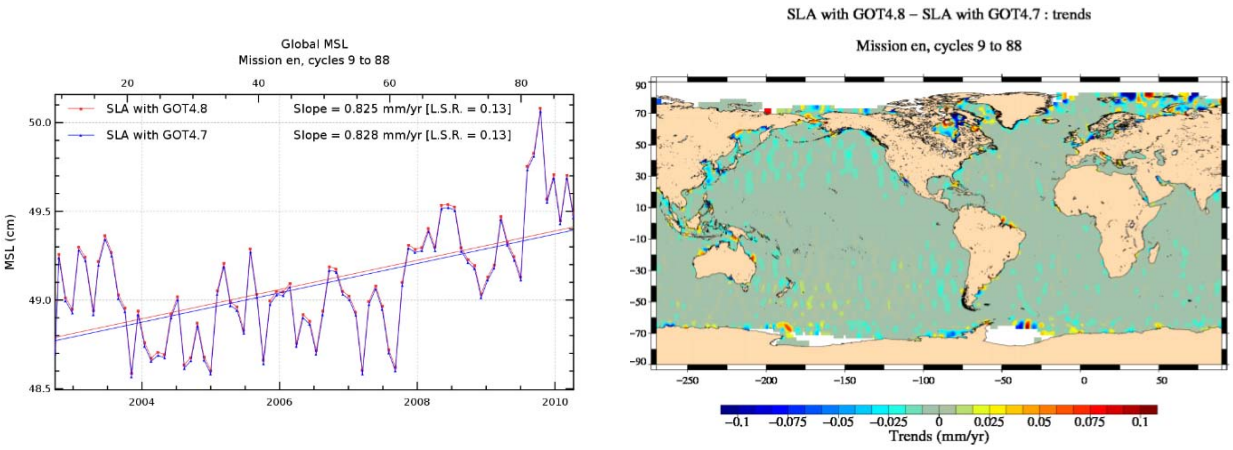

Figure 52: *Global and regional Mean Sea Level trend, using GOT 4V8 ocean tide model*

8.2. External analysis

8.2.1. Impact of orbits based on the latest gravity field: GFZ-GRGS EIGEN6S2

During the first years red patches collapsing after 2004 are observed when comparing Envisat and Jason-1 (53). They constitute a residual from the time gravity model taken into account in the GDR-D orbits (last standard available to users).

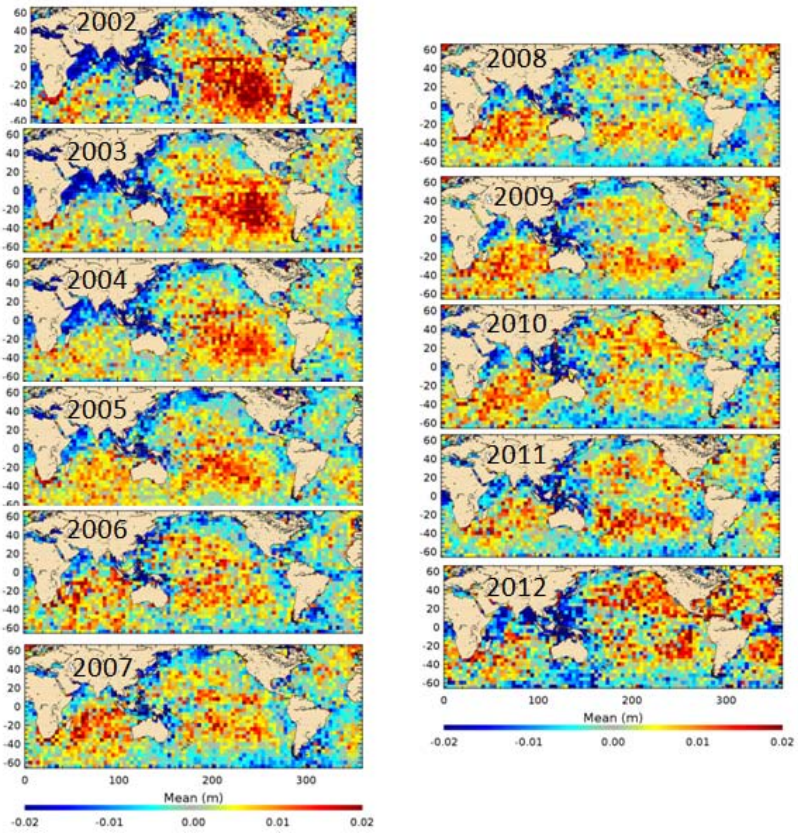

Figure 53: *Envisat/Jason-1 difference of SSH at dual-crossovers by year since 2003 using updated dataset for Envisat and GDR-D for Jason-1*

This remaining error identified last year was investigated and a new orbit, based on a more precise gravity field (EIGEN6S2) was computed and analysed:
- GDR-D standard includes the gravity field named EIGEN-GRGS_RL02bis_MEAN-FIELD (see Cerri et al. oral presentation, OSTST 2012): it is a linear fit over the GRACE period.
- for the new orbit, using the new gravity field named EIGEN6S2, the gravity field model is linear per piece over one year interval and includes interannual variability. An extrapolation is performed after 2012 with the last bias of this year and a null drift. For more information on this new gravity field consideration, please refer to http//grgs.obs-mip.fr/grace/variable-models-grace-lageos/mean_fields.

For the analyse, both orbits (GDR-D and EIGEN6S2) are compared to a test orbit, based on Grace only measured every 10 days without any model applied and constituting a very stochastic

reference considered as "the true gravity field" (Grace10days). The difference to this reference shows the errors of modeling of the gravity field.

8.2.1.1. Reduced error of the gravity fields model included in the POE

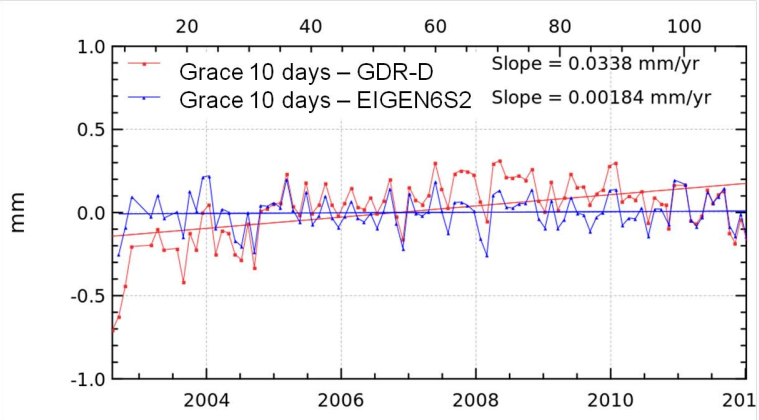

Figure 54: *Difference of orbit using 2 different gravity fields on the whole Envisat dataset with reference to GRACE 10-days gravity field)*

On Figure 54, a parabolic shape is observed on the difference between GDR-D - Grace10day POE (red curve). Conversely, using this very last EIGEN6S2 gravity field (GFZ-GRGS 2013) the (blue) curve representing the difference EIGEN6S2 - Grace 10days, is all flat.
Concerning the global long term drift, the new gravity field EIGEN6S2 has no impact (0.03mm/year, far lower than the significant limit of 0.1mm/year) but the interannual variability observed in GDR-D is well reduced. The maximum error between GRACE 10-days reference and GDR-D gravity field reaches an amplitude of 0.5mm. With the new gravity field, this error is reduced to 0.2mm and the interannual signal is well restituted.

Similarly, the regional East West patterns observed on Figure 55 between GDR-D and Grace10days (left) are well removed on the difference EIGEN6S2 - Grace 10days (right).

This study shows that taking the new gravity field into account in the POE is better to restitute the interannual variability of the signal.

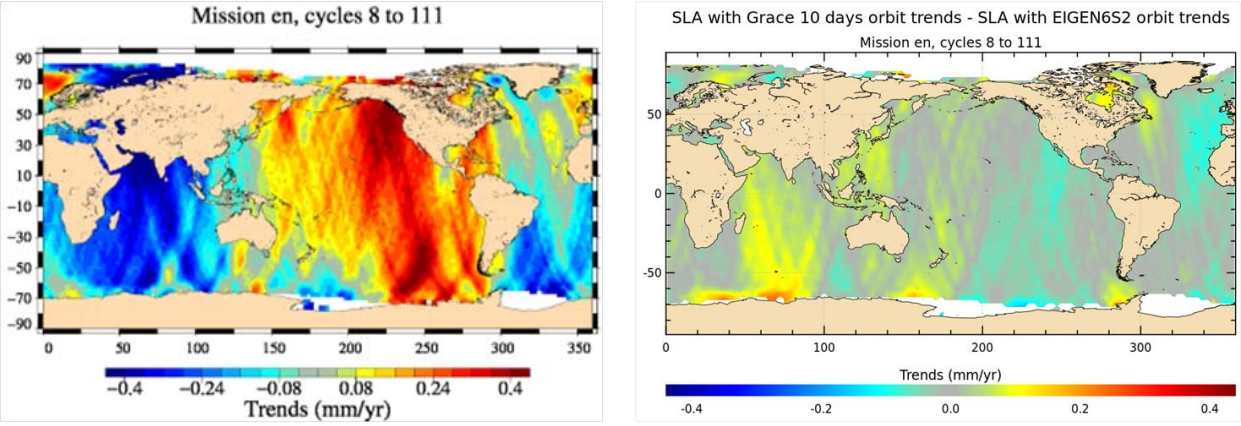

Figure 55: *Regional Mean Sea Level trend difference for Envisat using* ***Left)*** *GRACE 10 days-GDR-D* ***Right)*** *GRACE 10 days-EIGEN6S2*

8.2.1.2. Effects of gravity field update on all missions

Similar results are observed on Jason-1 and 2 (in a weaker way because they are less sensitive to the gravity due to their altitude and weight) see Figure 56.

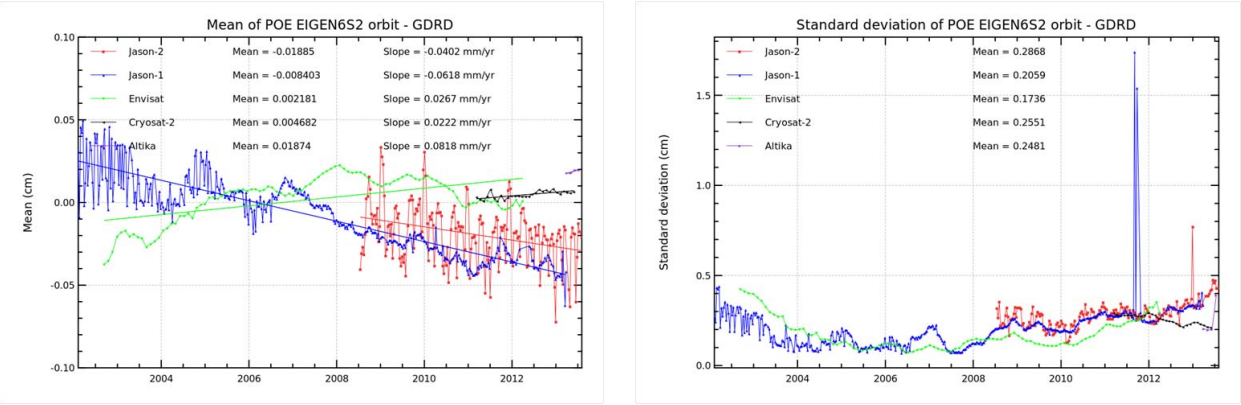

Figure 56: *Mean and standard deviation of difference EIGEN6S2/GDR-D for altimetrics missions*

For Jason-1 and Jason-2, the impact of the EIGEN6S2 gravity field compared to GDR-D is also negligible on global MSL and considered as small (but non negligible) on interannual signal.
Note that for missions with GPS (Jason-1 before mid 2006 + Jason-2) orbit difference is quite noisy. This was clarified on POD expert sides and will be solved for future standards.
The standard deviation of the difference is also higher at end of the period for the three altimetric missions, due to the fact that GDR-D gravity field was built on GRACE data for a period going from 2002 to 2011 only.

Thanks to an improvement of the gravity field modeling on different missions, the patches of dual crossovers EN - J1 are significantly reduced. Figure 57 presents the difference Envisat-Jason 1 SSH computed by year, each mission using the new EIGEN6S2 gravity field, on the whole Envisat

dataset. The East/West patches visible on this difference per year using GDR-D standard (see [16] and 53) are efficiently removed. Remaining patches now dominating between those missions (North/South effect for the beginning of the period (2002-2005)) are most probably due to a mix of other sources (wet tropospheric correction, ionospheric correction, SSB solutions,...).

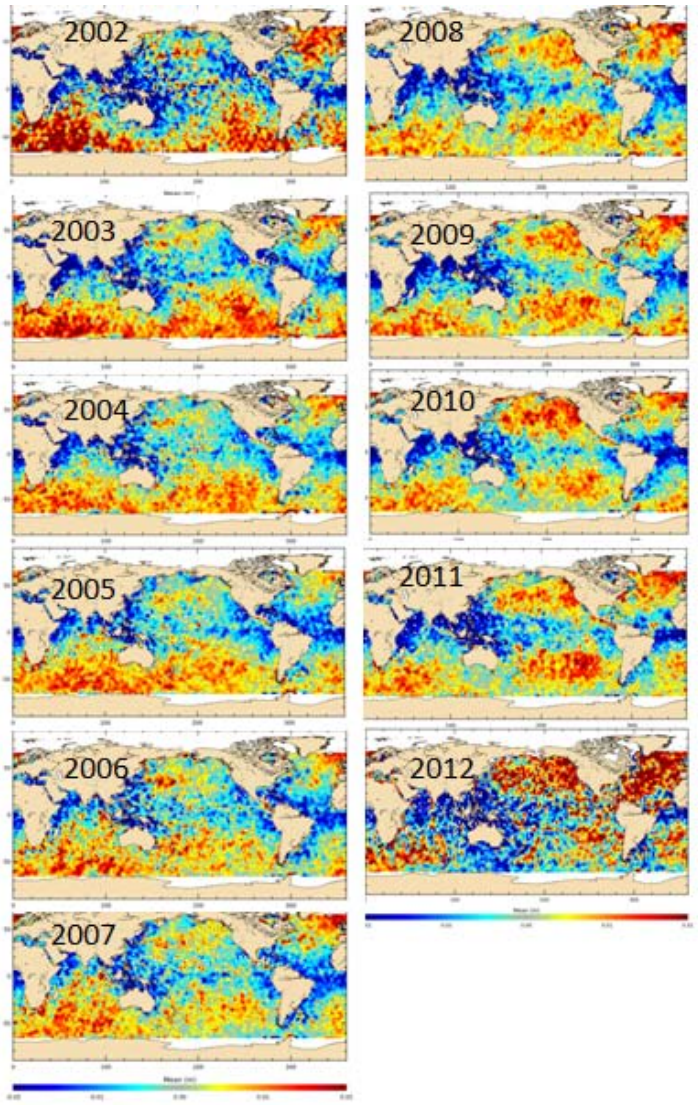

Figure 57: *[Envisat - Jason1] SSH using EIGEN6S2 gravity field for the two missions, by year*

The effect of gravity field evidenced above can be completed by the computation of Envisat-Jason 1 trend differences. This difference is presented on figure 58.
The improvement on East/West bias was clearly demonstrated using GDR-D standard, comparing to previous GDR-C standard (see [16]). With the EIGEN6S2 orbit solution, the improvement is limited, comparing to the GDR-D, but the Envisat-Jason 1 difference is more homogeneous, notably in South Pacific area.

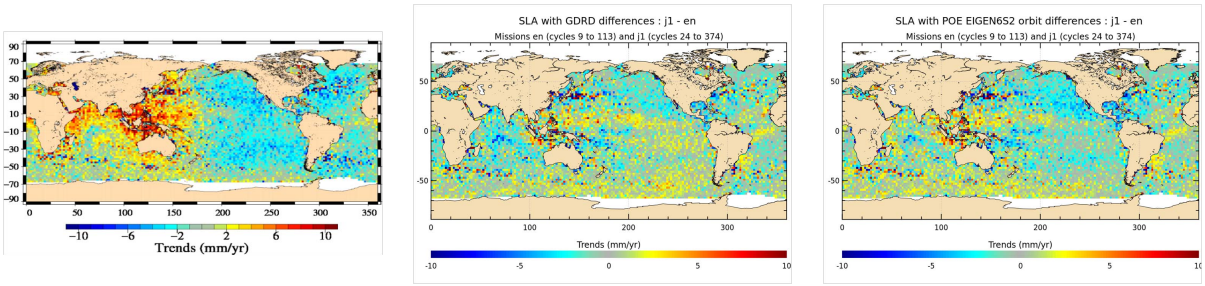

Figure 58: *Regional Mean Sea Level of dual crossovers Envisat (V2.1+)/Jason-1 using* ***Left:)*** *GDR-C orbit standard* ***Middle:)*** *GDR-D orbit standard* ***Right:)*** *EIGEN6S2 orbit standard*

8.2.1.3. Regional impact at crossovers

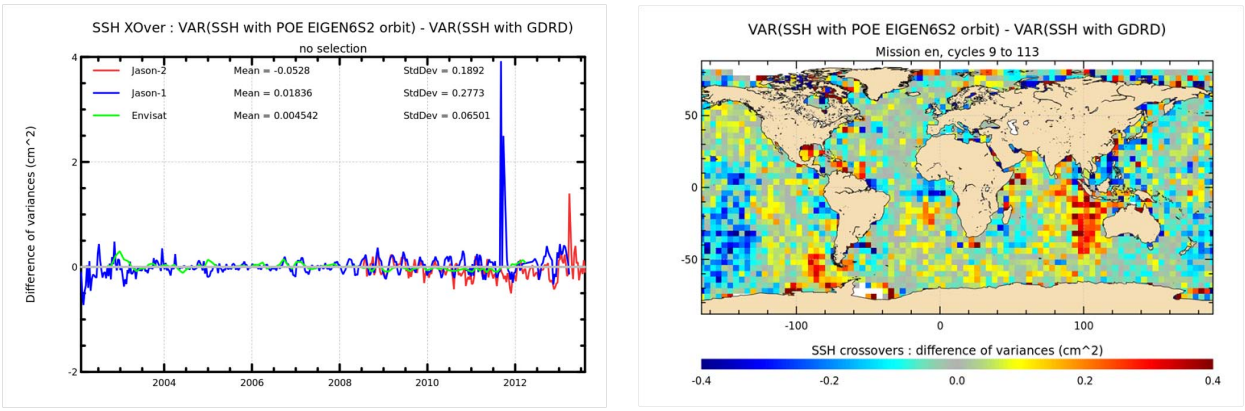

Figure 59: *Difference of variance of SSH using EIGEN6S2 gravity field against GDR-D* ***Left)*** *Long term impact for multi-missions* ***Right)*** *Regional impact for Envisat, on the whole dataset (cycle 6 to 113)*

To complete this study, the impact on mesoscale (10 days crossovers variance) is estimated and compared for both standards. Figure 59 shows a small, and not homogeneous impact (improvement in Pacific area, degradation in Indian Ocean). With the new gravity field the error made at mesoscale is comparable to the one obtained with GDR-D orbit solution.

8.2.1.4. Conclusion

Using the EIGEN6S2 gravity field instead of EIGEN-GRGS_RL02bis_MEAN-FIELD as in GDR-D standards has a negligible impact to restitute mesoscale, is not significant to change the global MSL but improves the long term evolution of regional mean sea level. Its use is recommended for Envisat and Jason-1 for climate oriented studies.

8.2.2. Envisat altitude consideration in GIM (Global Ionopshere Maps) model computation

Before the loss of the S-Band (cycle 65, 02/2008), the dual-frequency ionospheric correction is used in the SLA computation for Envisat. After this event, the ionospheric correction used is the GIM model corrected from a reference pattern (IRI: International Reference Ionosphere):

$$Ionospheric\ correction\ model = GIM\ model + IRI\ pattern$$

Another solution to compute ionospheric correction (see [100]) is to consider only a percentage of the GIM model, and not a correction factor as IRI pattern. This percentage would be linked to the position of Envisat in the ionosphere. In Sharroo et al. ([100]) purpose the ionospheric correction would be simply computed as a coefficient of GIM model. For Envisat, this coefficient is estimated at 0.856. Then the ionospheric correction model could be defined as

$$0.856 * GIMcorrection$$

A study was carried out in 2012 to analyse this new definition of ionospheric correction model and to compare GIM model with and without IRI pattern.
The potential effects on sea surface height and Mean Sea Level were also estimated.

The ionospheric correction, as defined by a coefficient of GIM model, is more consistent with filtered ionospheric correction for the beginning of the mission (before 2003). After this year, the phenomenon is reversed: the GIM model corrected from IRI pattern is more consistent with filtered correction throughout the Envisat mission, for odd and even tracks.

The mean difference between the two correction after cycle 65 reaches 1.1mm, but the trend of this difference on this period is 1 mm over 4 years (2008 to 2012).

In term of variance of SSH at crossovers, using GIM model without IRI pattern slightly degrades the performance on the whole Envisat dataset.
The impact on Mean Sea Level trend is very weak and limited to period after cycle 65.

After this analysis, **this solution won't be selected for the next reprocessing and the GIM correction which will be used will continue to take into account the IRI pattern** as the reprocessing performed in 2012.

Analysis of GIM without IRI correction in SLA computation

Impact on MSL

Subject

- For Envisat, before the loss of the S-Band (cycle 65, 02/2008), the bifrequency ionospheric correction is used in the SLA computation
- After this event, the ionospheric correction used is the GIM model corrected from a reference pattern (IRI: International Reference Ionosphere).

  Iono correction model = GIM model + IRI pattern (JPL)

- The GIM model takes into account the whole content of ionosphere. But Envisat IS in the ionosphere…

  ➔ Need to consider only the content of ionosphere UNDER the satellite? Via the IRI model (in RA2 products).

➔ BUT Remko Sharroo says that (Remko Scharroo/Walter H. F. Smith: A global positionning system-based climatology for the total electron content in the ionosphère/October 2010)

> For Envisat, using GIM+IRI is equivalent to 0.856*GIM

ENVISAT Altimetry Quality Working Group Meeting (#19)

Analysis of GIM without IRI/GIM beahviors

Regression coefficient, computed by cycle, for ascending (night)/descending (day) tracks between:

GIM Iono. correction Vs Filtered Iono. correction for GIM ionospheric correction with/without IRI pattern

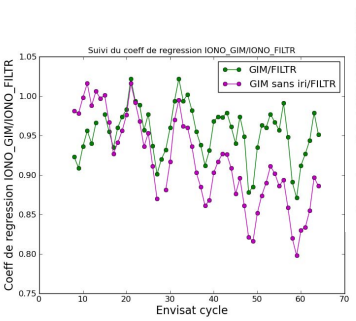

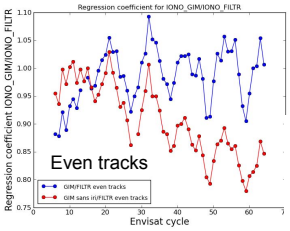

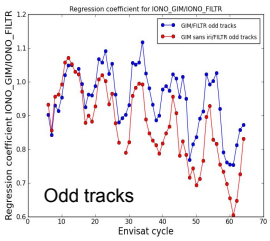

•Before 05/2003 (cycle 15): Iono. GIM without IRI pattern is more coherent with bifrequency iono. correction

•After 05/2003, the phenomenon is reversed : GIM model with IRI pattern is coherent with bifrequency iono.correction, whereas the regression is descreasing for GIM without IRI.

Iono. corrections differences

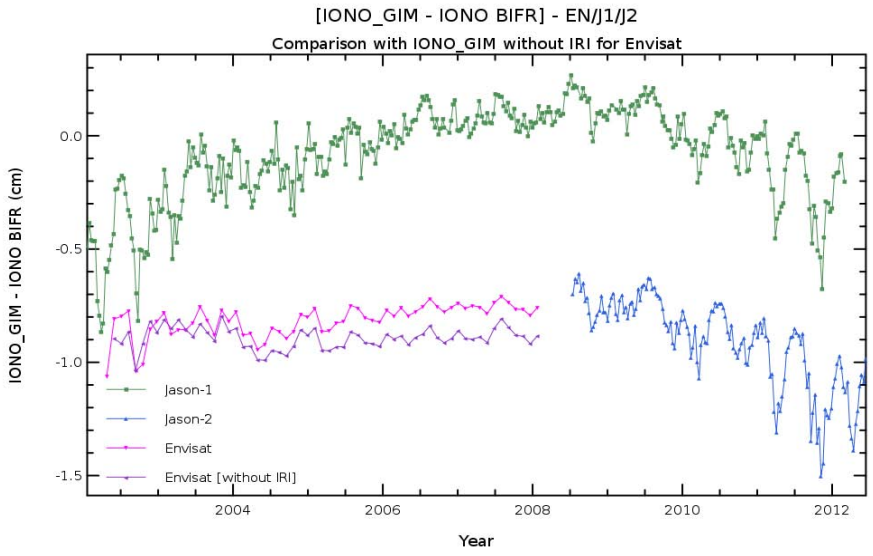

Statistics on difference: GIM without IRI/GIM

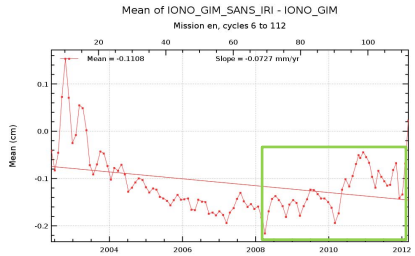

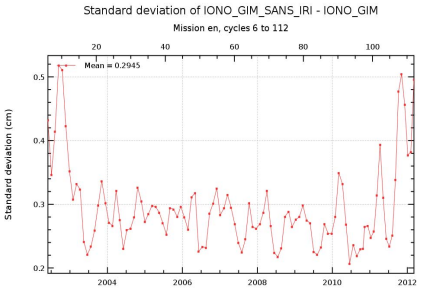

« GIM » = [GIM model] + [IRI pattern](JPL)
« GIM without IRI » = 0.856*[GIM model]

Mean bias between the two corrections: -0.11cm

If we consider the period during which the GIM correction is used (after cycle 65):

⇒The trend is close to 1mm over 4 years (2008 to 2012)

Impact on Envisat MSL

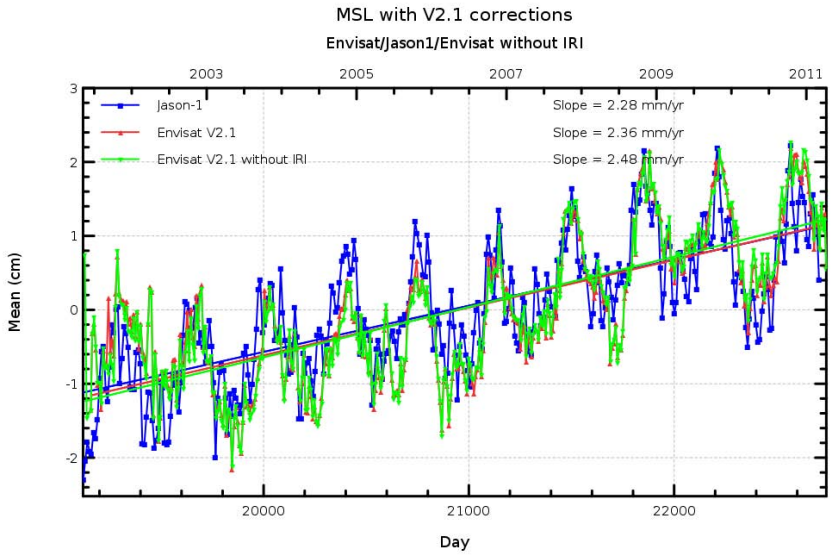

SSH at crossovers

• Degradation of variance of SSH at crossovers : +0.034 cm² on the whole serie.

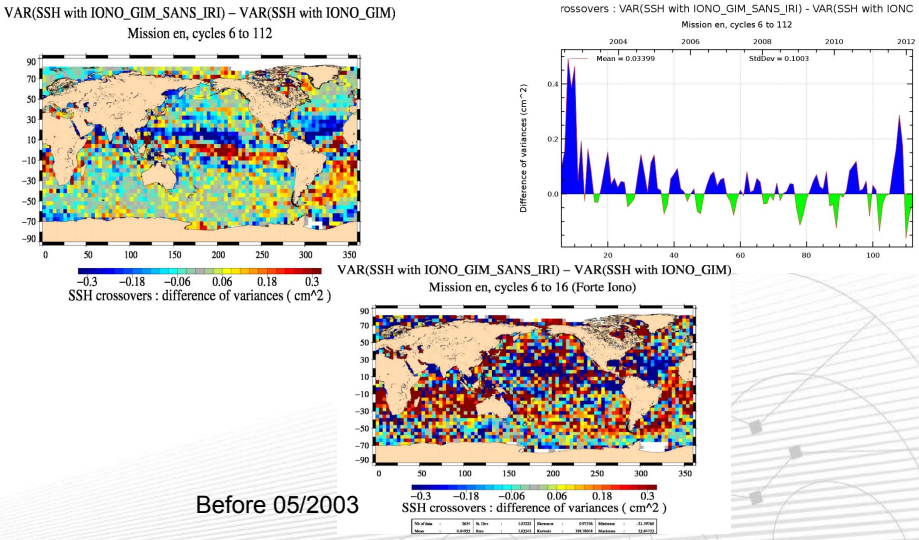

Before 05/2003

Conclusion

- Correction without IRI pattern consistency with bifrequency ionospheric correction is less stable than GIM corrected from IRI.
- Variance of SSH at crossovers is slightly degraded using GIM model without IRI pattern.
- MSL computed with GIM model without IRI pattern is similar, compared to the Envisat V2.1 and J1 mean sea level trends (impact limited to after cycle 65).
- Not recommanded for future reprocessing

8.2.3. Instrument effect suspected at QWG 19

The interannual variability of Envisat MSL is questionable (see detrended curve compared to Jason-1's).
An instrumental issue is not excluded and a potential correlation was suspected with a parameter related to the waveform (shape and jumps apparently simultaneous on msl and 2 parametres).
This parameter: the IFF slope (slope of the mask applied on waveforms) provided by isardSat was therefore superimposed to check the concomittence (figure 60) of the two curves. The consistency between both curves was not demonstrated and the pist was abandonned.

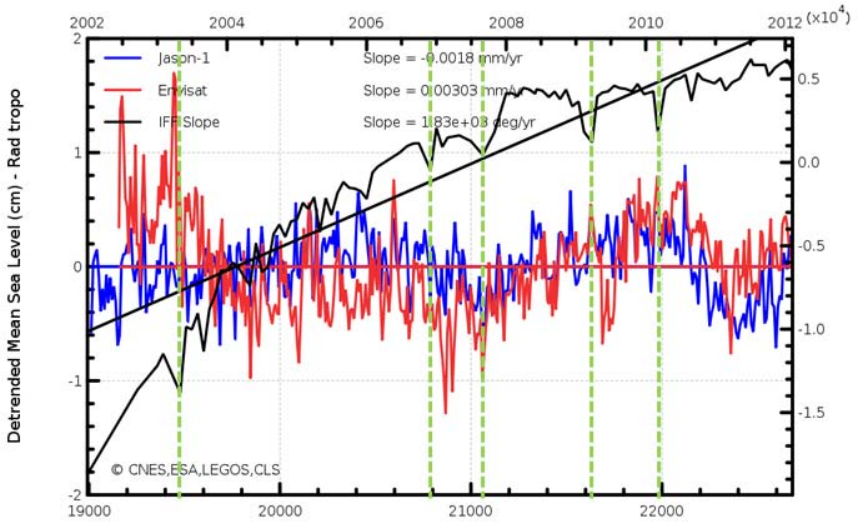

Figure 60: *Superimposition of MSL trend (CLS) and IFF Slope (isardSAT)*

Note that this exercise however evidenced the fact that during the B-side period, the waveform slope is extremely different than for the other periods (figure 61) and with an opposit sign. This is plotted here, for the record.

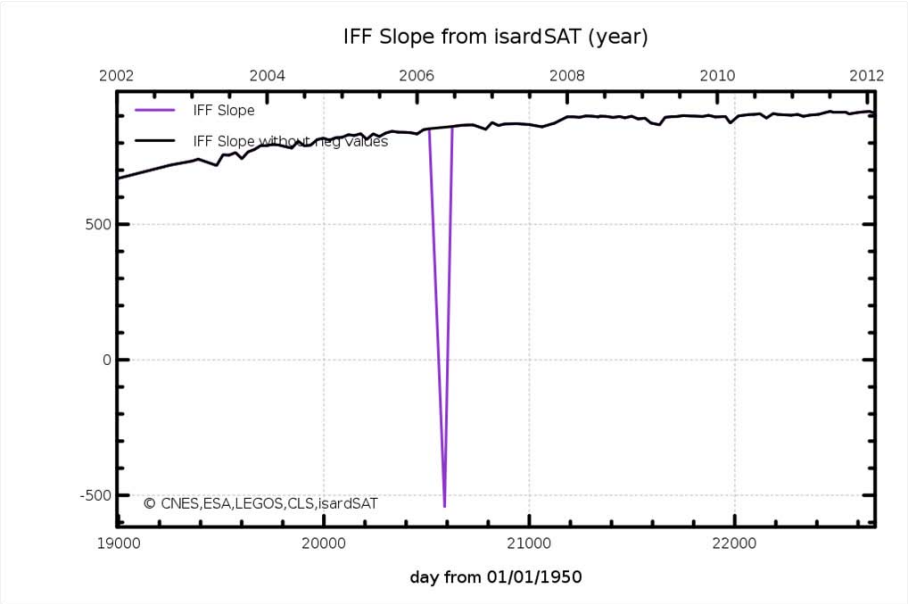

Figure 61: *Very different behavior of Side-B waveform slope.*

8.2.4. Significant Wave Height evolution towards a climate dedicated multimission product

This year a training course was realized at CLS to better characterize SWH estimated from altimetric missions. For this, comparisons between different missions were analysed directly. Comparisons to an external model from ECMWF (ERA-Interim) were performed too. This work was aiming at better characterising the biais and stability of the missions in estimating this parameter. Unexpectedly, the study also enabled to characterize the ability of the model taken as a reference to restitute the long term variations, potentially used for climate studies.

8.2.4.1. Selection of significant wave height data

The study was performed on a set of valid data of SWH, relying on a specific selection (less restrictive than the one usually used for SLA validation purpose). This selection takes into account the ice recognition, as it is currently made for SLA selection, but the maximum threshold on SWH data is relaxed to 20m and waveform mispointing values are limited at $[-0.2; 0.16] deg^2$. With this new selection applied for Envisat, the number of SWH data considered as valid is increased by 3% compared to the current valid data number. For instance measures without radiometer corrections are marked as invalid for SLA validation purpose but the correspondant values of SWH can be usable. The SWH data gained with the new selection for cycle 55 are presented on figure 62.

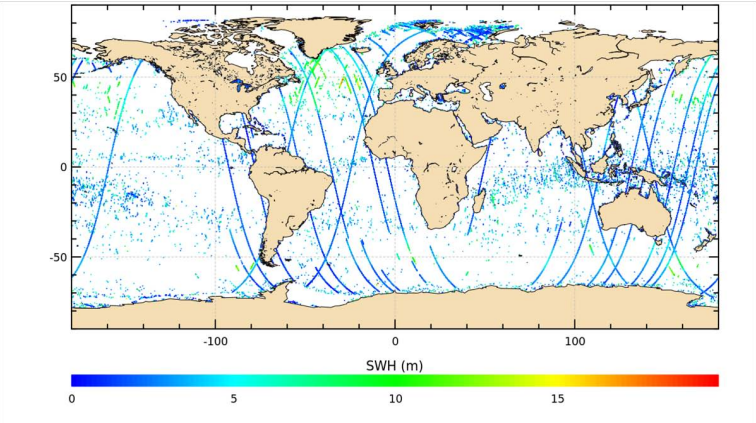

Figure 62: *SWH additionnal valid data, obtained with the new specific selection (cycle 55)*

Relevant values of SWH are recovered in North Atlantic (around 11m). Some entire tracks are now considered as valid on SWH critria.
This analysis shows that coherent waves can be recovered with a more refined selection, increasing the number of relevant SWH data for Envisat.

8.2.4.2. Long term SWH analysis

The long term analysis of SWH data (figure 63) shows that Envisat, Jason-1 and Jason-2 are globally in agreement whithin a variability of around 10cm (solid lines) and the bias compared to

ERA-Interim model is below 5 cm (on the plot 63, 50cm bias was introduced for more lisibility). Note that on Topex/Poseidon, a strong anomaly is observed between 1997 and 1999 whereas it is not present in model data. This effect is known and already published.

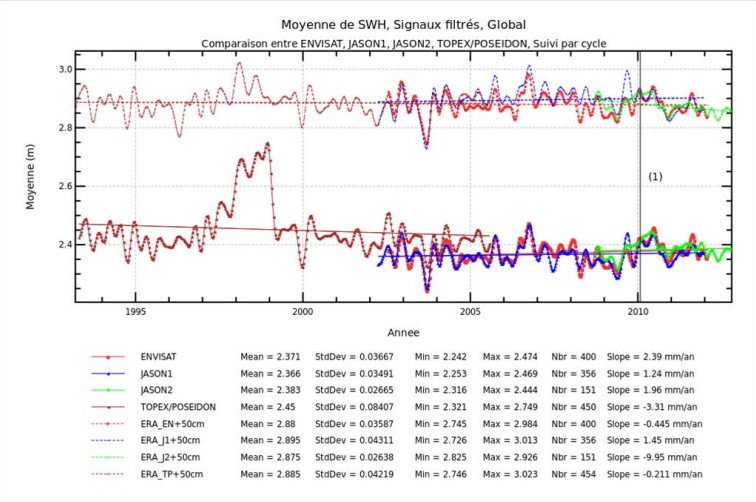

Figure 63: *Long term SWH signal for altimetric missions (Mean per box of* 2 deg*X*2 deg*, over 10 days)* ***Top curve:*** *ERA-Interim model* ***Bottom curve:*** *altimeter data - (bias of 50cm between the two curves introduced for more lisibility)*

The comparison of alti/model highlights that the dispersion between altimeter data are of the same order as the dispersion between models interpolated along track data. This highlights the fact that:
- altimeter data are consistent
- the differences are due to the sampling of a phenomenon with short correlation scales (for a same zone, satellites and models don't measure the same waves at the same moment).

Working on the difference between alti - model directly enables to get rid of most of the temporal/spatial variability (the model is sampled at 6 hours temporally and grids spatially).
The difference (figure 64) between altimetric and ERA-Interim model is below 5cm for Envisat, Jason-1 and Jason-2. But such plot also enables to show discontinuities in the series.
Knowing the standards used on altimetry side, the jump in 2010 is due to the model.
Actually, the model assimilates non homogeneous altimeter data (Nrt data, on the flow). For instance, they assimilate Envisat real time data, suffering from a jump at the time of standard upgrade in december 2010 (see [84]). The difference observed here is therefore a signature of the altimetry difference between before and after reprocessing Envisat off line products SWH data.
The discontinuities introduced by such time series assimilated affects the model and it is visible on the differences alti -model for all missions.
This phenomenon is interesting and underlines the fact that, even if ERA-Interim is a reanalyse, homogenous on the whole series in terms of model version, it does present some discontinuities via the data it assimilates. This limitation would prevent it from being a reliable model for climatic studies.

For such applications, the altimetric data should be homogeneous delayed time products.
By now, the GDR products only partly fills in such request...
A different dataset could be set in place, including a multimission merging, more relevant for climate

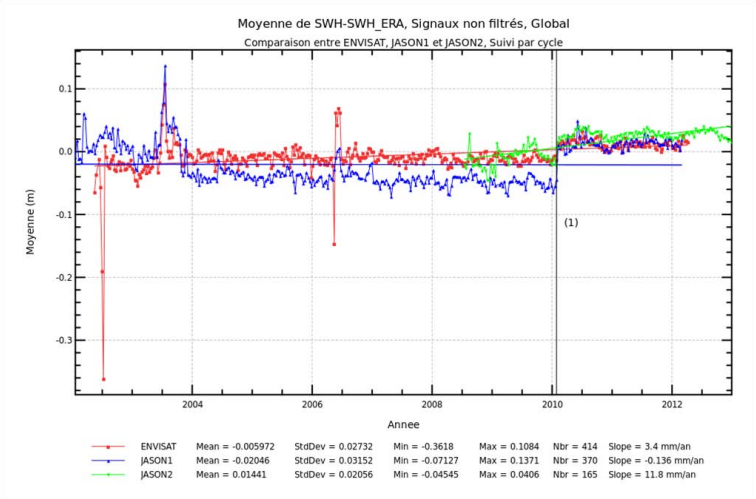

Figure 64: *Difference between SWH data and ERA-Interim model for Envisat, Jason-1 and Jason-2*

studies.
For ocean modeling, the assimilated altimeter SLA data consist of gridded (or along track) products merging all altimetric missions (DUACS system). The merging consists in computing biases map between mission, correlation distances.
This work could be envisaged for SWH.

8.2.4.3. Towards a SWH merged product in DUACS?

To obtain a multimission product, a merging would be necessary.
To merge data, bias would be estimated at large and smaller scales (equivalent of orbit error and Long WaveLength correction). But the bias can be estimated as long as the consistency between mission is sufficient enough. Therefore, an estimation of the maximum of correlation was done in order to determine the sampling period of SWH data.
The computation was made for Envisat and Jason-1, and a sampling period of 500 days was optimal to maximize the correlation between SWH data of the two missions, as visible on figure 65. Averaged over this period, the physical information is more correlated and would ease the computation of a multimission product.

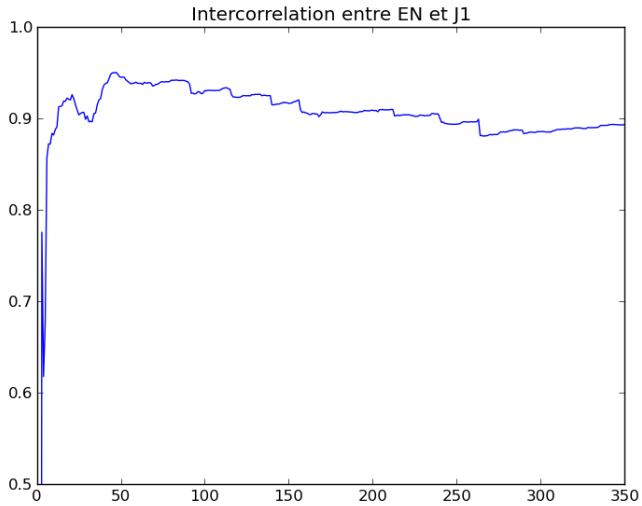

Figure 65: *Maximum of correlation for SWH data between Envisat and Jason-1, in 10-days unit*

8.2.4.4. Analysis of SWH dispersion

To estimate bias at smaller scales, systematisms between mission should be removed.
For this, the dependancy of SWH bias per class of SWH was computed, thanks to a comparison to a model in order to have finer and less noisy plots.
Figure 66 left presents the difference between altimetry and ECMWF-ERA model depending on waves ranges, for Envisat and the Jason's missions. This plot shows that the deviation from model is more important for low waves for Envisat ($< 1m$), contrary to the other missions (see error budget dedicated part). This effect was shown in 2013 (FPac activities, Thibaut et al.) to be solved by corrections tables computed by comparing retracked data with the real PTR or with an approximation of it.
For Jason-2 the plot is on the contrary very clean because such correction were already applied directly in the products.
On Figure 66 right hand, the same plot was done, after correcting altimeter SWH by empirical polynomial corrections described in [88] and obtained when comparing altimetry an in-situ data. The fact that the dependancy alti / ERA-interim model is reduced when using these corrections shows that the model is a good reference to estimate altimeter errors (as good as in situ data).

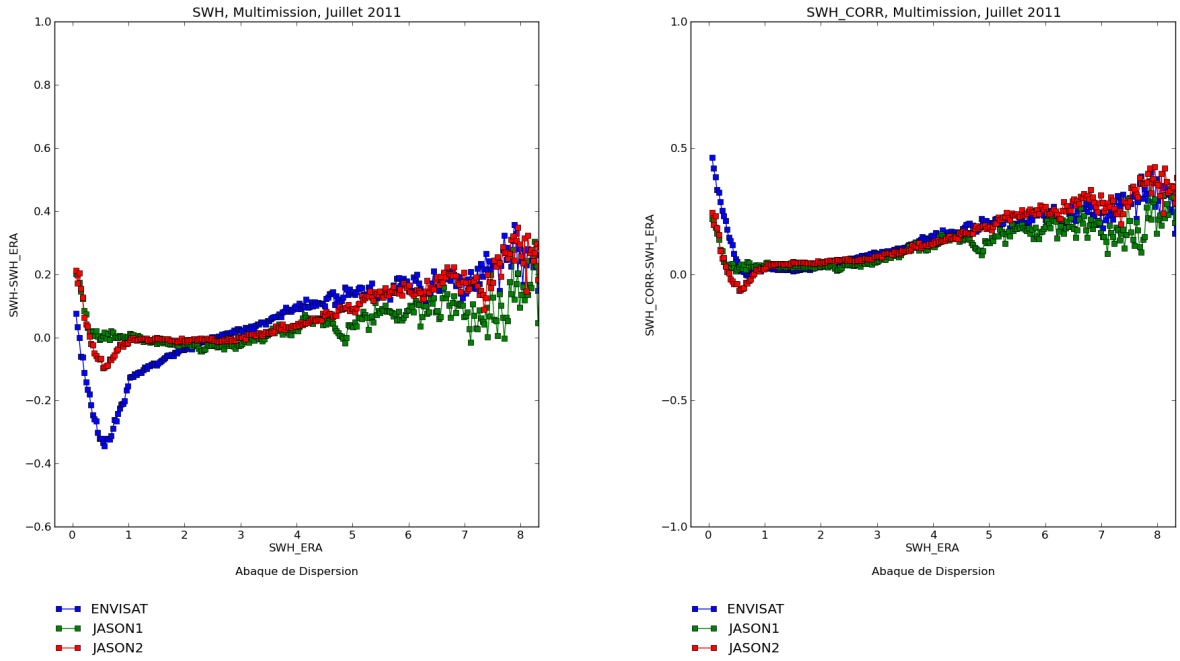

Figure 66: *Dispersion of difference SWH-ERA model against SWH altimetric data* ***Left:*** *before correction* ***Right****: after correction*

8.2.4.5. Conclusion and prospects

The use of ERA-Interim model in comparison to altimeter SWH estimation is very fruitful.
It enables to detect finer discrepancies between altimetric missions than what the direct comparison enables.
For short wavelength and systematism as function of SWH, this reference is very reliable (similar results to alti/in situ comparisons).
However, for climatic scales, the assimilation of Near Real Time altimetry in ERA-Interim model is a problem because it introduces jumps and inhomogeneity in the model.
To avoid this, 2 prospects are envisaged:
- The same exercise could be done again with non assimilated models (hindcast version of ECMWF).
- A homogeneous merged altimetry product could be created and given as an input to the models

The first prospect would enable a better characterisation of the long term trends on different missions.
It would also ease the bias computation used in the merging process proposed for the second prospect.
A merged dedicated altimeter product would be a good basis for models and could be analysed as a climate indicator itself.

Working on the production of SWH products for applications was already envisaged in the frame of the European GlobeWave project without the merging step.
In Duacs, SWH are made available also without the merging step. The experience of Duacs system on SLA side would certainly be a precious competency to improve such product.

9. Error budget of Envisat Altimetry Mission - October 2013 update - V2.1+ version, with anticipated updates

1. Introduction

This document is a synthesis of the error budget estimated for the whole mission for Envisat altimeter (RA-2)ś level 2 OFL products. This takes into account the homogeneous reprocessed data set, achieved in January 2012.
Estimating the error budget in altimetry is a hard work principally because of the lack of absolute reference. It can however be estimated by comparing corrections from different sources of estimation (typically measurements/models or measurements/in situ data,...)

The global Envisat altimeter error budget (for level 2 OFL products) may change during the mission lifetime considering corrections improvements (this effect is much reduced thanks to the reprocessing exercise), on ageing of devices or geophysical interannual effects.
In 2013 V2.1 reprocessed dataset was enhanced on several aspects. The V2.1+ dataset is an anticipation of future reprocessing in an expertise maintained database at CLS and for DUACS purpose. This dataset brings together the following altimetric corrections updates:
- PTR with an impact on Global Mean Sea Level (see [6] and Ollivier 2012 et al.);
- POE standard with an impact on Regional Mean Sea Level (see [6] and Ollivier 2012 et al.);
- Sea Surface Bias with an impact on performances at crossovers and on mean of SLA (see [7], particular investigation on SSB).
- The GOT 4V8 Ocean Tide Height is now the new correction used in SSH computation;
- The iterative filtered ionospheric correction is now used in SSH computation;
- Finally, a new radiometer wet tropospheric correction has been developped by CLS experts team to correct the degradation of mesoscale error observed after reprocessing.This new correction is named V2.1b.
These updates were analysed in the view of the next reprocessing.

The table hereafter sums up the Envisat altimeter error budget for the whole Envisat period compared to the specificationś allowed budget. The impact of anticipated updates is indicated if needed.
Each figure of the table is associated to a small paragraph including:

- comments on the method used to quantify them
- comments on the stability of the given value.
- reference documents.

Particular events:

- In 2012, Envisat was entirely on its drifting phase. The 35 day cycle was reduced to a 30day pseudo cycle with a small drift estimated to +/-1.7km per cycle maximum at respectively 50deg Latitude N/S, whereas it does not drift at 38deg N and S. Note that the drift was observed to be higher than the one theoretically expected (+/-600m per cycle maximum was expected). The impact on the data was already described in last year yearly report. Only a weak impact is noticed in the data quality (the visible impact concerns the SLA standard deviation) and the new Mean Sea Surface was shown to erase almost all this impact (see [5]).
- The Envisat whole mission reprocessing ended on January 2012. The ground processing chains had been upgraded to support reprocessing, this new standard is called V2.1. The

impact of this new version is detailed in [10], and the Error budget obtained with reprocessed data was available at the end of 2012 (see [7]).
The Error budget estimation presented hereafter is computed with the reprocessing version and the new V2.1+ updates cited above.

- On April, 8th 2012, the communication with Envisat mission was definitively lost. Its data quality remained stable and very good until the end. The end of operation was announced in May 2012, however, this Error budget document is likely to be updated after the end of the mission, thanks to delayed time future reprocessing and improvement of the global altimetric system.

2. Term by term altimetric error budget

2.1. a/ Altimeter noise

A slight seasonal signal is visible on the mean RMS of Ku 20Hz. Higher values correspond to higher waves occurring during the austral winter. The mean value is about 9.1 cm. This value represents a rough estimation of the 20 Hz altimeter noise (Zanife et al. 2003 [17], Vincent et al. 2003a [16]). Assuming that the 20Hz measurements have uncorrelated noise, it corresponds to a noise of about 2 cm at 1Hz.
The High frequency content of range parameter (noise level) reaches its maximum during the last cycle, but remains stable in 2012.

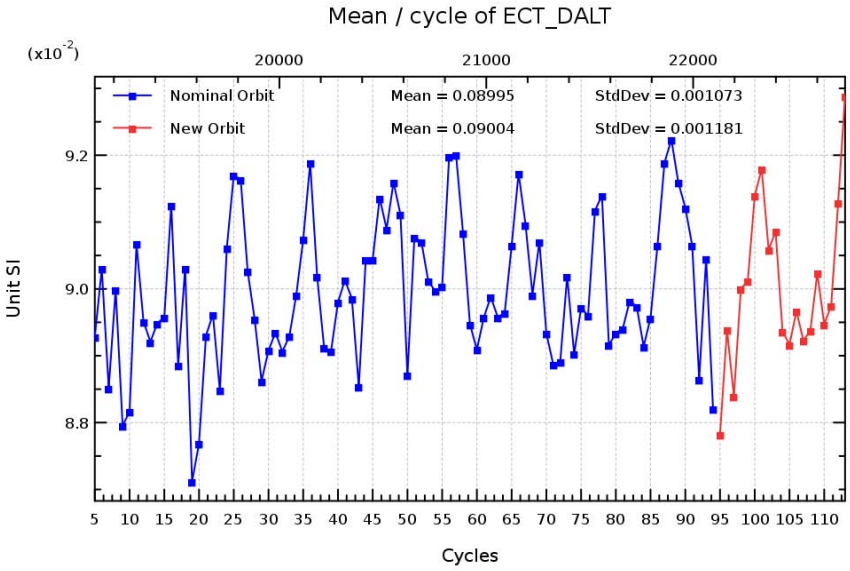

Figure 1: *Mean of range sdt. deviation, by cycle*

2.2. b/ Sea State Bias

Estimating the absolute sea state bias correction error is relatively difficult (see [13]). Since most SSB estimators are computed as a function of SWH and altimeter Wind Speed, the first approach is to use a Gaussian assumption, and a direct dependence between the random noises on the input parameters. Our current knowledge on SWH and SIG0 is synthesized in chapter 5.3 and 5.4 of [13].
This don't represent an absolute reference but long term monitoring mean and standard deviation of SSB give information on stability of this parameter. Studies concerning the SSB noise was also performed and explained during SLOOP project ([4]). This sea state bias mean is stable around -14cm with an annual cycle linked to the seasonal repartition of high/small waves. The standard deviation of SSB (including ocean variability) is now homogeneous on the whole time series, using the 2007 Labroue Non Parametric Bias. The standard deviation is between 6cm and 7.5cm according to a seasonnal signal and 6.3cm for 2012. A part of this standard deviation is linked to a slight degradation of the average SWH in the reprocessed version (see §3.2).

In 2012, a new SSB has been computed (Tran et al. OSTST 2012), not included in products yet.

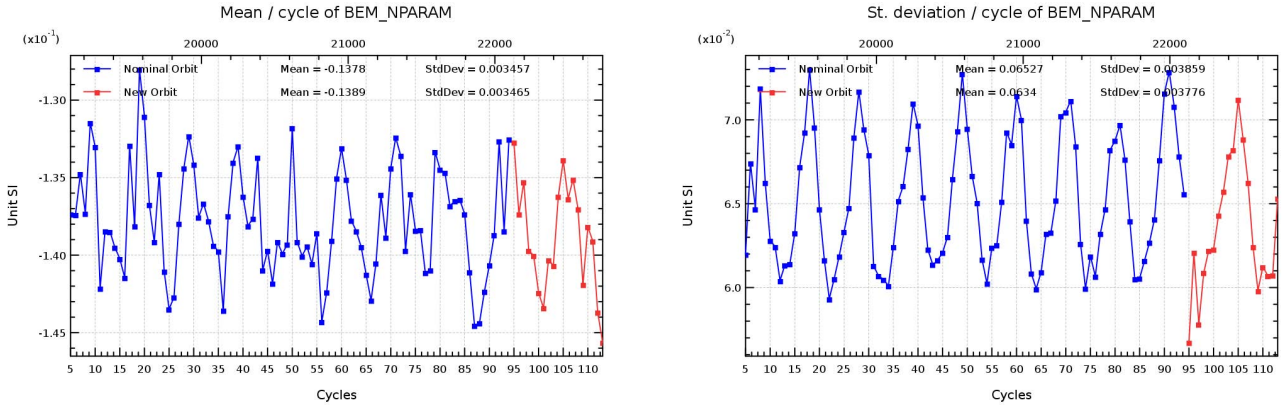

Figure 2: *Mean and Std. Dev of Sea State Bias by cycle*

2.3. c/ Ionospheric correction

Due to the S-Band loss on January 17th 2008, the bifrequency ionospheric correction is no longer available. A comparison to the GIM model ionospheric correction during 2007 and a cross comparison between Envisat and Jason-1/2 and the GIM model during 2010 enables to get an acceptable value. The comparison to the GIM model ionospheric correction during year 2007 gives a standard deviation of 0.7 cm. As described in Envisat Yearly report 2010, a 280km Lanczos Low pass filter enables to reduce this variability to 0.4 cm. Cross comparison of bifrequency ionosphere to the same GIM model ionospheric correction for Jason-1/2 shows that the statistics are rising slowly. This is related to the slight increase of solar activity.
The ionosphere quality is affected by the S-Band loss from January 2008 onwards. In 2012, the quality of the GIM ionosphere correction continued to be slightly degraded whereas it was stable until 2011. In fact, the degradation was observable in 2012 at crossovers as seen on figure 6 (last cycle of Envisat lifetime).

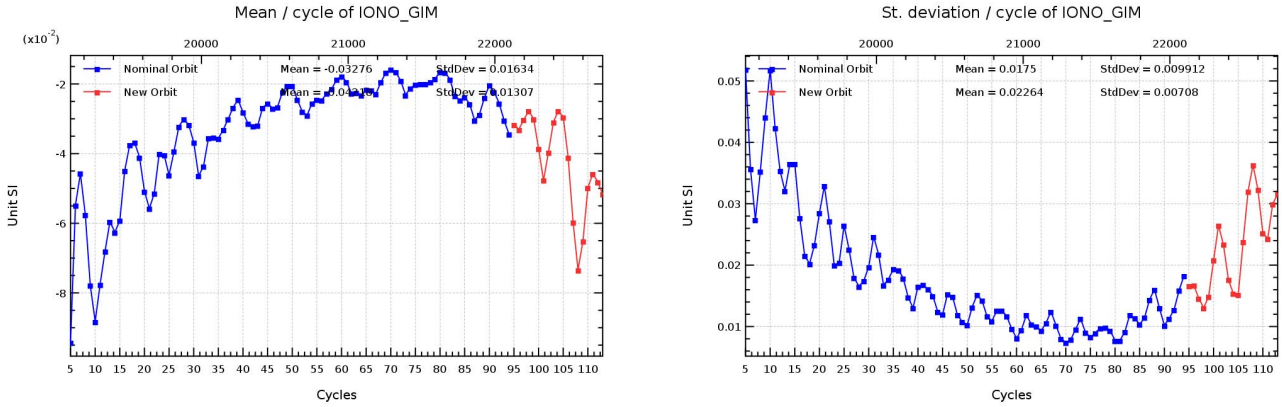

Figure 3: *Mean and Std. Dev of GIM ionospheric correction by cycle*

Since the S-Band loss, Envisat iono correction was efficiently replaced by the JPL GIM model. But the solar activity (reprensented by a higher value of the mean correction) is increasing again since mid 2009 following a 11 year period signal (see 4 left hand plot). The monitoring of the difference iono GIM-Bifrequency correction on Jason-1 and Jason-2 (see 4 right hand plot) enlights that the error on the model is higher when the solar activity increases (around 5mm more than in 2008). The GIM model is therefore becoming less and less efficient for Envisat as observed on the signature on plot 5 compared to 6.

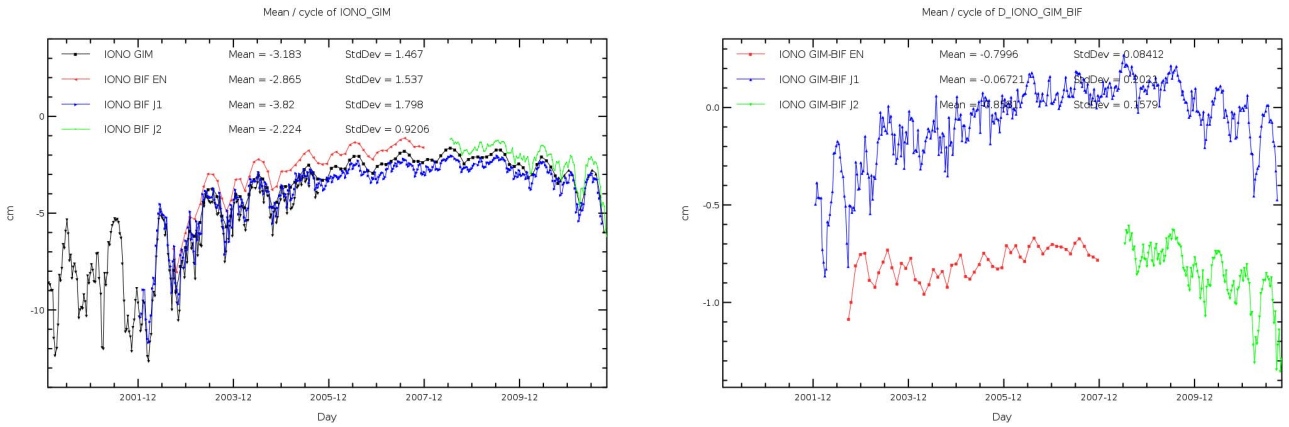

Figure 4: *Ionospheric content over the 11 last years observed by different missions (left). Difference to GIM reference (right).*

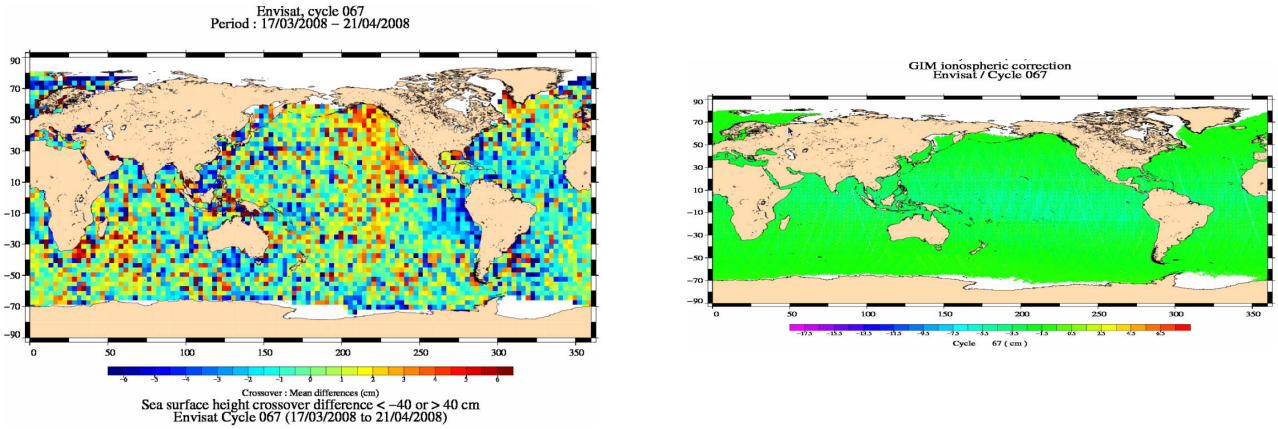

Figure 5: *Cycle 67, March 2008: X SSH at crossovers (left). GIM ionospheric correction (right).*

Another point can be underlined concerning the comparison of Envisat Bifrequency ionospheric correction to the GIM model over the first year. One can note that, unlike the other missions, the bias is not proportionnal to the ionospheric content. This was investigated this year, by comparing the GIM behavior using two different methods to take into account the portion of ionospheric correction under the altitude of Envisat. The first one uses the IRI95 correction from JPL and depending on the solar activity coefficients. The other one, proposed by Scharroo et al. 2010 ([12]), fixes the proportion of ionospheric content to a constant for the whole mission. The first method shows more consistent long term behavior with the bifrequency correction and suggests that the second method slightly degrades the data. Still, the change of behavior of the first year remains in both cases and should still be further investigated, as you can see in figure 7.

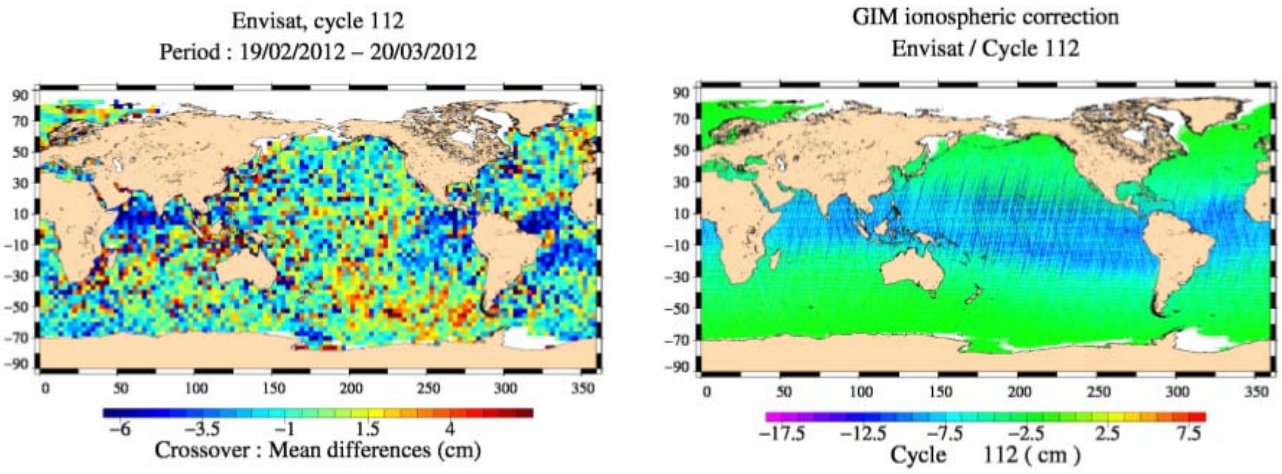

Figure 6: *Cycle 112, mars 2012: X SSH at crossovers (left). GIM ionospheric correction (right).*

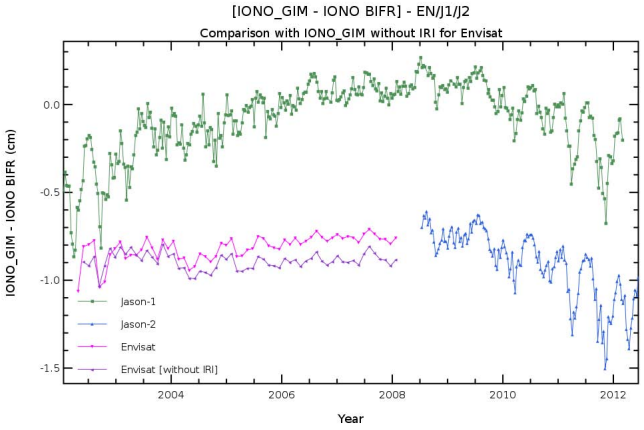

Figure 7: *Difference of ionospheric correction for Jason-1, Jason-2 and Envisat; without IRI95 correction for Envisat*

2.4. d/ Dry troposphere

See Salstein et al. (2008) [11].

2.5. e/ Wet troposphere

The standard deviation of the difference between MWR and ECMWF is variable throughout the mission. This variability can include the effect of the MWR ageing but it also includes ECMWF model changes. For the major part of the mission, it is rather stable around 1.8cm, whith slightly higher values (2cm) before cycle 12 (beginning 2003) and following an upgrade of the ECMWF model version on cycle 77 (end 2007). To prove this, a comparison to ERA Interim reprocessing ECMWF model is performed (see 9): no jumps are noticed. Convertely, a drift is observed on the difference of both corrections (0.5mm/year). Globally, MWR performance are better than ECMWF (0.6cm^2) as illustrated by the graph 8. This year, studies showed that this

could be improved (Ollivier et al., OSTST 2012). But feasability of a final improve of 1.1cm^2 has been shown too. Concerning the average stability, it is responsible for a non negligible part of the Mean Sea Level uncertainty (Ablain et al. 2010 [1]), around 0.6mm/year on Envisat as explained in ([6]). In 2013 a new radiometer wet tropospheric correction was developped, correcting the degradation observed after reprocessing. This new correction, name V2.1b is compared to ECMWF models on figure 10

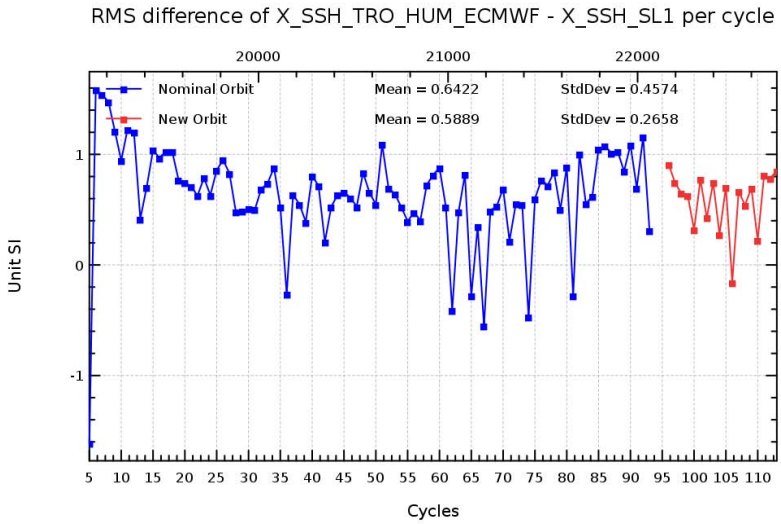

Figure 8: *RMS loss using ECMWF instead of MWR at crossovers, monitored by cycle*

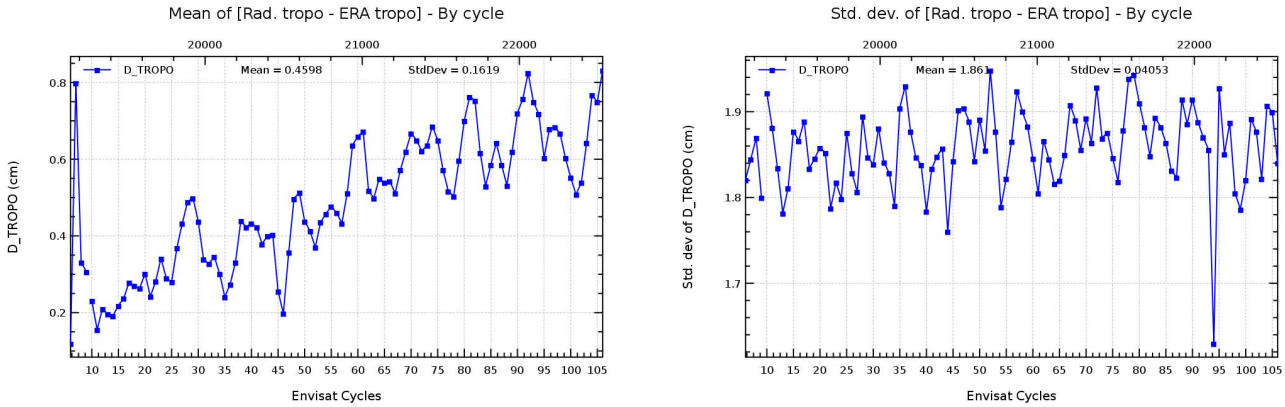

Figure 9: *Mean and Std. Dev of [radiometer-ERA model] correction by cycle*

We observe on figure 10 that V2.1b wet tropospheric correction gives a better agreement with models than V2.1, notably with ERA-Interim reprocessed series which has a reduced number of inhomogeneities.

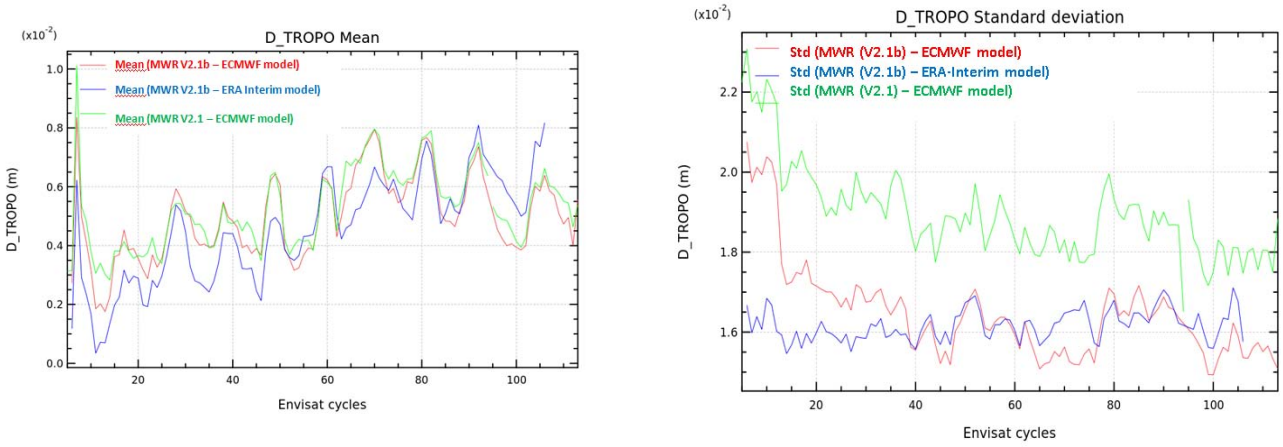

Figure 10: ***Left:*** *Mean and* ***Right****: Standard deviation of V2.1b wet tropospheric corrections: [radiometer - models] on the whole Envisat serie*

2.6. f/ Range drift/SSH

Extensive description of the in situ comparison is available in [14]. Note that a study was performed this year concerning the new sources of errors identified in Envisat RA2 system, notably concerning a wrong instrumental correction (PTR) with a 1 to 2mm/year impact on the global trend estimation. Also note that the errors are now monitored with a regional approach detailed in [5], §7.1.
Thanks to the recent updates, the accuracy of Envisat Mean Sea Level trend is now more realistic as detailled in Ollivier et al. 2012 [8]. The stability of the SSH can also be assessed by in situ data, as described in Valladeau and Leageais et al, 2012 [15].

2.7. g/ Radial Orbit Error

Absolute orbit quality is hard to determine, a criteria is the rms based on laser data. An increase is noticed in 2010 (from around 1.5 to 1.9cm). This increase seems to continue overs 2011 and 2012, with short periods of relative decrease (beginning of 2012). This increase could be due to a quality degradation of some stations included in the laser network. Furthermore, an internal quality criteria can also be given, based on consecutive orbits overlap comparison. This rms is reduced to around 0.6 cm for 2010 (1cm in 2009). The rms based on high elevation laser data gives a more reliable metric to assess the orbit quality. Orbit quality is stable despite the change of Envisat orbit and the slight increase of the solar activity.

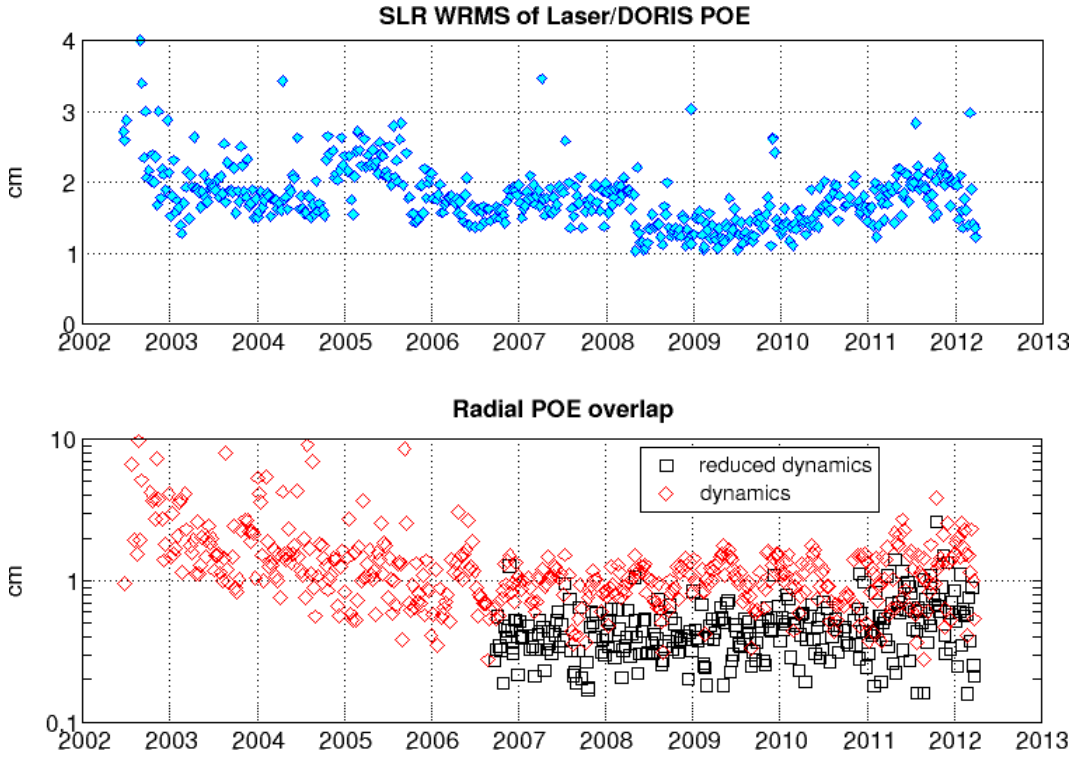

Figure 11: *Intrinsic POD quality criterion for Envisat (courtesy P. Yaya)*

2.8. h/ Significant Wave Height

See with Saleh Abdallah for ECMWF WAM outputs. In V2.1 version, the change of instrumental constant SigmaP has a direct impact on the SWH estimation, due to the following relation: $SWH = 2c\sqrt{(\sigma c^2 - \sigma p^2)}$
The SWH in V2.1 dataset is globally more compliant to buoys except for small waves, and to WAM model too. But both see stronger bias, around -13cm mean SWH bias, and a standard deviation degradation for SWH less than 3m. The noise increases from less than 7cm to 25cm for waves lower than 1m. This is presented in Figure 12. On figure 13 left, the blue curve corresponds to the chosen value of SigmaP, and the change of SWH behavior can be explained theoretically as a consequence of the non linear relation between SWH and SigmaP. This was explained in QWG_17 (A.Ollivier talk on SWH issue) and investigated this year on instrument expert side (see FPac activities, Thibaut et al., [18]). Theoretical analysis based on a numerical retracking have been carried out. A solution consists in applying corrections tables computed by comparing retracked data with the real PTR or with an approximation of it. This solution could be recommended for the next reprocessing.

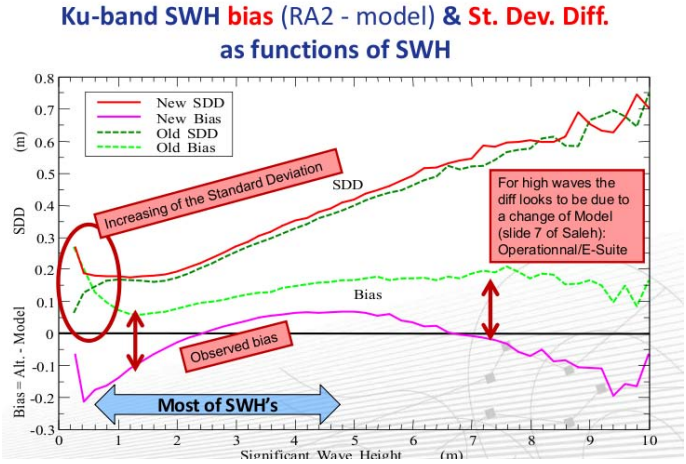

Figure 12: *Ku-band SWH bias and standard deviation difference as functions of SWH*

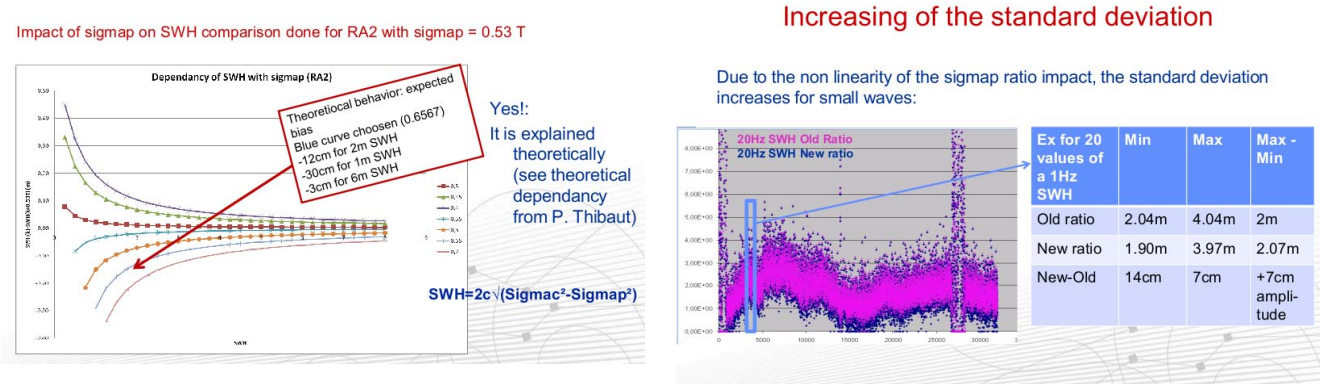

Ex for 20 values of a 1Hz SWH	Min	Max	Max - Min
Old ratio	2.04m	4.04m	2m
New ratio	1.90m	3.97m	2.07m
New-Old	14cm	7cm	+7cm amplitude

Figure 13: ***Left:*** *Dependancy of SWH with SigmaP* ***Right:****Standard deviation increase for small waves*

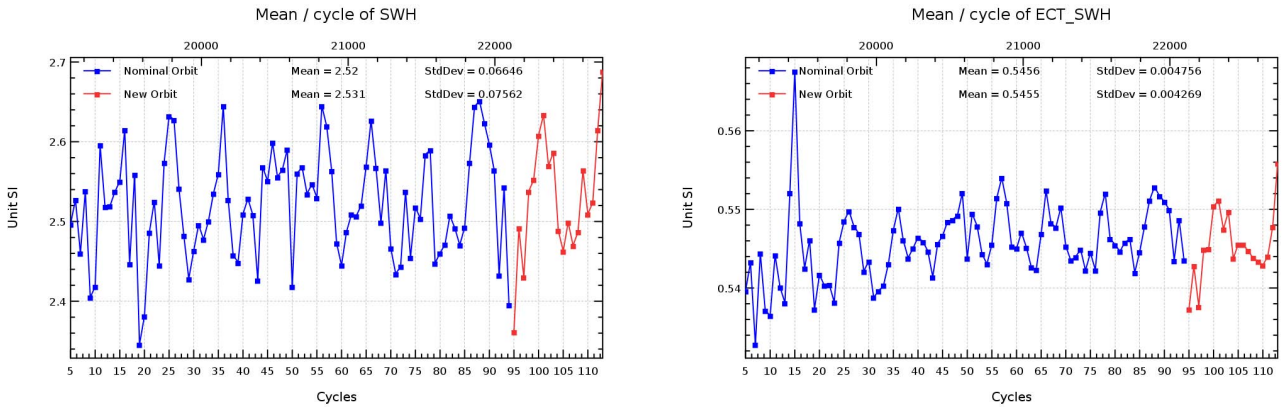

Figure 14: *Left) Mean Wave Height by cycle Right) Sdt. dev. of Wave Height by cycle*

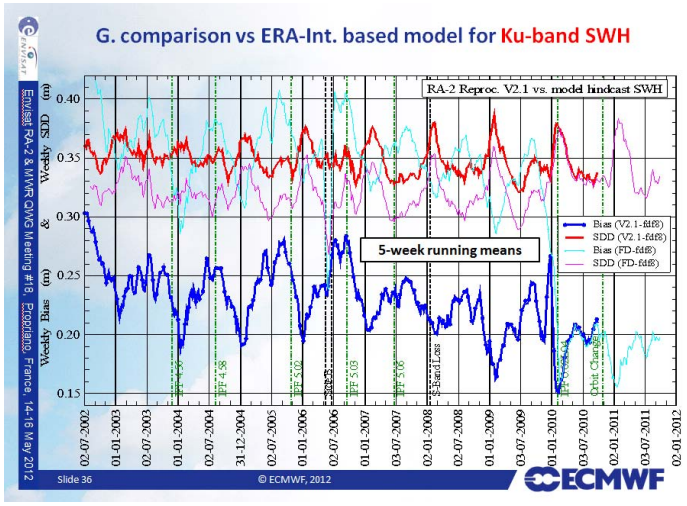

Figure 15: *Time series of Ku-Band SWH bias (RA2-model) and standard deviation difference (courtesy S. Abdalha ECMWF)*

2.9. i/ Wind speed

Obtained from a comparison between Sigma0 derived winds obtained with v1.0 tables and ECMWF gaussian grids wind outputs, with ocean data only (see editing specifications in Envisat Yearly report 2010 [5]). In 2012, a paper was also written on the stability of this parameter, evidencing a drift at the beginning of Envisat's period (Ablain et al. 2012 [2]).

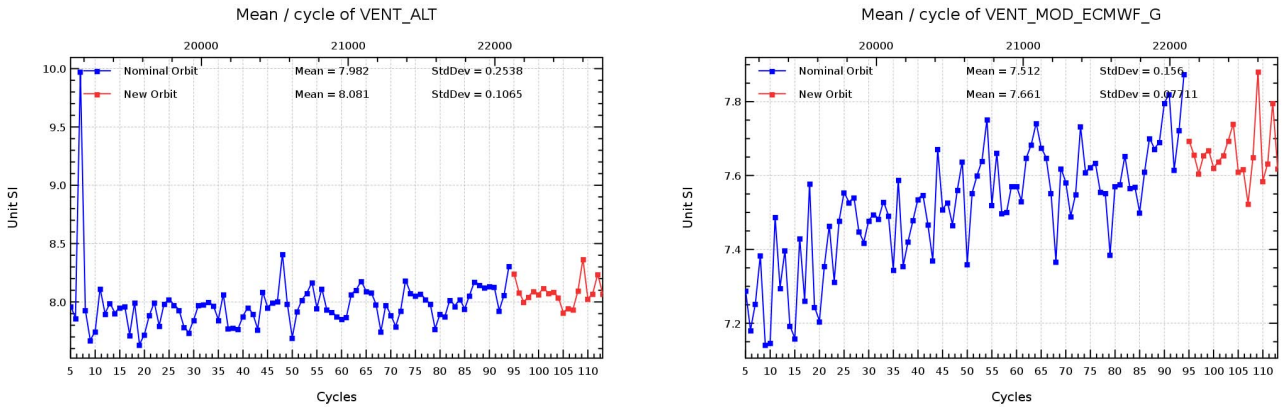

Figure 16: *Mean of Left) Altimetric Wind Speed Right) ECMWF Gaussian Wind Model, by cycle*

Envisat Altimetry	**Specified**	**Observed**	**Comments**
Altimeter noise	4.5cm	2cm	Altimeter noise computed on post launch data (see a/)
Sea State Bias	2cm	0.5cm	SSB error estimated from differences between different empirical models. Value at 2 m SWH. (see b/)
Ionosphere	0.2cm	0.7cm	Derived from cross-sensor comparisons (see c/)
Dry troposphere	0.7cm	0.7cm	From uncertainties in ECMWF atmospheric fields used to derive the correction. Value at 2-3 hPa sea level pression. (see d/)
Wet troposphere	1.4cm	1.8cm	Comparisons with ECMWF correction. (see e/)
Total range error (TRE): $\sqrt{\sum Terms^2}$	**5cm**	**2.9cm**	
Range drift/SSH	$<$ 0.5cm/y	0.2cm/y	From in situ tide gauge comparison over 2005-2010 (see f/)
Radial Orbit error (ROE)	2cm	1.7cm	From POD operational monitoring (see g/)
Sea height error: $\sqrt{(TRE)^2 + (ROE)^2}$	**5.4cm**	**3.5cm**	
Significant Wave Height	5% or 25 cm	25cm	Comparison versus ECMWF WAM global value (see h/)
Wind Speed	2.0m/s	1.3m/s	Comparison versus ECMWF global fields (see i/)

.

10. Conclusion

This report gathers the statistical evaluation of Envisat altimetric measurements on the whole dataset, corresponding to 10 years of data now available. Results presented here are based on GDR in V2.1 version and the last updates named V2.1+ version. A part of these updates are anticipated to prepare the next reprocessing. These anticipated updates are analysed in terms of performance of SSH at crossovers to quantify the global improvement of Envisat dataset.

The 10 years of data available and provided to users are homogeneous and allows to improve the computation of Envisat MSL. The impact of anticipated updates on MSL were analysed and described in this report too.

The major points to underline are:

- A very good availability of Envisat data on the last 2.5 years was noticed thanks to an improvement of the data dissemination since May 2008. Over the 10 years the availability of data is remarkable, reaching 94%.

- This year some studies were carried out in order to improve the quality of Envisat dataset, notably on anticipated updates:

  * A new radiometer wet tropospheric correction was computed and analysed. This update correct the degradation of quality observed in V2.1 dataset after reprocessing. This degradation is now corrected and the performance of SSH reach the quality obtained with the before reprocessing radiometer wet tropospheric correction. The impact of this new radiometer wet tropospheric correction on MSL trend is very weak and described in this report too.

  * Other anticipated updates were analysed and taken into account in SSH computation, such as iteratively filtered ionospheric correction or GOT 4.8 tide model.

- Cross comparisons continue to be developped with Jason-1, Jason-2, and Cryosat-2, which represents a new potential reference at high latitudes after the loss of Envisat. The behaviour of Cryosat-2 in terms of cross comparison allows to be confident in its use as a new reference solution for multimissions studies.
  However the cross comparisons with Jason's missions show some residual discrepancies on statistics of SSH at multimissions crossovers. Strange behaviors were highlighted on standard deviation comparing to Jason's missions. More investigations could allow to detect and analyse potential problems on Envisat side from multimission comparisons.

- Extensive studies of comparison to in situ data (Tide gauges and TS profile) were performed this year again, helping to characterize the differences between Jason-1 and Envisat missions. They also enabled to show the great improvement on global MSL trend (see [113]).

- After the loss of Envisat, the efforts concerning the computation of Envisat Mean Sea Level trend on the whole time series have been carried on. Sensitivity studies have been performed

.

and many improvements and updates over the whole time series allows to show similarity with Jason-1's MSL and tide gauges, which is very encouraging. In 2012, Envisat time series was updated notably with the PTR instrumental correction and the GDR-D POE standard, which insures a better consistency between other missions and in situ dataset (this drove to 2 official publications in Marine Geodesy: Ollivier et al. 2012 and Valladeau et al. 2012). These comparisons indicates that the Envisat MSL drift is greater than the one of Jason-1 over the period 2004/2012.

In terms of regional MSL, the effect of V2.1+ dataset is dominated by the GDR-D POE standard use. The geographical patterns on trend maps observed previously are now reduced.
Orbits based on a new gravity field are tested and compared to the GDR-D for Envisat and for Jason-1. The impact is negligible on mesoscale error and not significant on global Mean Sea Level, but the long term evolution of regional MSL is well improved. Its use is recommended for climate oriented studies for Envisat and Jason-1.
An effort was made to analyse MSL for the beginning of the period (before 2004). During this period, a great decreasing trend is observed. Some altimetric parameters have been shown as suspicious before 2004 (standard deviation of GIM/Bifrequency ionospheric correction, S-Band parameters, Ku-Band waveforms). The question of impact on MSL is still unresolved and should be carried on.

Efforts must continue to be performed to analyse the residual strange behaviors of Envisat dataset comparing to other missions in terms of SSH quality or relevant Mean Sea Level computation. This is important to refine our knowledge of the mission and to well prepare future reprocessings of Envisat dataset.

11. Bibliography

References

[1] Abdalla, S., "A wind retrieval algorithm for satellite radar altimeters", ECMWF Technical Memorandum, in preparation, 2006.

[2] Ablain, M., G. Pontonnier, B. Soussi, P. Thibaut, M.H. de Launay, J. Dorandeu, and P. Vincent. 2004. Jason-1 GDR Quality Assessment Report. Cycle 079. SALP-RP-P2-EX-21072-CLS079, May.

[3] M. Ablain., S. Philipps, Dorandeu J., 2006: Jason-1 validation and cross calibration activities. Yearly report. Technical Note CLS.DOS/NT/06-302, Contract N° 03/CNES/1340/00-DSO310 - lot2.C http://www.jason.oceanobs.com/documents/calval/validation_report/annual_report_j1_2006.pdf

[4] M. Ablain., S. Philipps, 2007: Jason-1 validation and cross calibration activities. Yearly report. Technical Note CLS.DOS/NT/06-302, Contract N° 03/CNES/1340/00-DSO310 - lot2.C http://www.jason.oceanobs.com/documents/calval/validation_report/annual_report_j1_2007.pdf

[5] Ablain M., A. Cazenave, G. Valladeau, and S. Guinehut. 2009: A new assessment of the error budget of global mean sea level rate estimated by satellite altimetry over 1993-2008. Ocean Sci, 5, 193-201.

[6] M. Ablain., S. Philipps, G. Valladeau, J.F. Legeais, H. Roinard 2011: Jason-1 validation and cross calibration activities. Annual report 2011. Technical Note CLS.DOS/NT/12-017, Contract N° SALP-RP-MA-EA-22056-CLS

[7] M. Ablain., S. Philipps, G. Valladeau, J.F. Legeais 2011: Jason-2 validation and cross calibration activities. Annual report 2011. Technical Note CLS.DOS/NT/12-005, Contract N° SALP-RP-MA-EA-22042-CLS

[8] Ablain M., Cazenave A., Guinehut S., Valladeau G., (submitted for publication), A new assessment of global mean sea level from altimeters highlights a reduction of global slope from 2005 to 2008 in agreement with in-situ measurements, submitted to Ocean Sciences.

[9] Ablain, M., A. Cazenave, G. Valladeau, and S. Guinehut. 2009: A new assessment of the error budget of global mean sea level rate estimated by satellite altimetry over 1993-2008. Ocean Sci, 5, 193-201.

[10] Ablain M., S. Philipps, M. Urvoy, N. Tran and N. Picot, 2012: Detection of long-term instabilities on altimeter backscatter coefficient thanks to wind speed data comparisons from altimeters and models, Marine Geodesy Vol 35.

[11] Faugere Y., Granier N., Ollivier A., 2007: Envisat RA-2/MWR ocean data validation and cross-calibration activities. Yearly report. Technical Note CLS.DOS/NT/08.006, Contract N° SALP-RP-MA-EA-21516-CLS

[12] Ollivier A.,Faugere Y., 2008: Envisat RA-2/MWR ocean data validation and cross-calibration activities. Yearly report. Technical Note CLS.DOS/NT/09.040, Contract N° SALP-RP-MA-EA-21633-CLS

[13] Ollivier A.,Faugere Y., 2009: Envisat RA-2/MWR ocean data validation and cross-calibration activities. Yearly report. Technical Note CLS.DOS/NT/10.018, Contract N° SALP-RP-MA-EA-21800-CLS http://www.aviso.oceanobs.com/fileadmin/documents/calval/validation_report/EN/annual_report_en_2009.pdf

[14] Ollivier A.,Faugere Y., 2010: Envisat RA-2/MWR ocean data validation and cross-calibration activities. Yearly report. Technical Note CLS.DOS/NT/10.018, Contract N° SALP-RP-MA-EA-21920-CLS http://www.aviso.oceanobs.com/fileadmin/documents/calval/validation_report/EN/annual_report_en_2010.pdf

[15] Ollivier A., Guibbaud M., 2011: Envisat RA-2/MWR ocean data validation and cross-calibration activities. Yearly report. Technical Note CLS.DOS/NT/12.021, Contract SALP-RP-MA-EA-22062-CLS http://www.aviso.oceanobs.com/fileadmin/documents/calval/validation_report/EN/annual_report_en_2011.pdf

[16] Ollivier A., Guibbaud M., 2012: Envisat RA-2/MWR ocean data validation and cross-calibration activities. Yearly report. Technical Note CLS.DOS/NT/12.292, Contract SALP-RP-MA-EA-22163-CLS http://www.aviso.oceanobs.com/fileadmin/documents/calval/validation_report/EN/annual_report_en_2012.pdf

[17] Commien L., S. Philipps, M. Ablain., 2008: Jason-1 validation and cross calibration activities. Yearly report. Technical Note CLS.DOS/NT/09-006, Contract N° 60453 - lot2.C http://www.jason.oceanobs.com/documents/calval/validation_report/annual_report_j1_2008.pdf

[18] Valladeau G. and Prandi P., 2013:Validation of altimeter data by comparison with tide gauge measurements for TOPEX/Poseidon, Jason-1, Jason-2 and Envisat (Annual report 2013). [SALP-NT-MA-EA-xxxxx-CLS, CLS.DOS/NT/13-262].

[19] Legeais J.F. and Ablain M., 2013: Validation of altimetric data by comparison with in-situ T/S Argo profiles (Annual Report 2013) [SALP-RP-MA-EA-22281-CLS, CLS.DOS/NT/13-256]

[20] Beckley, B. D., F. G. Lemoine, S. B. Luthcke, R. D. Ray, and N. P. Zelensky A reassessment of global and regional mean sea level trends from TOPEX and Jason-1 altimetry based on revised reference frame and orbits, Geophys. Res. Lett., 34, L14608, 2007, doi:10.1029/2007GL030002.

[21] Valladeau G., Ablain M., Validation of altimetric data by means of tide gauge measurements for TOPEX/Poseidon, Jason-1 and Envisat, Reference : CLS.DOS/NT/10-289, Nomenclature : SALP-NT-MA-EA-21922-CLS

[22] Legeais JF, Ablain M., Validation of altimetric data by comparison with in-situ T/S Argo profiles, Reference : CLS.DOS/NT/10-308, Nomenclature : SALP-NT-MA-EA-21921-CLS

[23] Carrère, L., and F. Lyard, Modeling the barotropic response of the global ocean to atmospheric wind and pressure forcing - comparisons with observations. 2003. Geophys. Res. Lett., 30(6), 1275, doi:10.1029/2002GL016473.

[24] Commien, L., 2009. Différences entre l'orbite des GDR-C et GDR-B Jason-1, NT08.338

[25] Commien, L., S. Philipps, M. Ablain, and N. Picot, 2008. SSALTO CALVAL Performance assessment Jason-1 GDR "C" / GDR "B". Poster presented at OSTST meeting, Nice, France, 09-12 November 2008. Available at: http://www.aviso.oceanobs.com/fileadmin/documents/OSTST/2008/commien.pdf

[26] Legeais JF. and Carrere L, July 2008, Complement de validation de la DAC_HR par rapport à la DAC , en zone cotiere, Technical Note CLS.DOS/08.189.

[27] Cazenave, A., et al.,1999: Sea Level Change from Topex/Poseidon altimetry and tide gauges, and vertical crustal motions from DORIS, G. Res. Let., 26, 2077-2080.

[28] Cazenave, A. and Nerem, R. S.: Present-day sea level change, Observations and causes, Rev. Geophys., 42, RG3001, doi:10.1029/2003RG000139, 2004.

[29] Celani C., B. Greco, A. Martini, M. Roca, 2002: Instruments corrections applied on RA-2 Level-1B Product. 2002: Proceeding of the Envisat Calibration Workshop.

[30] Cerri L., Berthias P., Bertiger W.I., Haines, B.J. Lemoine F.G., Mercier F., Ries J.C., Willis P., Zellensky P. and Ziebart M. Precision Orbit Determination Standards for the Jason Series of Altimeter Missions, Marine Geodesy Vol 33., 2010

[31] Cerri L., Couhert A., Houry S., Mercier F., OSTST 2011 presentation available at http://www.aviso.oceanobs.com/fileadmin/documents/OSTST/2011/oral/02_Thursday/Splinter%203%20

[32] Chambers, D., P., J. Ries, T. Urban, and S. Hayes. 2002. Results of global intercomparison between TOPEX and Jason measurements and models. Paper presented at the Jason-1 and TOPEX/Poseidon Science Working Team Meeting, Biarritz (France), 10-12 June.

[33] Dorandeu, J. and P.Y. Le Traon, 1999: Effects of Global Atmospheric Pressure Variations on Mean Sea Level Changes from TOPEX/Poseidon. J. Atmos. Technol., 16, 1279-1283.

[34] Dorandeu J., Y. Faugere, F. Mertz, F. Mercier, N. Tran, 2004a: Calibration / Validation Of Envisat GDRs Cross-calibration / ERS-2, Jason-1 Envisat and ERS Symposium, Salzburg, Austria.

[35] Dorandeu, J., M. Ablain, Y. faugere, F. Mertz, B. Soussi, 2004b, Jason-1 global statistical evaluation and performance assessment. Calibration and cross-calibration results Mar. Geod. 27(3-4): 345-372.

[36] Doornbos E., Scharroo R., 2005: Improved ERS and Envisat precise orbit determination, Proc. of the 2004 Envisat and ERS Symposium, Salzburg, Austria.

[37] ECMWF, The evolution of the ECMWF analysis and forecasting system Available at: http://www.ecmwf.int/products/data/operational_system/evolution/

[38] EOO/EOX, October 2005, Information to the Users regarding the Envisat RA2/MWR IPF version 5.02 and CMA 7.1 Available at http://earth.esa.int/pcs/envisat/ra2/articles/

[39] EOP-GOQ and PCF team, 2005: Envisat Cyclic Altimetric Report, Technical Note ENVI-GSOP-EOPG-03-0011 Available at: http://earth.esa.int/pcs/envisat/ra2/reports/pcs_cyclic/

[40] Eymard L., E. Obligis, N. Tran, February 2003, ERS2/MWR drift evaluation and correction, CLS.DOS/NT/03.688

[41] http://earth.esa.int/brat/html/alti/dataflow/processing/pod/orbit_choice_en.html

[42] Envisat RA-2 Range Instrumental correction: USO clock period variations and associated auxiliary file, ENVI-GSEG-EOPG-TN-03-0009

[43] Faugere Y., Mertz F., Dorandeu J., 2003: Envisat GDR quality assessement report (cyclic), Cycle 015. SALP-RP-P2-EX-21072-CLS015, May. Available at http://www.aviso.oceanobs.com/html/donnees/calval/validation_report/en/welcome_uk.html

[44] Faugere Y., Mertz F., Dorandeu J., 2003: Envisat validation and cross calibration activities during the verification phase. Synthesis report. Technical Note CLS.DOS/NT/03.733, ESTEC contract N°16243/02/NL/FF WP6, May 16 2003 Available at http://earth.esa.int/pcs/envisat/ra2/articles/Envisat_Verif_Phase_CLS.pdf

[45] Faugere Y., Mertz F., Dorandeu J., 2004: Envisat RA-2/MWR ocean data validation and cross-calibration activities. Yearly report. Technical Note CLS.DOS/NT/04.289, Contract N° 03/CNES/1340/00-DSO310 Available at http://earth.esa.int/pcs/envisat/ra2/articles/Envisat_Yearly_Report_2004.pdf

[46] Faugere Y., Estimation du bruit de mesure sur jason-1, December 2002, CLS.ED/NT.

[47] Y.Faugere, J.Dorandeu, F.Lefevre, N.Picot and P.Femenias, 2005: Envisat ocean altimetry performance assessment and cross-calibration. Submitted in the special issue of SENSOR 'Satellite Altimetry: New Sensors and New Applications'

[48] Yannice Faugere, JoÃ≪l Dorandeu, Fabien Lefevre, Nicolas Picot and Pierre Femenias, Envisat Ocean Altimetry Performance Assessment and Cross-calibration, Special Issue on 'Satellite Altimetry: New Sensors and New Application' Edited by Ge Chen and Graham D. Quartly, March 2006

[49] Faugere Y., Mertz F., Dorandeu J., 2005: Envisat RA-2/MWR ocean data validation and cross-calibration activities. Yearly report. Technical Note CLS.DOS/NT/04.289, Contract N° 03/CNES/1340/00-DSO310 http://www.jason.oceanobs.com/documents/calval/validation_report/en/annual_report_en_2005.pdf

[50] Faugere, Y., J. Dorandeu, N. Picot, P. Femenias. 2007. Jason-1 / Envisat Cross-calibration, presentation at the Hobart OSTST meeting

[51] Faugere, Y., Ollivier, A., 2007, Investigation on the differences between CLS and Altimetrics Envisat MSL trend, CLS.DOS/NT07-261

[52] Faugere, Y., Ollivier, A., 2008, Investigation on the High frequency content of Jason and Envisat, CLS.DOS/NT08-119

[53] Dibarbour, G., Bruit Jason et Analyse spectrale, March 2001, CLS.ED/NT

[54] G.Dibarboure, P.Schaeffer, P.Escudier, M-I.Pujol, J.F.Legeais, Y.Faugère, R.Morrow, J.K.Willis, J.Lambin, J.P.Berthias, N.Picot - Finding desirable orbit options for the "Extension of Life" phase of Jason-1 Submitted to Marine Geodesy - Jason-2 Special Issue Volume 3 - May 2011

[55] Imel, D., Evaluation of the TOPEX/POSEIDON dual-frequency ionosphere correction, J. Geophys. Res., 99, 24,895-24,906, 1994

[56] Labroue, S. and P. Gaspar, 2002: Comparison of non parametric estimates of the TOPEX A, TOPEX B and JASON 1 sea state bias. Paper presented at the Jason 1 and TOPEX/Poseidon SWT meeting, New-Orleans, 21-12 October.

[57] Labroue S. and E. Obligis, January 2003, Neural network retrieval algorithms for the ENVISAT/MWR, Technical note CLS.DOS/NT/03.848

.

[58] Labroue S., 2003: Non parametric estimation of ENVISAT sea state bias, Technical note CLS.DOS/NT/03.741, ESTEC Contract n°16243/02/NL/FF - WP3 Task 2

[59] Labroue S., 2004: RA-2 ocean and MWR measurement long term monitoring, Final report for WP3, Task 2, SSB estimation for RA-2 altimeter, Technical Note CLS-DOS-NT-04-284

[60] Labroue S., 2005: RA2 ocean and MWR measurement long term monitoring 2005 report for WP3, Task 2 SSB estimation for RA2 altimeter, Technical Note CLS-DOS-NT-05-200

[61] Labroue S., 2006: Estimation du Biais d'Etat de Mer pour la mission Jason-1, Technical note CLS-DOS-NT-06-244

[62] Labroue S., MH. Rio, Y. Faugere, A. Ollivier - Tâche 1.1 - Résolution des produits et filtrage SALP-NT-P-EA-21665-CLS

[63] Laxon and M. Roca, 2002: ENVISAT RA-2: S-BAND PERFORMANCE, S., Proceedings of the ENVISAT Calibration Workshop, Noordwijk

[64] Legeais J.F., Ablain M. 2011: Cal/Val in-situ annual report Altimetry / Argo T/S profiles. Validation of altimeter data by comparison with in-situ T/S Argo profiles. Ref. CLS/DOS/NT/11-305. SALP-RP-MA-EA-22045-CLS.

[65] Le Traon, P.-Y., J. Stum, J. Dorandeu, P. Gaspar, and P. Vincent, 1994: Global statistical analysis of TOPEX and POSEIDON data. J. Geophys. Res., 99, 24619-24631.

[66] Le Traon, P.-Y., , F. Ogor, 1998: ERS-1/2 orbit improvement using TOPEX/POSEIDON: the 2 cm challenge. J. G. Res., VOL 103, p 8045-8057, April 15, 1998.

[67] Le Traon P.Y. Y. Faugere, F. Hernandez, J.Dorandeu, F.Mertz, and M. Can We Merge GEOSAT Follow-On with TOPEX/Poseidon and ERS-2 for an Improved Description of the Ocean Circulation? ; June 2003, American Meteorological Society

[68] Lefèvre, F., and E. Sénant, 2005: ENVISAT relative calibration, Technical Note CLS-DOS-NT-05.074.

[69] Lillibridge J, R. Scharroo and G. Quartly, 2005: rain and ice flagging of Envisat altimeter and MWR data, Proc. of the 2004 Envisat and ERS Symposium, Salzburg, Austria

[70] Luthcke. S. B., N. P. Zelinsky, D. D. Rowlands, F. G. Lemoine, and T. A. Williams. 2003. The 1-Centimeter Orbit: jason-1 Precision Orbit Determination Using GPS, SLR, DORIS, and Altimeter Data. Mar. Geod. 26(3-4): 399-421.

[71] Martini A. and P. Féménias, 2000: The ERS SPTR2000 Altimetric Range Correction: Results and Validation. ERE-TN-ADQ-GSO-6001. 23 November 2000.

[72] Martini A., 2003: Envisat RA-2 Range instrumental correction : USO clock period variation and associated auxiliary file, Technical Note ENVI-GSEG-EOPG-TN-03-0009 Available at http://earth.esa.int/pcs/envisat/ra2/articles/USO_clock_corr_aux_file.pdf http://earth.esa.int/pcs/envisat/ra2/auxdata/

[73] A. Martini, P. Feminias, G. Alberti, M.P.Milagro-Perez, 2005: RA-2 S-Band Anomaly: Detection and waveform recontruction. Proc. of 2004 Envisat & ERS Symposium, Salzburg, Austria. 6-10 September 2004 (ESA SP-572, April 2005).

.

[74] Mertz, F., Y. Faugere and J. Dorandeu, 2003: Validation of ERS-2 OPR cycle 083-086. CLS.OC.NT/03.702 issue 083-086.

[75] Mercier, F., L.Cerri, S. Houry, A. Guitart, P. Broca, C. Ferrier, J-P. Berthias, 2006: DORIS 1b Product evolution, Symposium 15 Years of progress in radar altimetry, Venice.

[76] Mertz F., J. Dorandeu, N. Tran, S. Labroue, 2004, ERS-2 OPR data quality assessment. Long-term monitoring - particular investigations, Report of task 2 of IFREMER Contract n° 04/2.210.714. CLS.DOS/NT/04.277.

[77] Mitchum, G., 1994: Comparison of TOPEX sea surface heights and tide gauge sea levels, J. Geophys. Res., 99, 24541-24554.

[78] Mitchum, G., 1998: Monitoring the stability of satellite altimeters with tide gauges, J. Atm. Oceano. Tech., 15, 721-730.

[79] Obligis E., L. Eymard, N. Tran, S. Labroue, 2005: Three years of Microwave Radiometer aboard Envisat: In-flight Calibration, Processing and validation of the geophysical products, submitted

[80] Ollivier A.,Y. Faugere, P. Thibaut, G. Dibarboure, J. Poisson, 2008: Investigation on the high frequency content of Jason-1 and Jason-2, Technical note CLS-DOS-NT-09-027

[81] Ollivier, A., Y. Faugere and N. Picot, P. Femenias 2008. ENVISAT Jason-2 Cross calibration. Poster presented at OSTST meeting, Nice, France, 09-12 November 2008. Available at: http://www.aviso.oceanobs.com/fileadmin/documents/OSTST/2008/ollivier.pdf

[82] Ollivier A., Y.Faugere, N. Picot, M. Ablain, P. Femenias and J. Benveniste, 2012, Envisat ocean altimeter becoming relevant for Mean Sea Level Trend Studies, Marine Geodesy Vol 35

[83] Ollivier A., J.F. Legeais - N. Granier - Y.Faugere - F-PAC Calval Team CalVal status on the Envisat V2.1 reprocessing impact on main altimetric parameters, available on the ftp://diss-na-fp.eo.esa.int in a document distributed to users under the name: V2 1 reprocessing impact on altimetric parameters.pdf

[84] Ollivier A., M. Guibbaud - Envisat V2.1 reprocessing impact on ocean data, Technical Note CLS.DOS/NT/12.064, http://www.aviso.oceanobs.com/fileadmin/documents/calval/validation_report/EN/EnvisatReprocessingReport.pdf

[85] Pascual A., FaugÃ¨re F., Larnicol G., Le Traon P.Y, 2006, Improved description of the ocean mesoscale variability by combining four satellite altimeters, Geophys. Res. Let., Vol 33, L02611

[86] Picard B., M-L Frery, E. Obligis: ENVISAT Microwave Radiometer Assessment Report Cycle 039, Technical Note CLS.DOS/NT/05.147 Available at http://earth.esa.int/pcs/envisat/mwr/reports/

[87] Product disclaimer available on http://earth.esa.int/dataproducts/availability/

[88]

[89] Ray, R. (1999) - A global ocean tide model from Topex/Poseidon altimetry: GOT 99.2 - NASA Tech Memo 209478.

[90] R D Ray and R M Ponte, 2003: Barometric tides from ECMWF operational analyses, Annales Geophysicae, 21: 1897-1910.

[91] Roca M., A. Martini, 2003: Level 1b Verification updates, Ra2/MWR CCVT meeting, 25-26 March 2003, ESRIN, Rome

[92] Roca M., A. Martini, PTR Study, QWG meeting, November 2008, ESRIN, Rome

[93] H. Roinard, S. Philipps, Jason-2 reprocessing impact on ocean data (Cycle 001 to 145), CLS.DOS/NT/12.138

[94] Rudolph A., D.Kuijper, L.Ventimiglia, M.A. Garcia Matatoros, P.Bargellini, 2005: Envisat orbit control - philosophy experience and challenge, Proc. of the 2004 Envisat and ERS Symposium, Salzburg, Austria

[95] Salstein, D. A., Ponte, R. M., and Cady-Pereira, K.: Uncertainties in atmospheric surface pressure fields from global analyses, J. Geophys. Res., 113, D14107, doi:10.1029/2007JD009531, 2008.

[96] R. Scharroo and P. N. A. M. Visser, 1998: Precise orbit determination and gravity field improvement for the ERS satellites, J. Geophys. Res., 103, C4, 8113-8127

[97] Scharroo R., A decade of ERS Satellite Orbits and Altimetry, 2002: Phd Thesis, Delft University Press science

[98] Scharroo R., December 12, 2002, Routines for iono corrections, internet communication to the CCVT community

[99] Scharroo R., J. L. Lillibridge, and W. H. F. Smith, Cross-Calibration and Long-term Monitoring of the Microwave Radiometers of ERS, TOPEX, GFO, Jason-1, and Envisat, **Marine Geodesy, 27:279-297**, 2004.

[100] Scharroo, R., W.H.F.Smith - A global positionning system-based climatology for the total electron content in the ionosphere - October 2010

[101] Scharroo, R., RA-2 USO Anomaly: predictive correction model, Tech. Rep. N1-06-002, Altimetrics LLC, Cornish, New Hampshire, May 2006.

[102] Stum J., F. Ogor, P.Y. Le Traon, J. Dorandeu, P. Gaspar and J.P. Dumont, 1998: "An intercalibration study of TOPEX/POSEIDON, ERS-1 and ERS-2 altimetric missions", Final report of IFREMER contract N_97/2 426 086/C CLS.DOS/NT/98.070.

[103] Surface Topography Mission (STM) End to End Performance Budgets (SY-6) CLS-DOS-NT-08-2173-0 of 24/02/2010 - S3-TN-CLS-SY-00049

[104] Thibaut P., New assessment of the RA-2 instrumental corrections and impact on the Mean Sea Level P.Thibaut, J.C.Poisson, M.Roca, P.Nilo Garcia, Y.Faugere N.Picot, J.Benveniste, P.Femenias http://www.aviso.oceanobs.com/fileadmin/documents/OSTST/2011

[105] Tran, N., D. W. Hancock III, G.S. Hayne. 2002: "Assessment of the cycle-per-cycle noise level of the GEOSAT Follow-On, TOPEX and POSEIDON." J. of Atmos. and Oceanic Technol. 19(12): 2095-2117.

[106] Tran N. and E. Obligis, December 2003, Validation of the use of ENVISAT neural algorithm on ERS-2. CLS-DOS-NT-03.901.

[107] Tran N., E. Obligis and L. Eymard, 2006, Envisat MWR 36.5 GHz drift evaluation and correction. CLS-DOS-NT-05.218.

.

[108] Tran N. et al. Validation of Envisat Rain Detection and Rain Rate Estimates by Comparing With TRMM Data" N. Tran et al. IEEE Geoscience and Remote Sensing Letters, oct 2008

[109] Valladeau G., Ablain M., Validation of altimetric data by means of tide gauge measurements for TOPEX/Poseidon, Jason-1 and Envisat, Reference : CLS.DOS/NT/08-256, Nomenclature : SALP-NT-MA-EA-21589-CLS

[110] Valladeau G. 2011: Cal/Val in-situ annual report Altimetry / tide gauges. Validation of altimeter data by comparison with tide gauges measurements. Ref. CLS/DOS/NT/12-016. SALP-RP-MA-EA-22046-CLS.

[111] Valladeau G., Ablain M., Validation of altimetric data by comparison with tide gauge measurements for TOPEX/Poseidon, Jason-1 and Envisat, Reference : CLS.DOS/NT/09-115, Nomenclature : SALPNT-MA-EA-21691-CLS

[112] Valladeau G. and J.-F. Legeais, M. Ablain, S. Guinehut and N. Picot, Altimeter and in-situ sea level comparisons with tide gauges and ARGO profiles Marine Geodesy 2012, submitted

[113] Valladeau G. and J.-F. Legeais, M. Ablain, S. Guinehut and N. Picot, Comparing altimetry with tide gauges and Argo profiling floats for data quality assessment and Mean Sea Level studies, Marine Geodesy Vol 35.

[114] Thibaut P., Lasne Y., Poisson J.C, Numerical Retracking techniques applied on Envisat data, 2013-11-26, CLS-DOS-NT-12-143

[115] Vincent, P., S. D. Desai, J. Dorandeu, M. Ablain, B. Soussi, P. S. Callahan, and B. J. Haines 2003. Jason-1 Geophysical Performance Evaluation. Mar. Geod. 26(3-4): 167-186.

[116] Witter, D. L., D. B. Chelton, 1991: "A Geosat altimeter wind speed algorithm development", J. of. Geophys. Res. (oceans), 96, 8853-8860, 1991.

[117] Zanife, O. Z., P. Vincent, L. Amarouche, J. P. Dumont, P. Thibaut, and S. Labroue, 2003. Comparison of the Ku-band range noise level and the relative sea-state bias of the Jason-1, TOPEX and Poseidon-1 radar altimeters. Mar. Geod. 26(3-4): 201-238.

.